EVALUATION OF GROUNDWATER RECHARGE AND FLOW IN CRYSTALLINE TERRAIN IN THE MATLALA BATHOLITH, LIMPOPO, SOUTH AFRICA

Londolani Hope Maphala

Submitted in fulfilment of the requirements for the degree

Magister Scientiae in Geohydrology

in the

Faculty of Natural and Agricultural Sciences

(Institute for Groundwater Studies)

at the

University of the Free State

Supervisor: Dr FD Fourie

November 2021

DECLARATION

I, Londolani Hope Maphala, hereby declare that the dissertation hereby submitted by me to the Institute for Groundwater Studies in the Faculty of Natural and Agricultural Sciences at the University of the Free State, in fulfilment of the degree of Magister Scientiae, is my own independent work. It has not previously been submitted by me to any other institution of higher education. In addition, I declare that all sources cited have been acknowledged by means of a list of references.

I furthermore cede copyright of the dissertation and its contents in favour of the University of the Free State.

Londolani Hope Maphala

November 2021

ACKNOWLEDGEMENTS

I would hereby like to express my sincere gratitude to all who have motivated and helped me in the completion of this dissertation:

- I am grateful to the Lord God Almighty, for with him everything is possible.
- My supervisor Dr Francois Fourie. I am extremely grateful for the efforts and guidance, most importantly for picking me up while I was stranded.
- I place on record my sincere gratitude to Prof Kai Witthüser, for his valuable guidance and assistance thought the early stages of this research. I am really grateful.
- I am grateful to the Department of Water and Sanitation for the financial support.
- Special thanks to all my colleagues from the Department of Water and Sanitation (Geohydrology Section) in the Limpopo regional office. More especially Mr WH Du Toit for handing over the project to me for completion and to my supervisor Mr JM Mahlo who went above and beyond to assist me.
- I also thank my friends Maugana Vuledzani, Ligavha Mbelengwa Lufuno, Gomo Bernand, Nancy Ntseze, Blessing from GMC, and Maponya Kulanyane for their encouragement, assistance and support.
- I am grateful to my parents Mr and Mrs Matshivha and the rest of the family for support throughout this study.
- Lastly, my husband who stood by me from the first day till the last, staying up late, taking care of our toddlers. Words cannot describe how blessed and grateful I am.

TABLE OF CONTENTS

LIST OF FIGURES

LIST OF TABLES

LIST OF ABBREVIATIONS

CRD	Cumulative rainfall departure
CMB	Chloride mass balance
DWA	Department of Water Affairs
DWAF	Department of Water Affairs and Forestry
DWS	Department of Water and Sanitation
EC	Electrical conductivity
EM	Electromagnetic
MAP	Mean annual precipitation
NGA	National Groundwater Archive
SANS	South African National Standards
TDS	Total dissolved solids
WMA	Water management area
WTF	Water table fluctuation

LIST OF CHEMICAL SYMBOLS

Al	Aluminium
Ca	Calcium
Cl	Chlorine
F	Fluoride
Fe	Iron
HCO_3	Bicarbonate
K	Potassium
Na	Sodium
NaCl	Sodium chloride
SO_4	Sulphate
NH_3	Ammonia

NO_3	Nitrate
Si	Silicon
SiO_2	Silica (silicon dioxide)

LIST OF SYMBOLS

K	Hydraulic conductivity [L/T]
h	Hydraulic head [L]
i	Hydraulic gradient [-]
n	Porosity [-]
S	Storativity [-]
S_y	Specific yield [-]
T	Transmissivity [L^2/T]

LIST OF UNITS

d	days
km	kilometres
L/s	litres per second
m	metres
m^2/d	square metres per day
mamsl	metres above mean sea level
mbgl	metres below ground level
meq/L	milliequivalents per litre
mg/L	milligrams per litre
mm/a	millimetres per annum

CHAPTER 1:
INTRODUCTION

1.1 BACKGROUND

Groundwater is the water found below the earth's surface, be it in the weathered and fractured bedrock or in the pore spaces between mineral grains in the rocks. Water beneath the ground originates from water that falls onto the earth's surface as precipitation; some of the water runs off over the ground surface and some infiltrates into the subsurface and eventually percolates through the weathered material to the underlying solid bedrock. The rock units which store and allow the transmission of groundwater are referred to as aquifers.

Aquifers may occur in all rock types, including crystalline hard rock, which are also often referred to as basement aquifers. According to Wright (1992), these aquifers develop within fractured and weathered igneous and/or metamorphic rocks, mainly of Precambrian age. According to Holland (2011), topography, lithology, surface water bodies, and brittle tectonics control the development of fractures and fault zones in crystalline bedrock, as well as the nature and depth of the regolith. In this research, crystalline rocks refer to the metaphoric rocks (gneiss) and intrusive igneous rocks (granites and dolerite) found in the study area, namely the area around the Matlala Batholith.

The Matlala Batholith occurs a semi-arid area that receives little rainfall, with a mean annual precipitation (MAP) of less than 500 mm. The underlying aquifer is crystalline and complex, resulting in the irregularity of groundwater occurrence and availability. Previous studies have contributed largely to the understanding of the groundwater resource in the area. Du Toit (2001) investigated groundwater occurrence at a local scale around the Matlala Batholith to determine whether the contact between the Matlala Granite and surrounding Goudplaats-Hout River Gneiss is a potential groundwater target. The results obtained showed that groundwater occurs in the remnant roof section, which is highly fractured and weathered, and which produces blow yields of over 40 L/s.

Holland (2011) conducted investigations on a regional scale to estimate groundwater recharge using the chloride mass balance (CMB) method. He included the Matlala Batholith in his study and obtained a recharge estimate of 0.5% of the MAP at Chloe, which is located approximately 9 km north-north-east from the Matlala Batholith.

The Matlala Groundwater Monitoring Project was designed by the Department of Water and Sanitation to monitor groundwater levels in the study area. The primary objective of the groundwater monitoring network is to observe changes in groundwater quality and level in the regional aquifers.

Groundwater level data have been collected since 1998 but have not been analysed to estimate recharge in the area. Unfortunately, groundwater quality data were collected in only 1998 and 2017.

This study focusses on the characterisation of the crystalline aquifers of the Matlala Batholith, with a specific focus on the recharge to and flow within these aquifers. Although the study considers the batholith in its entirety, focus is placed on an area near the south-western boundary of the batholith outcrop where a wellfield (the Matlala wellfield) occurs and where several previous investigations have been conducted.

1.2 PROBLEM STATEMENT

People residing near the Matlala Batholith are dependent on the groundwater resource for their water supply. The Matlala wellfield occurs near the south-eastern perimeter of the batholith outcrop. This wellfield could in future supply the local residents with water for drinking and domestic purposes. However, the groundwater level response to rainfall and the groundwater flow patterns within the study area are not well understood, and the amount of water that enters and leaves the system is not well-defined.

This poor understanding of the crystalline aquifer system in the study area can negatively impact the sustainable use of groundwater in future. Some of the existing boreholes in the well field could in future be handed over to the community for domestic water supply, and the risk of aquifer depletion exists if over-abstraction from the aquifer takes place. It is therefore important to understand the underlying aquifer system in terms of recharge and groundwater flow to allow determination of a sustainable abstraction rate. This knowledge will guide future developments in the area which will likely depend on the groundwater resource.

1.3 RESEARCH QUESTIONS

This study attempts to address the following research questions:

- What is the general groundwater flow patterns in the aquifer system exploited by the Matlala wellfield?
- What is the rate of groundwater recharge to the Matlala Batholith aquifer?
- What are the dominant recharge mechanisms?
- What is the quality of the groundwater in the study area?

1.4 AIMS AND OBJECTIVES

Groundwater is currently pumped from the Matlala wellfield with little knowledge of the recharge to the aquifer system. The main aim of this study is to understand the water level response to rainfall and to estimate the recharge, and to understand the groundwater flow in the aquifer system in order to develop a general conceptual hydrogeological model of the area.

To address the aims and research questions of the study, the following objectives are identified:

- To gain an understanding of the characteristics of crystalline aquifers, as well as the groundwater quality and groundwater recharge mechanisms specific to crystalline aquifers.
- To examine water level variations in the Matlala Batholith aquifer and their relationship to rainfall.
- To estimate recharge to the Matlala Batholith aquifer as a percentage of the MAP.
- To develop a conceptual model representing the geohydrological condition of the Matlala wellfield based on ground observations and data analysis.
- To make recommendations for future studies to determine the sustainable abstraction rate from the aquifer.

1.5 RESEARCH METHODOLOGY

During the investigations, the following actions were taken: a literature review, data acquisition, data analysis, and data evaluation.

Literature review

- A review of existing literature on the characterisation of crystalline aquifers, groundwater quality and groundwater recharge specific to crystalline aquifers was performed, with a specific focus on the groundwater research previously conducted in the study area.

Data acquisition

Data required to achieve the objectives of the studies were obtained from the following institutions:

- Rainfall data from South Africa Weather Service (SAWS).
- Recently collected and archived groundwater level data and groundwater quality data from the Department of Water and Sanitation (DWS).
- Hydrological data of the Matlala Groundwater Monitoring Project from the project manager (Mr. du Toit, DWS).

- Existing groundwater information from GRIP (Groundwater Resource Information Project) and the National Groundwater Database (NGDB) of the DWS.

Data analysis

Analysis of the data entailed:

- Plotting groundwater level and rainfall data in an Excel spreadsheet in order to produce graphs to assist in evaluating the relationship between the two variables.
- Plotting geochemical data using the AqQA, software program to generate Piper diagrams that assist in classifying water types in the area.
- Estimating recharge using the chloride mass balance (CMB) method, water table fluctuation (WTF) method and cumulative rainfall departure (CRD) method.
- Creating a cross-plot of the static groundwater level and surface topography using an Excel spreadsheet to evaluate the general groundwater flow in the study area.
- Finally, compiling and collating all the results obtained to construct a conceptual geohydrological model of the Matlala Batholith.

Evaluation

- This phase of the project entailed a discussion of the results obtained from the data analysis, and their relation to studies previously conducted in the area. The evaluation aimed at addressing how future groundwater supply and management will be affected by the results of this study.

1.6 LIMITATIONS OF THE STUDY

Du Toit (2001) previously investigated groundwater occurrence around the Matlala Batholith and drilled 25 boreholes for his investigation. However, the last phase of the project, which would have focussed on determining the relationship of rainfall to groundwater level and developing a conceptual geohydrological model for the area, was not done, mainly due to financial constraints and vandalism of the boreholes. For the current study the author had to rely heavily on previously collected groundwater data. The limitations of this study related to data availability include:

- Groundwater quality data could be obtained for only two sampling events (1998 and 2017) separated by almost two decades. In addition, the available water quality data were obtained for different groundwater sites, which precluded an evaluation of temporal groundwater quality trends.

- In this study, three different methods are used to estimate groundwater recharge to the aquifer system of the Matlala Batholith. However, the available chemical and water level elevation data meant that different boreholes had to be used when applying the different estimation methods. No direct comparison of the estimation results could therefore be obtained for the boreholes used in this study.
- Although this study does encompass investigations over the entire Matlala Batholith, specific focus is placed on the Matlala wellfield near the south-eastern perimeter of the batholith outcrop where more data on groundwater elevations were available. The aquifer system near the wellfield may not be representative of the aquifer systems at other locations on the batholith.
- Due to vandalism of a rainfall gauge, no rainwater chloride data from the study area were available to use in the CMB method of recharge estimation and a value obtained from a previous publication had to be used.
- No long-term mean dry chloride deposition data were available for the study area. The dry deposition of chloride was therefore assumed to be zero during the recharge estimation with the CMB method.
- For recharge estimation using the CMB method, the chloride concentrations measured in different boreholes during a 1998 sampling event were used. During this sampling event, samples were collected at the depths of the main water strikes after purging of the boreholes. However, since most boreholes had multiple water strikes, and since no information on which water strikes were the main strikes is available, the measured chloride concentrations may be representative of different aquifers. The calculated recharge rates will therefore also represent recharge to the different aquifers at indeterminate depths.

1.7 DISSERTATION STRUCTURE

This dissertation is structured as follows:

Chapter 1 introduces the research framework, aims and objectives, research methodology, and limitation of the study, while **Chapter 2** gives a review of the literature for groundwater studies conducted in and around the study area, and general characterisation of the crystalline aquifers. It further gives an introduction to three different groundwater recharge estimation methods and their application in crystalline aquifers.

Chapter 3 gives a detailed description of the study area in terms of its regional setting, geological setting, topography and drainage, climate, geomorphology and water resources. In **Chapter 4**, the research methods used in this study to address the aims and objectives are described in detail. In

Chapter 5 the results of the study are presented and discussed, and compared to those obtained during previous investigations in and around the study area. A conceptual geohydrological model is developed for the Matlala Batholith near the Matlala wellfield by incorporating the recharge estimates, groundwater quality information, ground geophysical results, and geophysical borehole logging data. Different geological units and structures in the subsurface are identified. Possible recharge mechanisms are discussed.

Lastly, in **Chapter 6** conclusion are drawn from the results obtained from all different recharge estimation methods and their correlation as well as their relationship to groundwater chemistry and the underlying geology. A way forward is made for future studies that could assist in fully understanding the aquifer system in the area and determining a sustainable yield for the Matlala wellfield.

CHAPTER 2:
LITERATURE REVIEW

2.1 INTRODUCTION

Chapter 2 is a review of existing literature documentation on characterisation of crystalline aquifers, groundwater quality and groundwater recharge specific to crystalline aquifers, paying close attention to groundwater research previously conducted in the area of study. This chapter is divided into three sections: Section 2.2 reviews previous groundwater studies at the Matlala Batholith, Section 2.3 looks at the general characterisation of crystalline aquifers and lastly Section 2.4 gives a review of groundwater recharge estimation methods specific to crystalline aquifers, as well as different case studies of recharge investigations in and beyond South Africa.

2.2 PREVIOUS WORK CONDUCTED AROUND THE MATLALA BATHOLITH

A number of studies were conducted in the study area under the supervision of the Department of Water and Sanitation (DWS). These studies, however, investigated groundwater occurrence in the contact between the intruding Matlala Batholith and the host Goudplaats-Hout River Gneiss, with the main focus on borehole siting through geophysical surveys. In these studies, the components of aquifer recharge and water balance were not defined or considered during the borehole siting.

Research conducted by Du Toit (2001) indicated that groundwater is controlled by local structures and it mostly occurs in the fractured and weathered remnant roof sections. He further concluded that the main aquifer is 1) semi-confined and highly weathered and fractured, 2) a double porosity aquifer system with fractures that are highly permeable with low storage, against a rock matrix with low permeability and high storage. The main aquifer produced a maximum blow yield of >40 L/s.

More recently, Holland (2011) conducted a study that focused on the hydrogeological characterisation of crystalline basement aquifers in the Limpopo Province in South Africa. This research also included the Matlala area; however, the study was focused on a larger scale, covering 23 500 km^2 in the province. Similar to the study conducted by Du Toit (2001), Holland's study also indicated that groundwater occurrence in the area is structurally controlled and that the area has a complex geology, He concluded that the remnant roof section is important for recharge and groundwater storage and transmission of water to the fractured bedrock.

The groundwater levels in the area indicate that although local flow is controlled by fracture orientation, the regional flow gradient is towards the lower lying areas (Holland, 2011). The author discussed the conditions of the aquifer system at regional scales and concluded that most aquifers in

the crystalline bedrocks in Limpopo are semi-confined and capable of receiving diffuse recharge. This was also supported by the results presented by Du Toit (2001) with the Cl^-/HCO_3^--ratio indicating the presence of young, fresh water.

2.3 CHARACTERISATION OF CRYSTALLINE AQUIFERS

In order to understand the behaviour of crystalline basement aquifers, a thorough overview of their characteristics is required. This section focuses on reviewing the available literature regarding groundwater occurrence, flow, quality and also the development of the weathered and fractured aquifer system within crystalline rocks.

2.3.1 Groundwater occurrence

The occurrence and availability of groundwater depend on the hydrogeological characteristics of the underlying aquifer. For crystalline aquifers, however, the occurrence and availability of groundwater are irregular and are also affected by the lithology, surface water bodies, brittle tectonics, and aquifer properties that govern groundwater storage and movement such as porosity (n), hydraulic head (h), hydraulic gradient (i), hydraulic conductivity (K), transmissivity (T), storativity (S), and specific yield (S_y). According to Holland (2011) topography, lithology, surface water bodies, and brittle tectonics control the development of fractures and fault zones, as well as the nature and depth of the regolith. In crystalline bedrock, the composite aquifers are developed in the weathered overburden and fractured zones (Wright, 1992; Gustafson and Krásný, 1994; Holland, 2011).

2.3.2 Development of weathering and fracturing in crystalline aquifers

Weathering occurs when the rocks, soils, and minerals are in contact with the earth's atmosphere and water. The weathered material is reduced in size and its original form is changed due to the erosion of some of the original material. Jones (1985) and Wright (1992) indicated four important factors that contribute and influence the weathering of crystalline rocks, namely:

- **The presence and stress components of fractures**. Generally, granitic rocks do not have weakness planes. Weathering in these rocks occurs quite slowly compared to other layered rocks. However, in cases where these rocks are fractured, weathering is very common. When water enters the fractured zones, if the fractures are not interlinked, the water is trapped in the fractures and this results in a longer reaction time between the water and the silicate minerals in the granites. With time, the silicate minerals are converted to clay, which eventually results in the rock cracking. Once the cracks are formed, water can flow and is trapped easily in the rocks.

- **Geomorphology of the terrain**. The geomorphology and topography of the terrain have a large influence on weathering, as well as on the direction of groundwater flow. Landforms with a steeper gradient have much more active weathering than those on low-lying areas. As rainfall, strong winds, and tectonic activities occur, physical weathering takes place, and the boulders roll down the hill and abrade the rocks that are exposed on the surface. As this process occurs, the rocks wear away due to the friction caused between them. The rocks disintegrate, which forms cracks and as a result water will flow through the rocks and some water will be trapped in the rocks.
- **Temperature and occurrence of groundwater**. Temperature affects the type and rate of weathering in different conditions. High rainfall and temperature influence chemical reactions, as explained below (Figure 2.1). In colder regions, however, frozen water in joints and fractures expands and causes the rock to disintegrate, resulting in more cracks in the rock. The open cracks can serve as a flow medium for water and some of the water can be trapped and stored within the rock mass.
- **The mineral content of the basement rock**. The mineral content affects the rock's susceptibility to weathering. Rocks weather differently depending on their mineral content and the surrounding environment, as shown in Figure 2.1 where Bowen's reaction series is presented schematically.

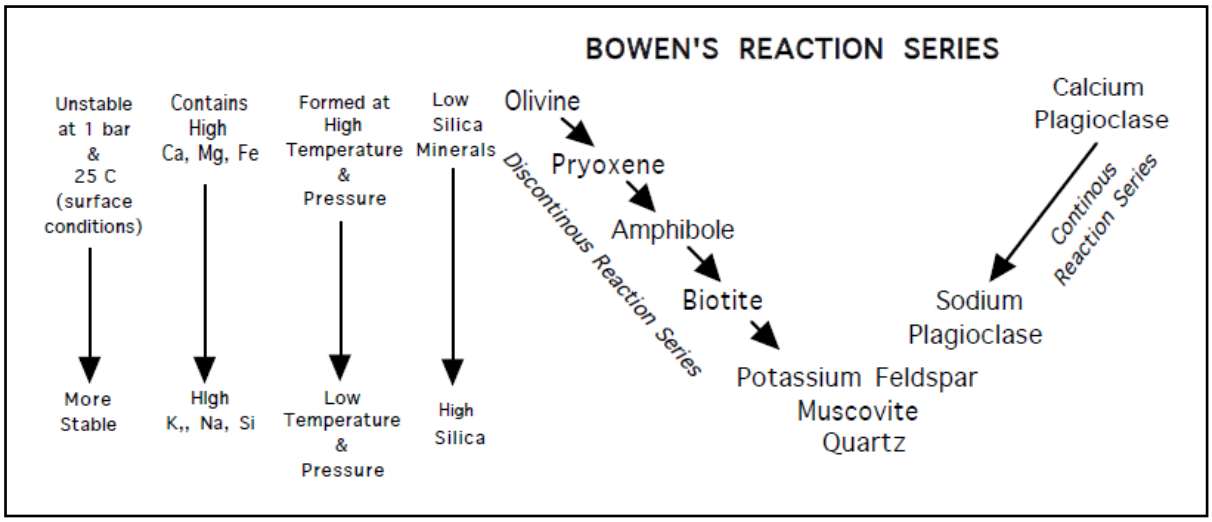

Figure 2.1: Bowen's reaction series (Bowen, 1922)

Following Bowen's reaction series, minerals are stable at the temperature at which they form. If minerals that form at higher temperatures are exposed to the surface (water), they weather faster compared to low-temperature minerals on the surface. Granitic rocks consist of three main minerals, namely alkali feldspar (silica and alumina), plagioclase feldspar (sodium and calcium), and quartz, as well as small and variable amounts of hornblende and biotite mica, which are low-temperature

minerals. As the silicate minerals in the rocks come into contact with water, they are converted to clay. As the silicate grains decay and cracks develop in the rock with time as the process occurs, more cracks develop and this results in the disintegration of the rock, which leads to the weathering of crystalline rocks.

Furthermore, Twidale and Romaní (2005) indicated that differential subsurface weathering (deep weathering) is one of the stages that attribute to the development of crystalline terrains. The process results in irregular weathering because of chemical weathering, which occurs due to a reaction between water and rocks as well as the physical disintegration of the rocks. The prolonged deep weathering produces unconsolidated weathered material (McFarlane, 1991; Taylor and Howard, 1998, 2000), as shown in Figure 2.2.

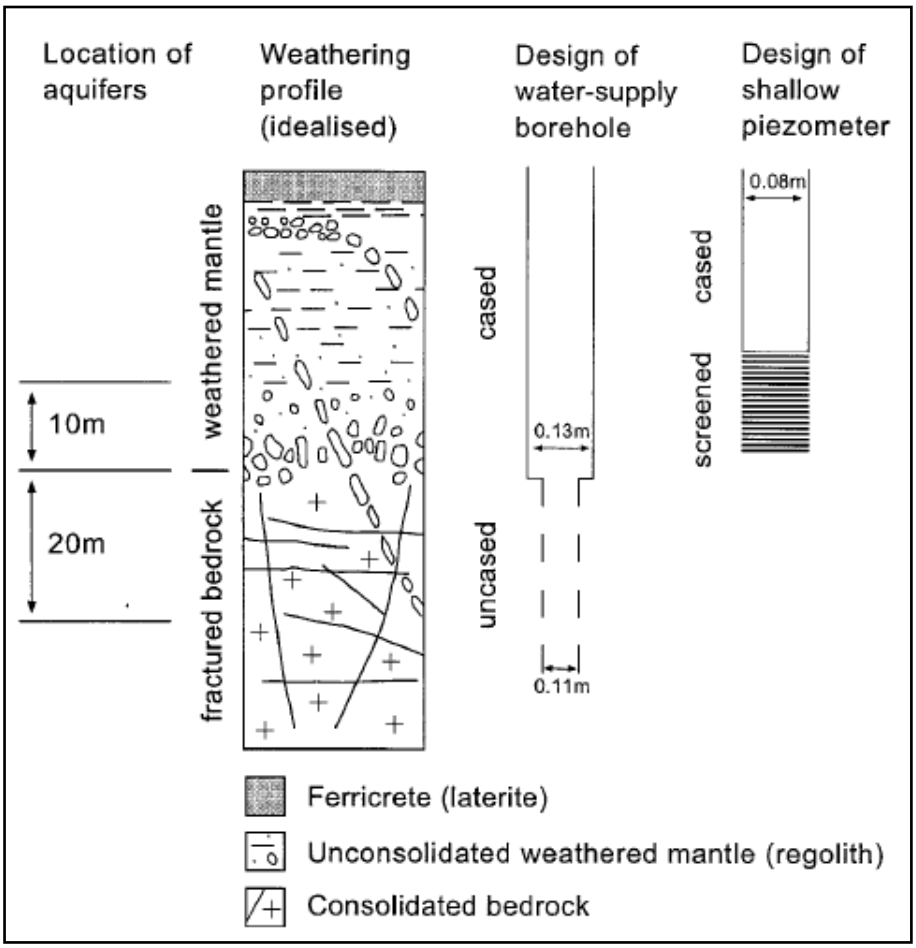

Figure 2.2: Vertical representation of weathered crystalline aquifer, including aquifer location (depth) and well construction (Taylor and Howard, 2000)

Fracturing, on the other hand, occurs as rocks are subjected to stress or force. Fractures are surfaces along which the rocks have broken. Unlike faults, fractures do not show any movement parallel to the fracture surface. In granitic terrains, fractures are mostly important for the movement of water in the bedrock.

2.3.3 Groundwater flow, hydraulics, and storage

Groundwater flow, hydraulics, and storage in crystalline aquifers are very complex because of the spatial arrangement (i.e., varying lithology and fracture network) of these aquifers. Steyl (2011) indicated that the irregular distribution of high and low transmissivity zones complicates the estimation of groundwater hydraulic parameters. The general groundwater flow in crystalline aquifers is suggested to be in the shallow weathered and fractured zones of the aquifer, approximately up to 50 m below ground level mainly because in these zones the permeability is high and the overlying regolith acts as a storage medium (Du Toit, 2001; Holland, 2011).

It is also important to note that water will not always flow only in the direction of the fracture; it can also be influenced by the effects of channelling (Dippenaar *et al*., 2009). Channelling occurs when the water in the fractures prefers to flow along a certain path, resulting in highly irregular flow velocities and flow paths that are difficult to predict (Krásný and Sharp, 2007) (see also Figure 2.3).

According to Tsang and Tsang (1987), in situ stress causes all fractured flow to be channelled at depths greater than 500 m to 1 000 m. As water infiltrates into the soils, some of the water percolates through fractures that are exposed on the surface to the saturated zone. As recharge takes place, these fractures directly feed the saturated zone. The weathered and fractured regolith acts as a reservoir because of the associated double porosity, and as it is recharged with water, it feeds water to the underlying bedrock through the fractures (Adams *et al*., 2003).

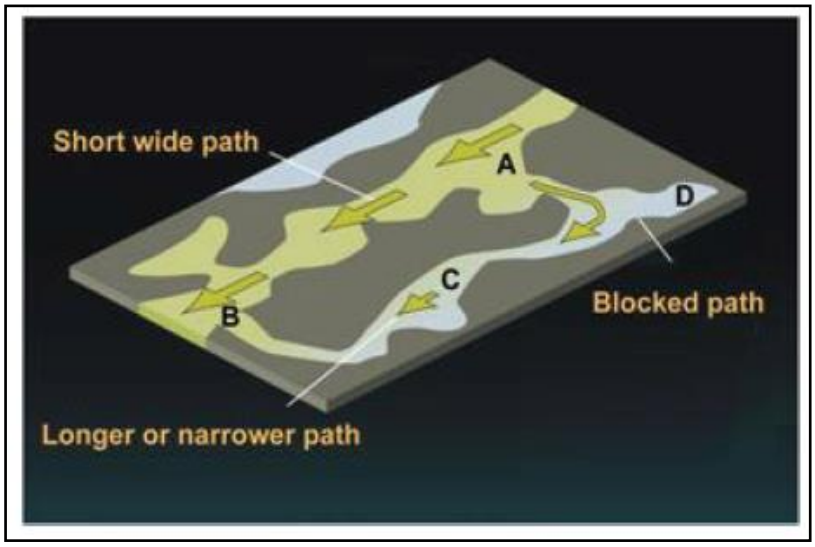

Figure 2.3: Flow in fractured rock aquifers (Kirchner, 2009)

According to Adams *et al*. (2003), fracturing and weathering decrease with increasing depth due to the increase in lithostatic pressure, which results in the closing of fractures and resistance to groundwater flow. Bisson and Lehr (2017) indicated that fractured rocks that are likely to transmit a greater volume of water will:

- receive adequate recharge,
- have a high density of fractures,
- have fractures with wide apertures,
- be parallel to the gravitational gradient, and,
- be overpressured.

Furthermore, Kellett and Bauman (2004) also indicated that not all fractures intersected during drilling will yield water, but rather that regional flow in bedrocks will only occur within major interconnected fracture systems. These hard rock aquifers have negligible matrix porosity and matrix permeability, which contribute considerably to their inherent small storage capacity (Clark, 1985; Gustafson and Krásný, 1994) According to Rebouças (1993), water within the underlying unweathered crystalline rocks is stored in isolated interconnected fractures, joints, and fissures controlled by regional tectonism.

Chilton and Foster (1995) illustrated the variation in the hydraulic properties of the typical lithologies found in the weathered and fractured regolith as well as the solid bedrock in the crystalline aquifers (Figure 2.4). According to Acworth (1987), the clay in the regolith reduces the permeability of the regolith and increases its porosity. The regolith acts as a reservoir; when it is fully saturated with water, it slowly feeds water downward into fractures in the bedrock, as illustrated in Figure 2.5. Figure 2.4 also indicates that the porosity of the weathered material decreases with depth until the fresh rock is reached. The unweathered fresh bedrock is permeable only where fractures are present (Gustafson and Krásný, 1994). The fractures in the bedrock significantly increase the hydraulic conductivity because they are the main flow conduits in the whole system, but fractures filled with lower permeable material than the host rock restrict the flow of groundwater. Unlike sedimentary rock aquifers that have primary porosity, crystalline aquifers have secondary porosity caused by the weathering and fracturing of rocks, which result in limited flow and storage of water.

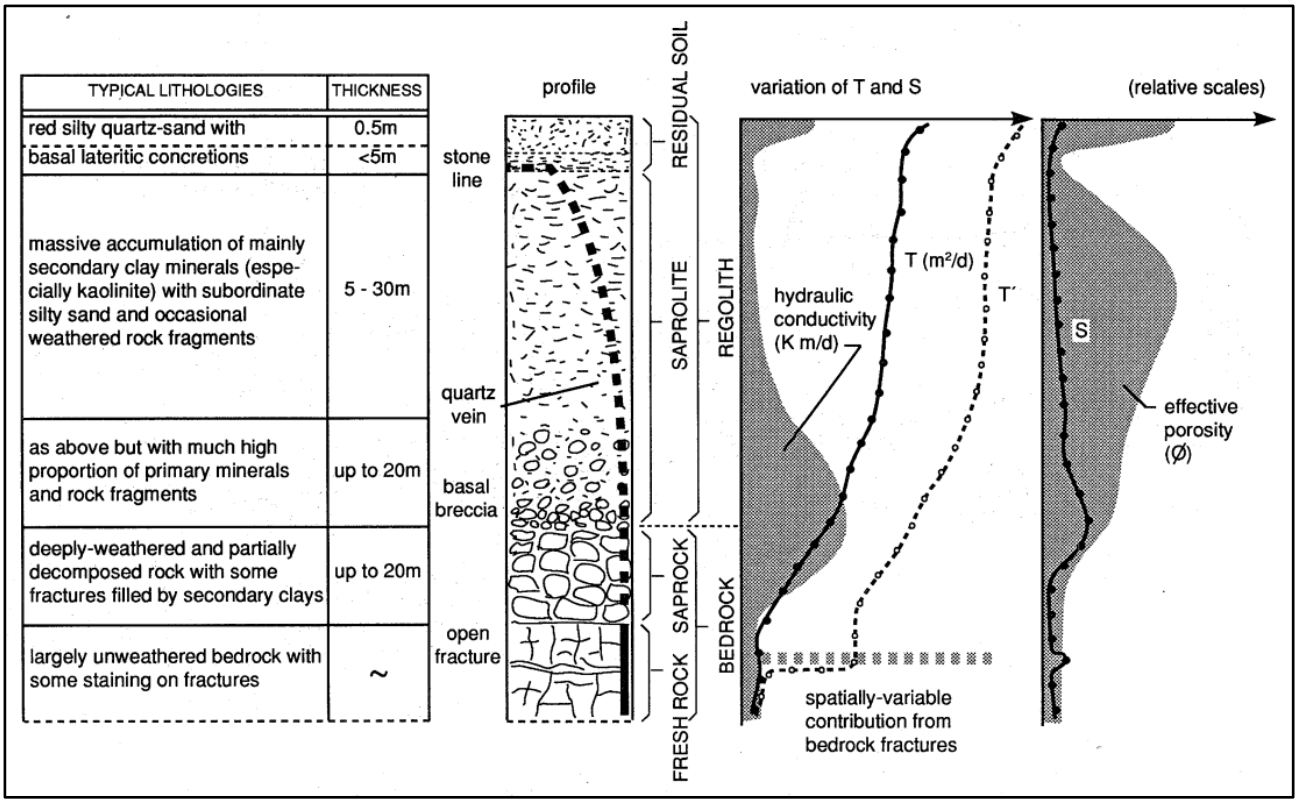

Figure 2.4: Permeability and porosity in basement aquifers (Chilton and Foster, 1995)

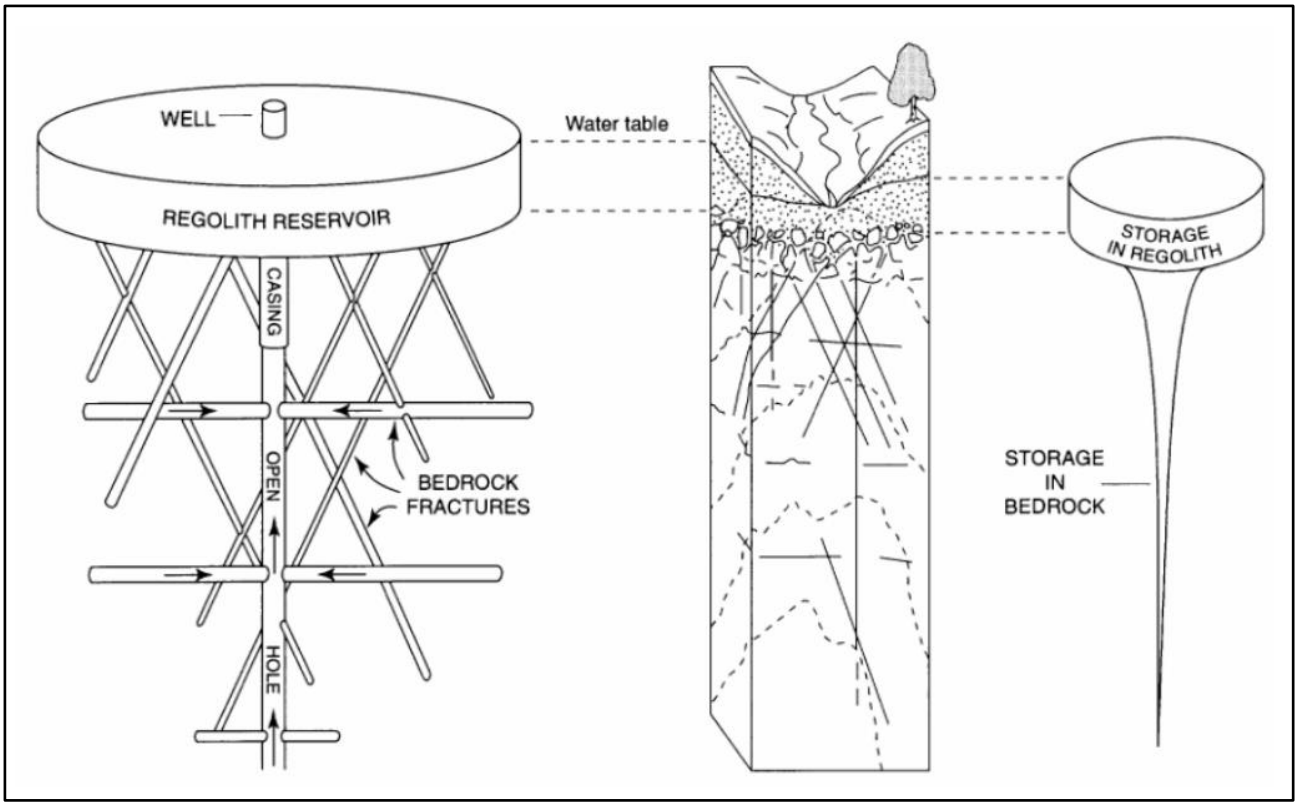

Figure 2.5: The reservoir-pipeline conceptual model of the Piedmont groundwater system and the relative volume of groundwater storage within the system (Baloochestani, 2008)

2.3.4 Groundwater quality

The groundwater quality for crystalline aquifers is considered to be generally acceptable (Clark, 1985; MacDonald and Davies, 2000; Chimphamba *et al*., 2009) because only small amounts of minerals are dissolved when water is in contact with crystalline rocks (containing insoluble minerals) and the water flows rapidly over a short flow path. The water of these aquifers typically has neutral to slightly acidic pH and is low in salinity.

Geology, topography, inflow of water (rainfall, recharge, and surface and groundwater interaction) and outflow of water (evaporation, and over-abstraction of boreholes) can influence the quality of groundwater in crystalline aquifers. Titus (2002) also identified hydraulic conductivity as a factor that influences groundwater quality/chemistry because the rate at which groundwater flows has an influence on the reaction rate with which minerals can influence groundwater quality.

Geology plays a major role in water quality in cases where weathering is common. For example, in the central Namaqualand area, fluoride is generally high as a result of geology (dissolution of fluoride-bearing minerals); however, topography and hydraulic properties also influence the presence of fluoride in the same area. It was found that groundwater in areas with a steeper gradient had lower fluoride concentrations than the groundwater from areas with gentle slopes, influenced by the rate of groundwater flow (Adams *et al*., 2009). Another example is in the Dowa West Integrated Project area in Malawi, where a groundwater study was undertaken by Smith-Carrington and Chilton (1983). The study was conducted in one village on different boreholes which are a few hundred metres away from each other, but the groundwater quality results obtained varied greatly, with some boreholes having an electric conductivity (EC) of 4 000 µS/cm, while others recorded values around 1 000 µS/cm.

According to Pietersen (2009) the poor quality of groundwater in some crystalline aquifers is associated with low rainfall, because low rainfall results in slow circulation of water. Furthermore, in most semi-arid regions, the rate of evaporation is higher than that of the precipitation, resulting in the accumulation of high levels of soluble salts on the surface. After rainfall events, these salts can be flushed into the saturated zone and affect the groundwater quality. Shallow aquifers and exposed weathered and fractured bedrock aquifers are furthermore highly susceptible to natural and anthropogenic pollution affecting the water quality.

2.4 GROUNDWATER RECHARGE ESTIMATION

Recharge estimations are important for the management of the groundwater resources. However, due to spatial factors such as geology, soil types, topography, precipitation, and abstraction, major challenges are experienced during the estimation of recharge. Moreover, in crystalline terrains the recharge estimation is more complex because of the heterogeneous conditions of randomly distributed

fractures and narrow openings in the rocks. For this study groundwater recharge estimation will conducted using the tracer and physical methods. Due to the purpose of study and availability of data, only one tracer method (the chloride mass balance (CMB) method) and two physical methods (the cumulative rainfall departure (CRD) and water table fluctuation (WTF) methods) will be considered.

The CMB, CRD, and WTF methods remain practical and reliable approaches of estimating groundwater recharge (Allison and Hughes, 1978, Sophocleous, 1991) and these methods can be applied with high certainty as they have been in use for more than three decades in arid and semi-arid region in southern Africa (Xu and Beekman, 2003). These methods estimate groundwater recharge by linking information from precipitation, the unsaturated zone and the saturated zone. Researchers have studied and used these methods to estimate groundwater recharge to understand and manage the geohydrological system (Eriksson, 1960; Wood and Sanford, 1995; Bazuhair and Wood, 1996; Holland, 2011).

2.4.1 Recharge estimation methods

This section is limited to a discussion of groundwater recharge estimation methods applicable to arid and semi-arid regions, namely the CMB, WTF and CRD methods.

2.4.1.1 The chloride mass balance (CMB) method

This method is a tracer method which investigates the chloride concentration of the precipitation in a study area and compares it to the chloride concentration of the groundwater. Water that is evaporated from the unsaturated zones causes an enrichment of the hydrogeochemical composition, and a resulting change in the chloride concentration. The method is quick and inexpensive to apply and can be used in both saturated and unsaturated zones at a scale ranging from 0.1 m^2 to 10 000 m^2. It can estimate recharge rates ranging from 0.05 mm to 300 mm per year (Scanlon *et al*., 2002). In the unsaturated zone, the method gives site-specific recharge estimates (up to 1 m^2). The principle in both the saturated and unsaturated zones is that the amount of chloride that enters the system is equal to that which leaves the system; neglecting any surface runoff (Selaolo, 1998); however, in the unsaturated zone alone the principle is that the drainage in the zone is inversely proportional to the chloride in the pore water (Beekman *et al.*, 1996).

The natural concentrations of chloride and chloride-36 have been and are still in use for recharge estimation in semi-arid to arid regions (Allison *et al*., 1985; Gee and Hillel, 1988; Phillips, 1994; Cook *et al*., 2001), among other environmental tracers such as deuterium, tritium, oxygen-18, and bromide. Chloride and chloride-36 are often used, mostly because they are less expensive compared to the other environmental tracers (Allison *et al*., 1994). The method is based on the mass balance of chloride in precipitation and in the groundwater system; it equates the mass balance of chloride at the

ground surface to the saturated zone where evapotranspiration does not take place. The method is represented by Equation 1 (Kinzelbach and Aeschbach, 2002).

$$R_t = \frac{P * Cl_p + D}{Cl_{gw}} \quad 1$$

where R_t is the total groundwater recharge (mm per time), P is the precipitation (mm per time interval), Cl_p is the chloride concentration in the precipitation (mg/L), D is the dry deposition (in mg per m^2 per time interval) and Cl_{gw} is the chloride concentration in groundwater (mg/L).

The method can be used in three different approaches, which are:

- Estimating the moisture flux using the chloride concentration of rain and soil moisture in the unsaturated zone;
- Estimating the average groundwater recharge with the chloride concentration in the saturated zone; and
- Defining the recharge mechanism by comparing the first two approaches.

The success of the method is based on certain assumptions:

1) Precipitation is the only source of chloride in the groundwater system

   According to (Dettinger, 1989), it is assumed that precipitation is the only source of chloride when estimating the mean annual recharge using the CMB method in arid and semi-arid areas. This means any other sources of chloride such as weathering or human activities are ignored. Low rates of recharge are generally associated with high chloride concentrations and vice versa.

2) Chloride is stable in the system

   The chloride concentration increases in the soil water through the root zone as evapotranspiration takes place. It is assumed that the chloride in the system cannot be taken up by plants and it therefore remains constant below this depth (Scanlon *et al.*, 2002).

3) Chloride cannot be replenished in the basin.

4) There is no surface runoff leaving the aquifer area.

5) Steady-state conditions are maintained in long-term precipitation and chloride concentration in that precipitation.

6) Groundwater evaporation does not occur upstream from the sampling point.

For the successful application of the method, the following are required:

- The groundwater chloride concentration.

- The chloride concentration in soil moisture, and the dry chloride deposition data.
- The mean annual precipitation.
- Undisturbed soil profiles.

The method is applicable in areas where the annual rainfall exceeds 600 mm with a terrain that is naturally permeable.

2.4.1.2 Physical methods

These methods involve taking direct measurements of water levels from a site. The estimates from these methods are easy to calculate and the results obtained can be used to calibrate models of other recharge estimation methods. The disadvantages of these methods are that 1) the results obtained are local for a specific site, structure, soil type, and vegetation, and 2) in arid regions recharge is not uniform.

The estimation of recharge through water balance involves comparing the input (precipitation) and output (evapotranspiration, runoff, and abstraction) of water in a system and the difference is regarded as the estimated recharge (Kinzelbach and Aeschbach, 2002).

2.4.1.2.1 The cumulative rainfall departure (CRD) method

The principle of the CRD method is that the water level response in an aquifer is proportional to the cumulative rainfall departure (Van Tonder *et al*., 2001). According to Bredenkamp *et al*. (1995), a dynamic equilibrium can be reached between the average annual precipitation and the groundwater level response despite the variation in annual precipitation. The method is represented by Equation 2 (Beekman and Xu, 2003):

$$CRD_i = \sum_{i=1}^{N} R_i - \left(2 - \frac{1}{R_{av} i} \sum_{i=1}^{N} R_i\right) i R_t \qquad 2$$

where R_i is the rainfall [L/T] for month i and R_t is a threshold value representing aquifer boundary conditions. R_t may range from 0 to R_{av}, with 0 representing a closed aquifer (no outflow), and R_{av} representing an open aquifer system (for instance controlled by spring flow). The cumulative rainfall average would conform to R_{av} if R_i does not show a trend ($R_t = kR_{av}$). This means that any change in the monthly water level is as a result of the CRD if the other stress is constant. If the cumulative departure is positive the groundwater level will rise and if the cumulative departure is negative this will result in a decline to the groundwater level, since:

$$rCRD_i = S_y\left[\Delta h_i + \left(Q_{pi} + Q_{out}\right)/\left(AS_y\right)\right] \qquad 3$$

where r is that fraction of a CRD which contributes to recharge, S_y is specific yield, Δh_i is the water level change during month i [L], Q_{pi} is the groundwater abstraction rate [L^3/T], Q_{out} is the natural groundwater outflow, and A is the recharge area [L^2].

The CRD method relies on easily obtainable data (water table hydrographs, rainfall, area, etc.). Another advantage of this method is that the changes in water level may be from other causes such as abstraction and not only a response to rainfall. The shortcomings of the CRD method are that it is only applicable to unconfined aquifers and not to deep (multi-layered) aquifers, is sensitive to the specific yield, requires estimates of the total inflow and outflow to the aquifer, and requires long-term data recorded over time periods of years.

2.4.1.2.2 The water table fluctuation (WTF) method

The principle of the WTF method is that the groundwater level response is proportional to recharge or discharge with the extent of the influence of the two components being controlled by the specific yield (S_y) (Bredenkamp et al., 1995, Varni *et al*., 2013). According to Beekman and Xu (2003), this method is inexpensive, easy to use, and accurate when applied in semi-arid areas. The method uses the storage parameter to link the water level response to the groundwater recharge. This method uses hydrographs, which are constructed using the change in water levels at a certain location over a period of time (Prathapar and Sides, 1993). The method is represented in Equation 4 (Healy and Cook, 2002):

$$R = \Delta S_{gw} = S_y \frac{dh}{dt} \sim S_y \frac{\Delta h}{\Delta t} \qquad 4$$

where R is the recharge, S_y is the specific yield of the aquifer [-], Δh is the water table rise [L], Δt is the time period [T] within which the rise occurred. The rise in the water level (Δh) is expressed as the difference between the peak of the water level rise and the extrapolated antecedent recession curve at the time of the peak.

This method calculates the ratio of water table rise to total rainfall in the area of interest. According to Duke (1972) and Sophocleous (1985), after a rainfall event the height at which the water table rises gives an estimate of the specific yield (S_y) through the open pore spaces in the unsaturated zone and S_y can vary with the depth of the water table. In order for the recharge estimate to represent the whole area of interest, data from multiple wells must be used. However, there is some uncertainty related to the estimation of specific yield of the aquifer when using this method (Healy and Cook, 2002),

The method is mostly applicable in wet climate zones where the difference between rainfall and evaporation is small and where water level fluctuations are more pronounced. The shortcomings of

this method are that it is less applicable in areas where depth to groundwater is significant, and where the inflow, outflow, and S_y are unknown.

2.4.2 Recharge studies in crystalline aquifers

Recharge is referred to as the portion of rainfall that reaches the saturated zone; it is dependent on climate, geomorphology, geology, soil content, moisture, and vegetation. For crystalline bedrock, the soil cover and weathered zones are important for recharging the aquifer. Water from rainfall infiltrates the soil (characterised by high storage capacity and high recharge probability) and weathered zones (moderate storage and moderate recharge probability) and is then transmitted through the interconnected fractures (low storage and moderate recharge probability) directly to the saturated zone. Figure 2.6 illustrates how recharge takes place in crystalline aquifers. These processes are described below with reference to Figure 2.6.

- **Point 1**: Water on the ground surface infiltrates the weathered bedrock, and some of the water on the surface runs off to the low point of the topography. Water in the weathered bedrock then penetrates to the underlying rocks through the interconnected fractures and flows to the saturated zone.
- **Point 2**: Rainwater that reaches the alluvial zone is absorbed, and once the alluvial zone is saturated, water then penetrates the underlying weathered bedrock and the process continues as explained in Point 1.
- **Point 3**: Water infiltrates the fractured bedrock and some runs off on the ground surface to the lower-lying areas, which in this case is Point 2. The fractures can be responsible for surface and groundwater interaction because some of the fractures are connected to the ground surface down the hill, which results in water flowing from the fracture to the ground surface and then running off to Point 2. The water in the fractured bedrock then flows through interconnected fractures to the saturated zone.

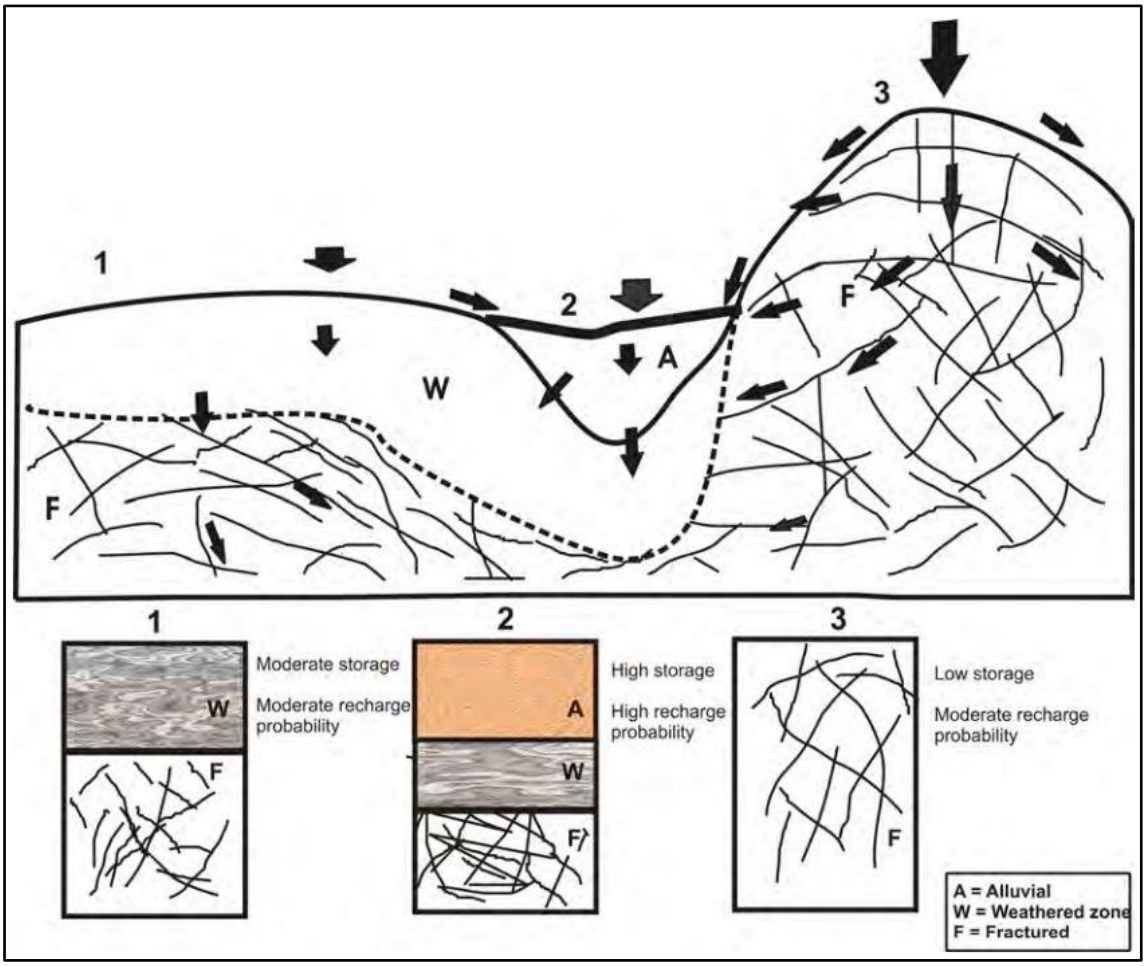

Figure 2.6: Conceptual recharge model of basement aquifers (Adams *et al.*, 2003)

According to Harte and Winter (1993), four factors influence recharge patterns in crystalline bedrocks, namely:

- the relief of the land and bedrock surfaces above groundwater discharge areas,
- lateral trends in bulk-rock horizontal conductivity,
- local topographic features, and,
- local drift stratigraphy.

In other words, recharge can occur in different ways, depending on the conditions of the area. Recharge can be direct, indirect, and/or even localised (Lerner *et al*., 1990). In semi-arid regions such as the Limpopo Province, Beekman and Xu (2003) indicated that there are several conventional methods for recharge estimation that can be considered, provided that assumptions associated with that particular method are taken into consideration.

Adams *et al*. (2003) conducted recharge investigations in Namaqualand, South Africa, a semi-arid region, underlain by basement rocks with a fractured and weathered aquifer system. The authors used different recharge estimation methods, including the CMB method, the CRD method, the saturated

volume fluctuation (SVF) method, the statistical approach, and the geographical information systems (GIS) approach. The selection of the methods was based on the availability of data. The data included water levels, rainfall information, borehole abstraction rates, water chemistry, and the position of boreholes.

Although the conditions of the area did not meet all the assumptions associated with the CMB method (see Table 2.1), the method was used for a first approximation of recharge due to its simplicity. According to Cook (2003), the CMB method should be used with caution when working with fractured rock aquifers due to the heterogeneity of the aquifer media in correspondence with the associated different porosities. Banks *et al*. (2009) also indicated that when using this method, the rate of recharge obtained should be considered only as a minimum rate due to the addition of other sources of chloride that may have resulted due to the weathering of rocks. The CRD method, however, seemed to be the most promising method in this study area, mainly because the method accommodated most of the data obtained (water level and pumping rates). This led to the conclusion that the use of different recharge estimation methods provides more accurate results compared to the use of only a single method.

Table 2.1: Assumptions when using the CMB method and the situation in Namaqualand (Adams *et al.*, 2003)

Assumption	**Met?**
Chloride in groundwater originates only from precipitation (no unmeasured chloride mass from overlying, underlying or adjacent aquifers and no unmeasured run-on occur).	×
Chloride is conservative in the system.	✓
The chloride mass flux has not changed over time.	?
There is no recycling or concentration of chloride within the aquifer.	×
No evaporation of groundwater occurs upgradient from the groundwater sampling points.	?
The adsorption of chloride in soils and the vegetation uptake is considered negligible.	✓

× = not met; ✓ = met; ? = uncertain

Internationally, there is a vast amount of literature reviews on groundwater recharge in basement aquifer. In Zimbabwe alone, different studies have been carried out by different authors in attempts

to estimate groundwater recharge into the crystalline basement aquifers. Values obtained ranged between 4% and 22% of the annual rainfall (Table 2.2). Houston (1992) reviewed the hydrogeology of crystalline basement aquifers in Zimbabwe and Nigeria. He used a combination of baseflow analysis, chloride balance and soil moisture methods to determine recharge rates of between 10% and 17% of the annual rainfall (950 mm) in Nigeria and 2% to 5% of the annual rainfall (600 mm) in Zimbabwe. He indicated that in the south-east of Zimbabwe (Masvingo Province), recharge was almost negligible (ranging between 0.05% and 0.5%) where annual rainfall was less than 400 mm.

Smith-Carrington and Chilton (1983) assessed the groundwater resource in Malawi by using a catchment water balance, stream hydrograph analysis, flow nets as well as groundwater level fluctuation and obtained recharge values between 1% and 5% of the annual rainfall for the weathered basement aquifer and 1% to 7% for the alluvial aquifer.

These results suggest that as annual rainfall decreases, groundwater recharge, as a percentage of annual rainfall, also decreases.

Table 2.2: Groundwater recharge estimates done in Zimbabwe (Nyagwambo, 2006)

Area	Estimated recharge (mm/a)	% of MAR	Estimation method	Author(s)
Nyatsime Catchment	131.0	16.4	Water table fluctuation	Mudzingwa (1998)
	130.0	16.3	Chloride mass balance	
	74.0	9.3	Reservoir method	
	162.0	18.0	Flux analysis	
Marondera Grasslands	136.0	15.1	Chloride mass balance	McCartney (1998)
Research Catchment Chiweshe, Mazowe	185.0	20.5	Chloride mass balace	Jarawaza (1999)
	190.0	22.0	Water table flactuation	
Research Catchment Chiweshe, Mazowe	71.6	8.5	Chloride mass balance	Mjanja (2000)

Nyagwambo (2006) conducted a detailed groundwater recharge study in the Nyundo catchment located in Zimbabwe. The catchment is dominated by Karoo sediments, underlain by basement rocks (Nyagwambo, 2006). The topography of the area is flat to gentle, with over 60% of the area used for farming. The main objective of the study was to investigate how the common recharge estimation methods are applicable in crystalline aquifers and also to develop a different method of estimating recharge in these aquifers by using simple field hydrological and physical data.

The methods selected to investigate recharge were as follows: 1) water balance (WB) method, 2) water table fluctuation (WTF) method, 3) chloride mass balance (CMB) method, and 4) groundwater flow modelling using MODFLOW. The WB, WTF, and CMB methods were selected because they

have been widely used in the Southern African Development Community. The WB method has a limitation that the method generally yields better results where annual rainfall was higher than potential evaporation (Lerner *et al*., 1990; Simmers *et al*., 1997). However, for this study area, the long-term daily average rainfall of the area was generally lower than the potential evaporation. Nevertheless, recharge was estimated over a shorter period using water balance at small time steps where rainfall was higher than evaporation and adding all the values together to determine recharge for a longer period. The results from the WB method revealed that more than 80% of recharge into the aquifer system occurred through preferential flow.

The CMB method was used to estimate the magnitude of recharge and also address the factors influencing the estimation. The magnitude of recharge was determined by estimating the chloride concentration in rainfall and in the groundwater. This was done by collecting samples daily during the 2000/1 and 2001/2 rainfall season. The average chloride concentration results from rainfall were 1.10 mg/L and 9.15 mg/L in groundwater, and the annual recharge rate was estimated at 12% of the annual rainfall. According to Nyagwambo (2006), it is evident that recharge estimation for the Nyundo catchment was also influenced by other factors, as can be seen through the chloride deposition which is higher compared to other values obtained from other crystalline basement aquifers in Zimbabwe (Table 2.3).

Table 2.3: Groundwater chloride concentrations in basement aquifers in Zimbabwe (mg/L) (Nyagwambo, 2006)

Location	Min	Mean	Max
Buhera	0.5	1.4	31.9
Chikomba	3.9	7.9	15.2
Goromonzi	0.2	1.5	68.2
Harava	2.0	5.7	290.0
Hwedza	1.0	5.8	36.0
Marondera	1.0	3.3	45.0
Murehwa	2.3	5.5	94.2

A minimum of 4.3 mg/L, maximum of 25.5 mg/L and mean of 9.15 mg/L were obtained in the groundwater chloride concentration. Nyagwambo (2006) suggested that these higher values correlate with land use, through the use of fertilisers to enhance the productivity of the sandy soils in the area. The relationship between rainfall and recharge, residence time of groundwater as well as the total annual recharge in the catchment was determined using the WTF method. This was based on the

selected specific yield value. The specific yield is an important parameter when using the WTF and for this study, it was based mostly on values obtained from literature. The method estimated a recharge magnitude of between 2% and 28% of the annual rainfall that occurs through both preferential and diffuse flow and showed that groundwater resides in the unsaturated for approximately 3 to 4 months.

In conclusion, the methods used in the area did not give the same distribution of groundwater recharge because of the different limitations and assumptions associated with them. The WB and WTF method gave clues when groundwater recharge occurs for daily time steps, while the CMB gave results for annual recharge rates. Table 2.4 shows the overall comparison of the methods. The WB method underestimated recharge and the WTF gave middle ranges, while the CMB overestimated groundwater recharge. These methods revealed that the overall groundwater recharge in the area is between 8% and 15% of the annual rainfall.

Table 2.4: Average groundwater recharge estimates from different methods over different time intervals (Nyagwambo, 2006)

Method	Recharge estimate (mm/time unit)								
	Year			Month			Day		
	Max	Ave	Min	Max	Ave	Min	Max	Ave	Min
Water balance (WB)	78.0	62.1	30.8	22.9	4.8	1.0	1.5	0.2	0.0
Chloride mass balance (CMB)	235.8	94.6	39.3	-	-	-	-	-	-
Water table fluctuation (WTF)	212.5	86.2	15.6	30.1	7.2	2.0	8.2	0.5	0.0

2.4.3 Recharge studies around Ga-Matlala

The water that enters the subsurface from different surface and subsurface sources recharges the groundwater system. Recharge to groundwater resources in the study area is dependent on effective rainfall. After runoff, evaporation, and transpiration, the water that infiltrates the ground to the saturated zone is responsible for recharging the groundwater system. The study area generally has no perennial rivers that can also recharge the groundwater through surface and groundwater interaction (baseflow).

Very few groundwater recharge studies have been conducted in the area of interest. The Groundwater Assessment Projected II (GRA II) (DWAF, 2006) dataset, which is based on the chloride method, depth to groundwater, land cover and slope assumes a regional recharge estimate of 3% of the MAP for the A62E quaternary region.

In a study conducted by Holland (2011) on crystalline basement aquifers within the Limpopo Province, the CMB and CRD methods were used to estimate recharge in the Limpopo water management area (WMA), in which the study area of the current research project is located. For the CMB method, local recharge was estimated using the concentration of chloride in groundwater and rainfall, and the Kriging technique was then used to interpolate the results obtained from the CMB. It was found that active recharge zones are associated with main surface water drainage divides on higher ground. Table 2.5 shows the results obtained, including that the area has an average recharge rate of 0.4% of MAP.

Table 2.5: Recharge rates based on the CMB method (modified from Holland, 2011)

Locality	Annual rainfall (mm)	Chloride conc. (mg/L)		Estimated average recharge	
		Cl_{rf}	Cl_{gw}	mm/year	% of MAR
Chloe (Matlala)	365	0.6	147.3	1.5	0.4

With the CRD method, the Excel-based recharge calculation spreadsheet developed by Xu and Van Tonder (2001) was used to simulate recharge for selected monitoring stations. The simulated CRD recharge rate was 1.4% of MAP, as indicated in Table 2.6.

Table 2.6: Recharge rates based on the CRD method (modified from Holland, 2011)

Locality	Station	Date		Estimated recharge (% of MAR)	Area (km^2)
		Start	End		
Chloe (Matlala)	A6N0586	Mar 06	Aug 09	1.4	15

The large difference in the recharge values was due to the limited period of monitoring for the CRD simulation, compared to the longer and more extensive period of monitoring with the CMB method.

2.4.4 Conclusions

This chapter examined the available literature on the characterisation of crystalline aquifers, groundwater quality and groundwater recharge specific to crystalline aquifers. The chapter focussed on groundwater recharge in crystalline aquifers, identifying and describing suitable groundwater recharge estimation methods which can be applicable to the current study area. The review identified no direct recharge studies carried out in the current study area; however, several studies have been conducted in nearby regions.

CHAPTER 3:
SITE DESCRIPTION

3.1 INTRODUCTION

This chapter provides a description of the study area which includes the Matlala Batholith. The main focus of this chapter is to understand and describe the following aspects of the study area: its regional setting, the regional geology, the geomorphology of the area, the vegetation and land use in the area, the climate of the area, and the different water resources within the study area.

3.2 REGIONAL SETTING

The Matlala Batholith is located approximately 40 km north-west of Polokwane and 50 km north of Mokopane in the Limpopo Province of South Africa (see Figure 3.1). The study area around the batholith falls within the Aganang Local Municipality, which was in 2016 merged with the Polokwane Local Municipality within the Capricorn District.

3.3 REGIONAL GEOLOGICAL SETTING

The Matlala Batholith is a fine-grained biotite granite intrusion of Randian and Vaalian age (3 600 to 3 200 million years old) (SACS, 1980). It occurs in host rock consisting of the Goudplaats-Hout River Gneiss (Figure 3.2). The grain size of the host rock varies from medium- to coarse-grained, and these rocks also show banding and layering (Brandl, 1986). A photograph of a contact between the granite of the Matlala Batholith and the host rock gneiss is shown in Figure 3.3.

The western perimeter of the batholith occurs near a south-to-north contact with rocks of the Bushveld Igneous Complex (BIC). These rocks predominantly consist of gabbro, norite, anorthosite and pyroxenite. Large diabase intrusions occur within the rocks of the BIC, while diabase dykes extend through the Goudplaats-Hout River Gneiss and intersect the Matlala Batholith, forming ridges in the modern surface topography (Brandl, 1986). During a study conducted by Du Toit (2001), some of the diabase intrusions were intersected during the drilling phase and the geological logs revealed a north-easterly or north-westerly strike. Holland (2011) also indicated that these dykes have a mean strike direction of 51^{o}.

Faulting in the area is apparent from the lateral displacement of the contact between the BIC and the Goudplaats-Hout River Gneiss. Quaternary deposits in the form of alluvium occur along the non-perennial rivers that flow across the Matlala Batholith.

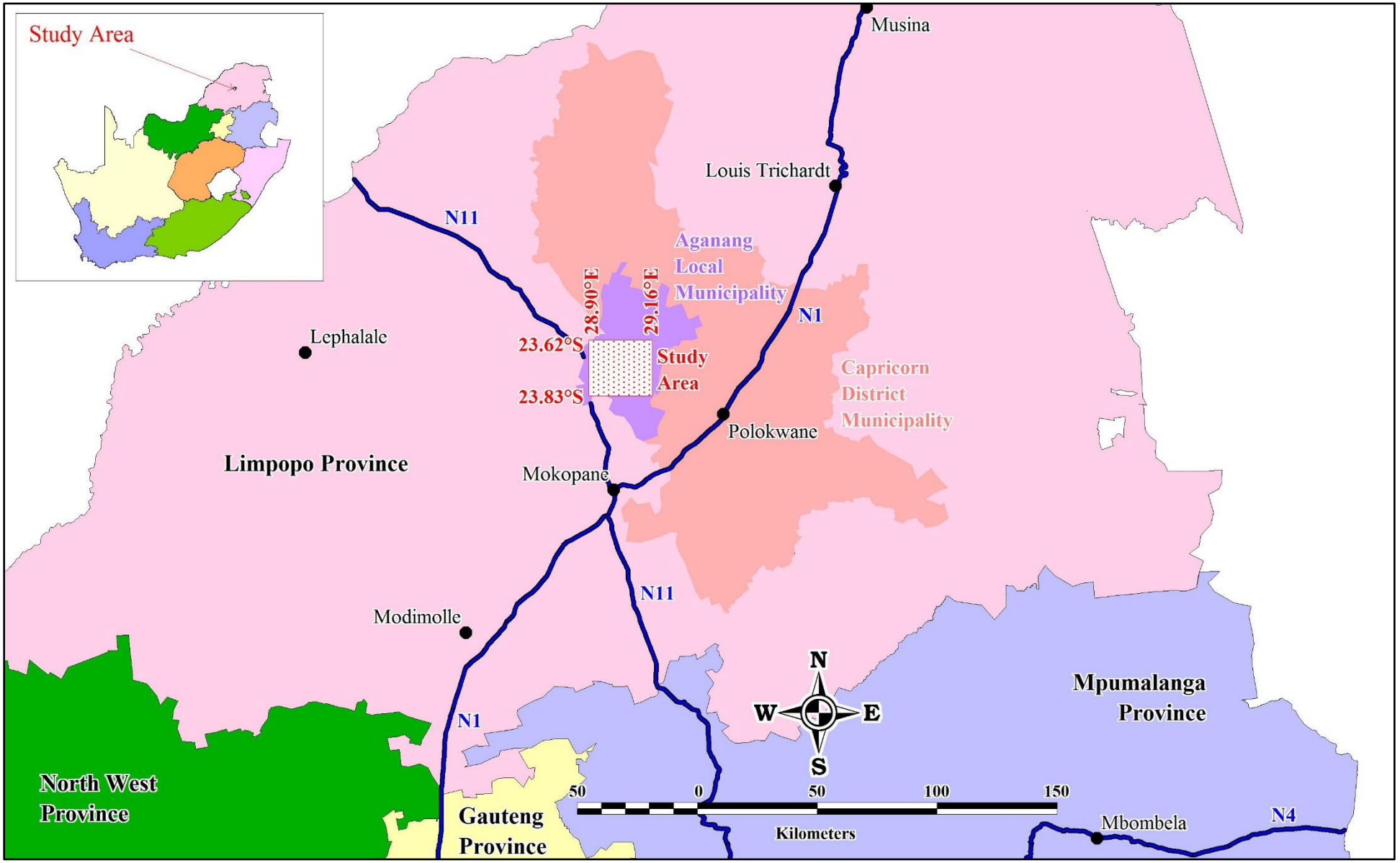

Figure 3.1: Regional setting of the study area

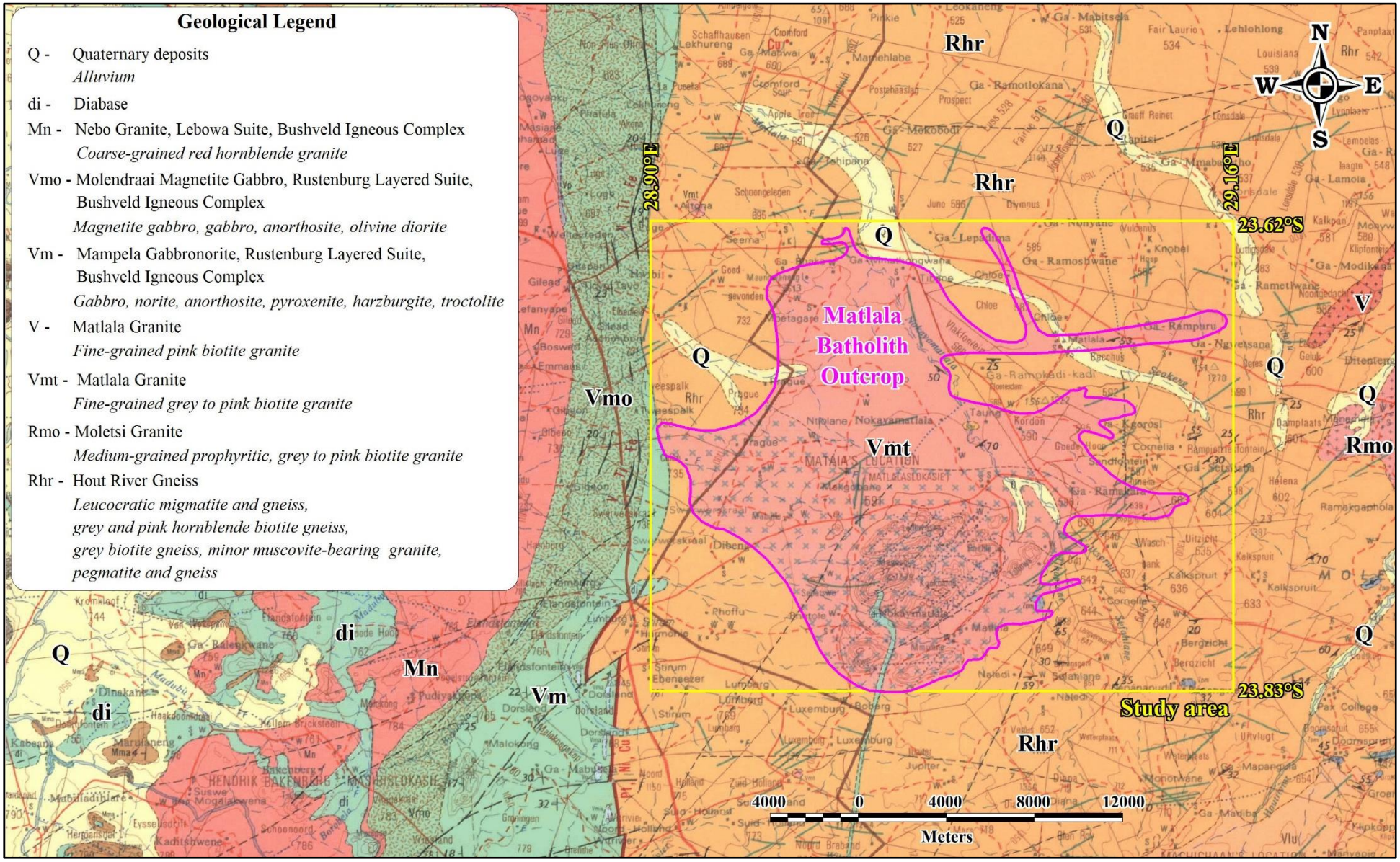

Figure 3.2: Regional geological setting of the study area

Figure 3.3: Contact between the Matlala Granite and the Goudplaats-Hout River Gneiss (Du Toit, 2001)

Du Toit (2001) discovered that the Matlala Batholith has three separate intrusions, occurring near different villages in the area. The batholith has been named according to these villages, and the three intrusions are now known locally as the Matlala, Tibane, and Chloe Batholiths. Of these three, the Matlala Baholith is the largest. Table 3.1 lists the lithostratigraphic units of the Matlala area.

Table 3.1: Lithostratigraphic units of the Matlala area (modified from Holland, 2011)

Era	Lithostratigraphic unit	Formation	Lithology
Randian	Matlala Granite		Biotitic-granodioritic composition
	Goudplaast Gneiss		Gneiss, banded gneiss, magmatite
	Hout River Gneiss		Leucocratic migmatite and gneiss, biotite, and pegmatite rocks
Randian to Swazian	Pietersburg Group	Zandrivierspoort	Mafic metalava interlayered with magnetite quartzite
		Mothiba	Ultramafic metavolcanics: Amphibolite chlorite schists

3.4 REGIONAL GEOMAGNETIC SETTING

An airborne magnetic map covering the Matlala Batholith is shown in Figure 3.4. Comparison with the geological map (Figure 3.2) shows that the area to the west of the batholith is associated with large positive magnetic anomalies due to the presence of the Molendraai Magnetite Gabbro. The batholith itself has no strong magnetic signature, but a number of magnetic dykes cut through it. These dykes have south-west/north-east, west-south-west/east-north-east and west-north-west/east-south-east strikes, and are likely diabase dykes of Vaalian age and/or dolerite dykes of Jurassic age.

3.5 CLIMATE

The climate conditions of the Matlala area are considered semi-arid with very hot summers and mild winters. The area receives most rainfall in summer between September and May, while it is usually dry during winter (see Figure 3.5). The annual rainfall data at weather station 0677802BX from the South African Weather Services (SAWS) reveal that the area received >400 mm rainfall per year from 2007 to 2014, except in 2008 when rainfall was 386 mm. In 2013, the area received a maximum rainfall of 636 mm for the observation period, which was around 150 mm more than the average rainfall (Figure 3.6). The mean annual precipitation (MAP) received for the period 2007 to 2014 is 484 mm.

The temperature varies significantly throughout the year; with summer temperatures reaching a maximum of ±39 C, usually in November to January, whereas in the winter the temperatures can drop to a minimum of -8 C, usually between June and July. The mean annual temperature of the area is around 18.5 C.

3.6 TOPOGRAPHY AND DRAINAGE

The western, eastern and northern parts of the study area display an undulating topography with gentle slopes towards the east and north-east. However, a few localised hills occur near the western and northern perimeters of the outcrop of the batholith. By contrast, the southern part of the batholith outcrop is characterised by sharp topographic variations in the form of numerous steep hills (Figure 3.7). Local surface drainage is predominantly to the north-west along the non-perennial Matlala and Seokeng Rivers.

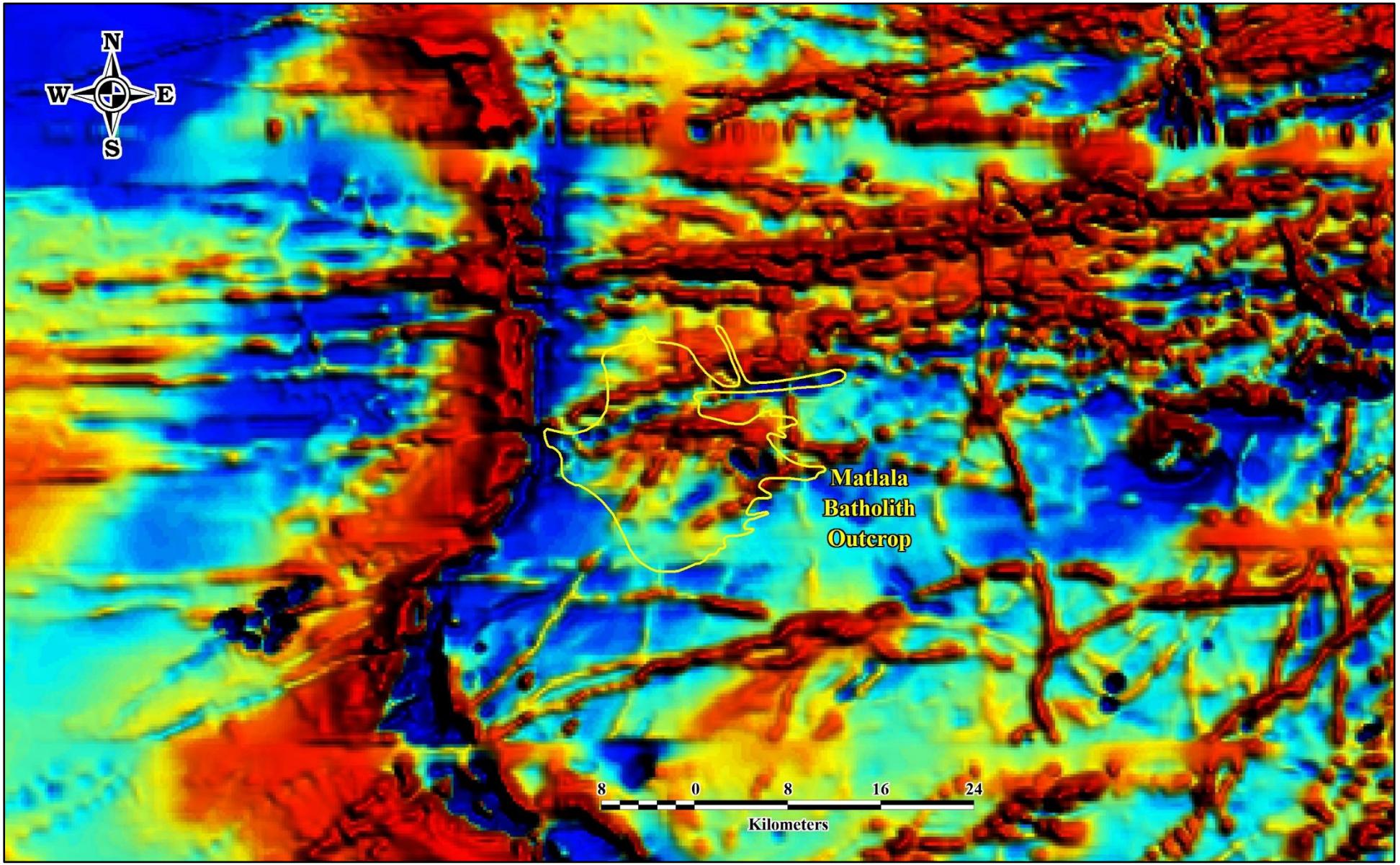

Figure 3.4: Regional geomagnetic setting of the study area

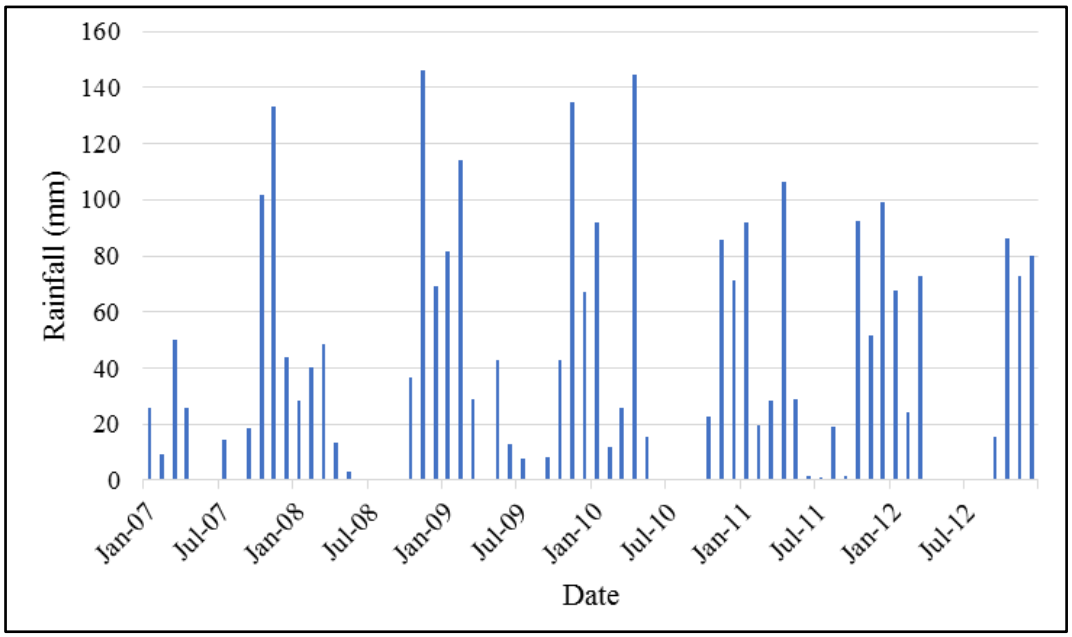

Figure 3.5: Monthly rainfall in Matlala, Jan 2007 – Dec 2012

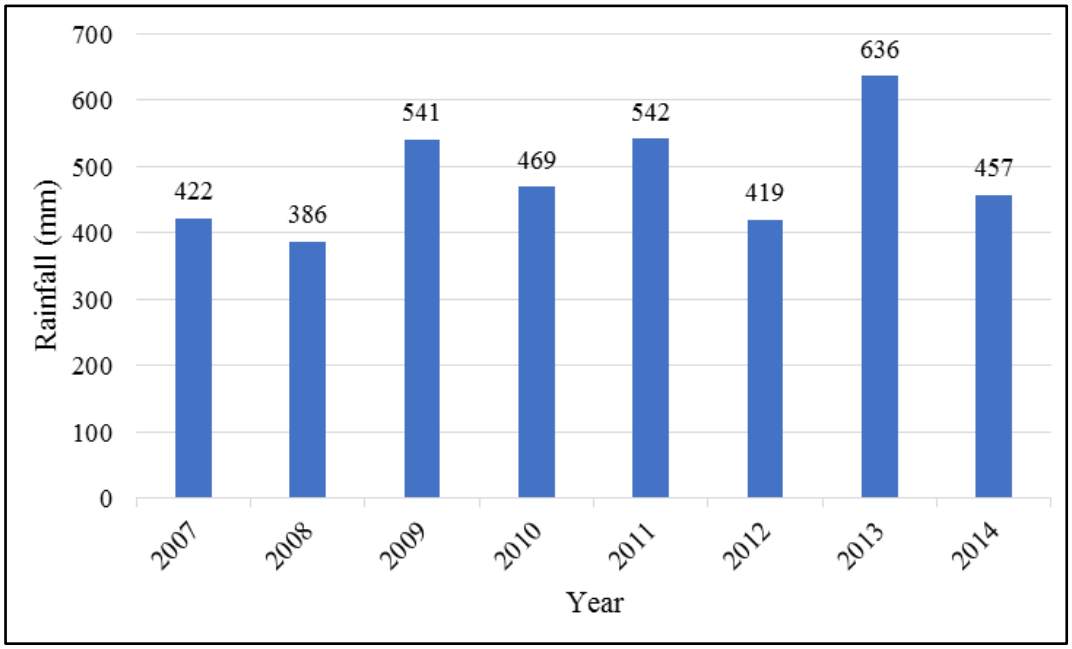

Figure 3.6: Annual rainfall in Matlala, 2007 – 2014

The study area falls within Quaternary Sub-Catchments A62E, A62F and A62H within the Limpopo Plateau region (Figure 3.8). Drainage from these sub-catchments is to the north-west. The Seokeng River is confluent with the Matlala River approximately 4 km north of the northern boundary of the study area. From here the Matlala River continues its north-western flow before joining the Mogalakwena River at a position approximately 28 km north-west of the study area. This river usually sustains flow after heavy rainfalls, typically from September to May, but its tributaries are typically dry during the dry season. The Mogalakwena River flows northwards before joining the Limpopo River approximately 120 km to the north.

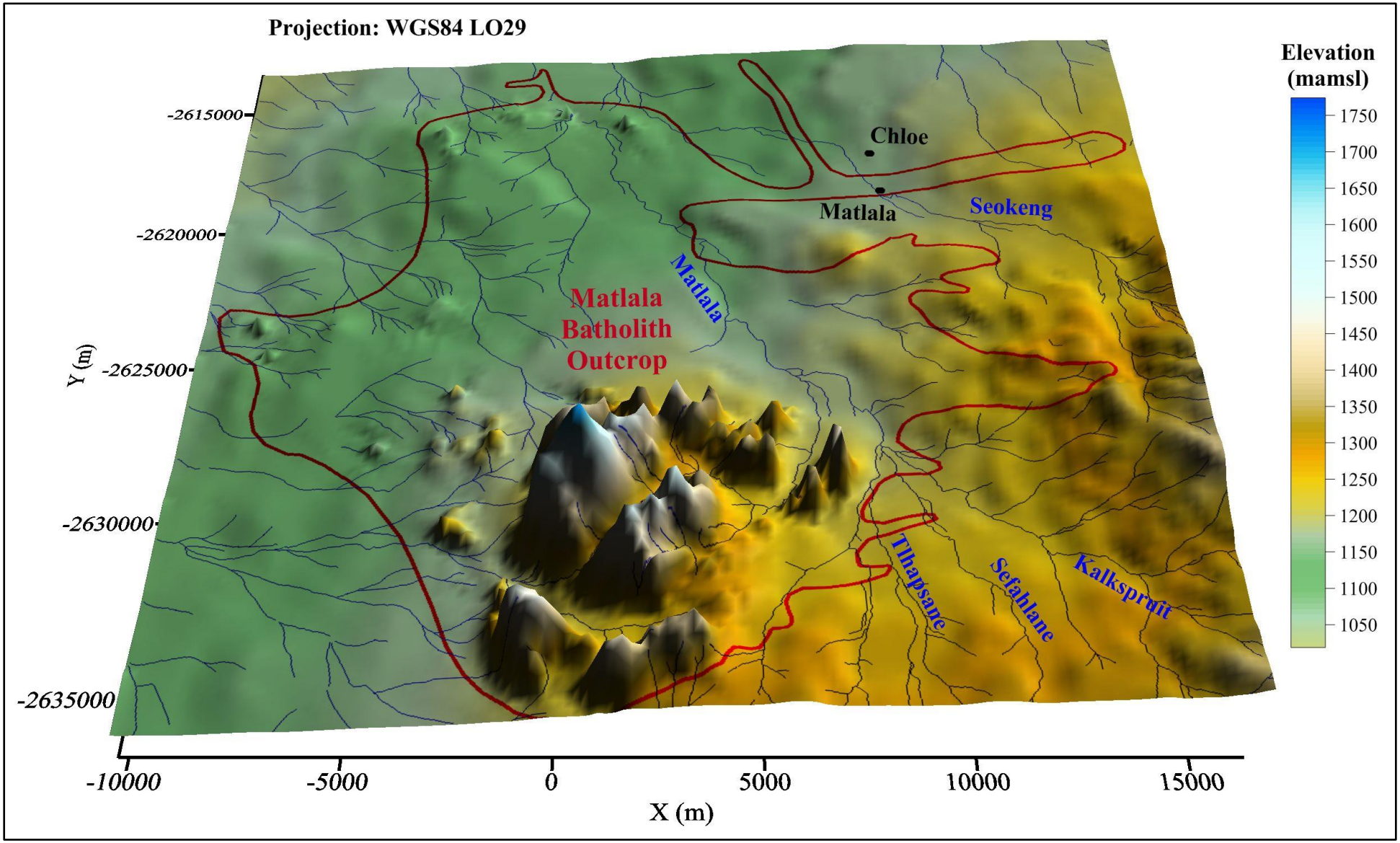

Figure 3.7: Local topographic elevations and drainage within the study area

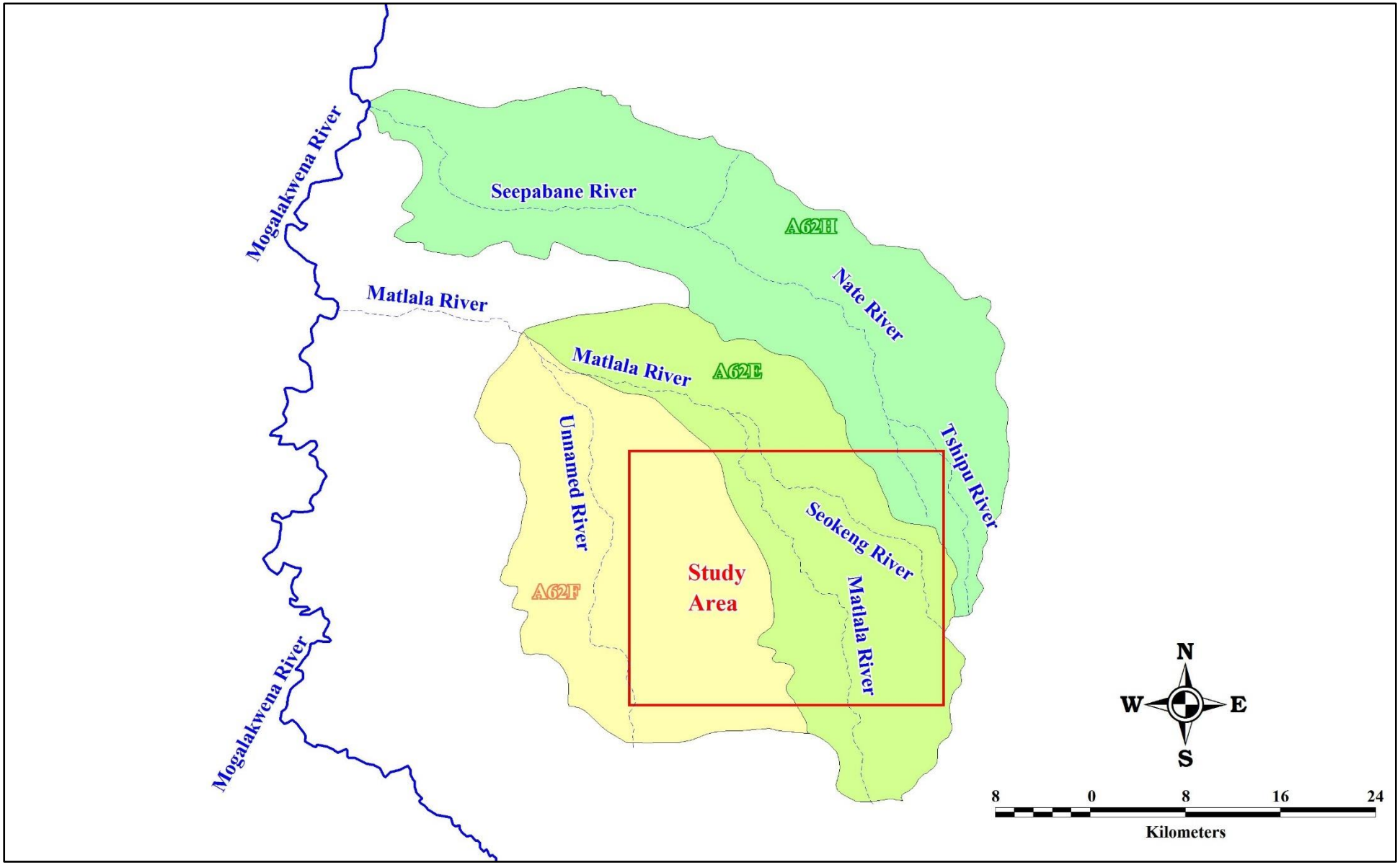

Figure 3.8: Drainage from the study area

3.7 GEOHYDROLOGY

3.7.1 Hydrological region

The Mogalakwena River Basin is classified into seven hydrological regions (Table 3.2). The study area falls within the eastern upland hydrological region. The region is dominated by crystalline rocks associated with geological structures (faults and dykes). Most of the aquifers in the region are low yielding and are associated with dykes, faults and weathered contacts. Weathering of bedrocks is shallow (around 10 m). Groundwater recharge is estimated to be low at 3% of the MAP (Scot and Wijers, 1992).

Table 3.2: Hydrological regions in the Mogalakwena River basin (adapted from Scot and Wijers, 1992)

Hydrological region	Main aquifer				Recharge potential (% of MAP)	Water quality		Target features for drilling
	A	W	S	C		EC (mS/m)	Problem species	
Nyl valley	*	*	*	*	2-4	<300	Nitrate, fluoride	Alluvium, faults, dykes
Plains	*	*	*	*	4-5	100-700	Chloride	Faults, dykes contacts, lithological contacts
South-eastern uplands	*				5	10-200		Faults, weathered zones, alluvium
Upper Mogalakwena Valley	*	*	*		5	50-800	Iron, chloride	Alluvium, faults, weathered zones
Basement lowlands		*	*	*	3	100-750	Nitrate, fluoride	Faults, weathered zones
Eastern uplands			*	*	3	<300	Fluoride	Faults, dykes, weathered contacts
Western uplands		*	*	*	3-10	70-500	Nitrate, iron, manganese, chloride	Dyke contacts, faults, weathered zones

A - Alluvium *S - Structural* *MAP - Mean Annual Precipitation*
W - Weathered *C - Contact* *EC - Electrical conductivity*

3.7.2 Aquifer types and conditions

Groundwater occurs in two different aquifer systems in the area, namely (1) the regolith (weathered) zone, and (2) the fractured bedrock. These aquifer systems are closely interlinked (hydraulically connected). The overlying regolith serves as a recharge system to the underlying fractured bedrock as the water level is exposed to the atmosphere. The highly weathered remnant gneissic roof section is a good target for groundwater development (Acworth, 1987). Du Toit (2001) showed that the contacts between the host rocks and intrusive rocks are poor targets for groundwater exploration, as the boreholes drilled along these contacts had very low yields compared to those drilled in the regolith.

3.7.3 Aquifer hydraulic parameters

Pumping tests are conducted in order to estimate the distribution of hydraulic parameters of a groundwater system. The hydraulic parameters such as hydraulic conductivity, transmissivity, and storage coefficients are estimated depending on the hydrogeological environment as well as the short-term and long-term objectives of the investigation. Du Toit (2001) used three different tests for the purpose of his study namely:

- **Step-drawdown tests:** To determine the optimum pumping rate of each borehole, well efficiencies at various pumping rates, and also the suitable rates for the subsequent constant-discharge test (CDT) which is used to stress the aquifer. Four step tests of equal duration (100 minutes) were conducted on four boreholes, and five step tests of 100 minutes on one borehole.
- **Constant discharge tests:** To determine the volume of water that a borehole can yield for a longer period and to determine the transmissivity (*T*) and storativity (S) of the aquifers. 72-hour tests were conducted on four boreholes and a 48-hour test on one borehole.
- R**ecovery test**: The test is conducted immediately when the CDT ends. It gives a representation of the groundwater inflow in the borehole. The water levels were monitored until a 95% of the total drawdown was recovered.

Information on the pumping tests performed by Du Toit (2001) is listed in Table 3.3. The results obtained from the pumping tests were analysed using the flow characterisation (FC) program developed by Van Tonder *et al.* (2001) to determine aquifer parameters and flow characteristics.

Based on the results obtained from the different methods and programmes, Du Toit (2001) concluded that the total T-values vary from 3 to 57 m^2/d for the fractured bedrock and from 151 to 205 m^2/d for the weathered roof section, with the S-values vary from 10^{-2} to 10^{-5}. He, however, pointed out that the heterogeneity of the aquifer system together with the varying distances between observation and

abstraction boreholes might have resulted in a variation in the calculated *S*-values, and therefore, the S-values should be used with caution. The through-flow value of the aquifer ranges from 0.12 to 0.15 m^3/d. Table 3.4 shows the maximum and minimum *T*- and *S*-values for all five tested boreholes, also illustrated graphically in Figure 3.9.

Table 3.3: Results obtained from the step test, constant discharge test and recovery test (after Du Toit, 2001)

Site name	G45282	G45278	G45227	G45229	G45287	G45302
Step-Drawdown						
Rate 1 (L/s)	2.37	0.9	3,695/90	4,07/92	7.14	0.44
Well efficiency (%)	71	98	90	92	98	34
Rate 2 (L/s)	3.94	1.9	7.01	8.07	13.62	0.85
Well efficiency (%)	59	94	83	85	96	21
Rate 3 (L/s)	8.91	3.7	11.0	12.26	21.0	1.275
Well efficiency (%)	39	89	76	79	94	15
Rate 4 (L/s)	Failed @	5.4	14.62	16.63	28.47	Failed @
Well efficiency (%)	14 L/s	85	70	74	93	1.8 L/s
Rate 5 (L/s)	-	-	-	-	35.17	-
Well efficiency (%)					91	
Constant-Discharge						
Rate (L/s)	No test	5.5	14.65	12.41	25.28	0.99
Duration (hours)	No test	48	72	72	72	72
Recovery						
Duration (hours)	24	108	138	171	149	72
% Recovered	99.7	100	100	98.3	92.1	98.5

Table 3.4: Transmissivity and storativity values of five boreholes around the Matlala Batholith (Du Toit, 2001)

Site number	Main lithology	Total transmissivity (*T*) (m^2/d)		Total storativity (*S*)	
		Min	Max	Min	Max
G45227	Gneiss / Granite	51	58	8.55×10^{-5}	8.52×10^{-4}
G45229	Gneiss	32	57	3.61×10^{-5}	7.73×10^{-4}
G45278	Granite	3	7	1.13×10^{-4}	1.82×10^{-3}
G45287	Gneiss / Granite	151	205	5.12×10^{-4}	1.02×10^{-2}
G45302	Gneiss / Diabase	3	10	2.25×10^{-5}	1.39×10^{-3}

Figure 3.10 gives an illustration of the spatial distribution of the transmissivity around the Matlala Batholith in the study area. Most boreholes have a *T*-value >5 m^2/d, while many have a *T*-value >25 m^2/d. Eight boreholes have a *T*-value >150 m^2/d. The even distribution of high *T*-values indicates the presence of deeper zones of weathering with higher storage capacities and conductivities, which

are able to transmit groundwater throughout the entire saturated thickness of the weathered zone. The boreholes with low *T*-values may also represent the presence of a confined aquifer in the system. The *T*-values of the weathered and fractured granitic zone of the roof section range from 20 to 60 m^2/d and the low permeability gneiss/granite contact has a *T*-value of <20 m^2/d.

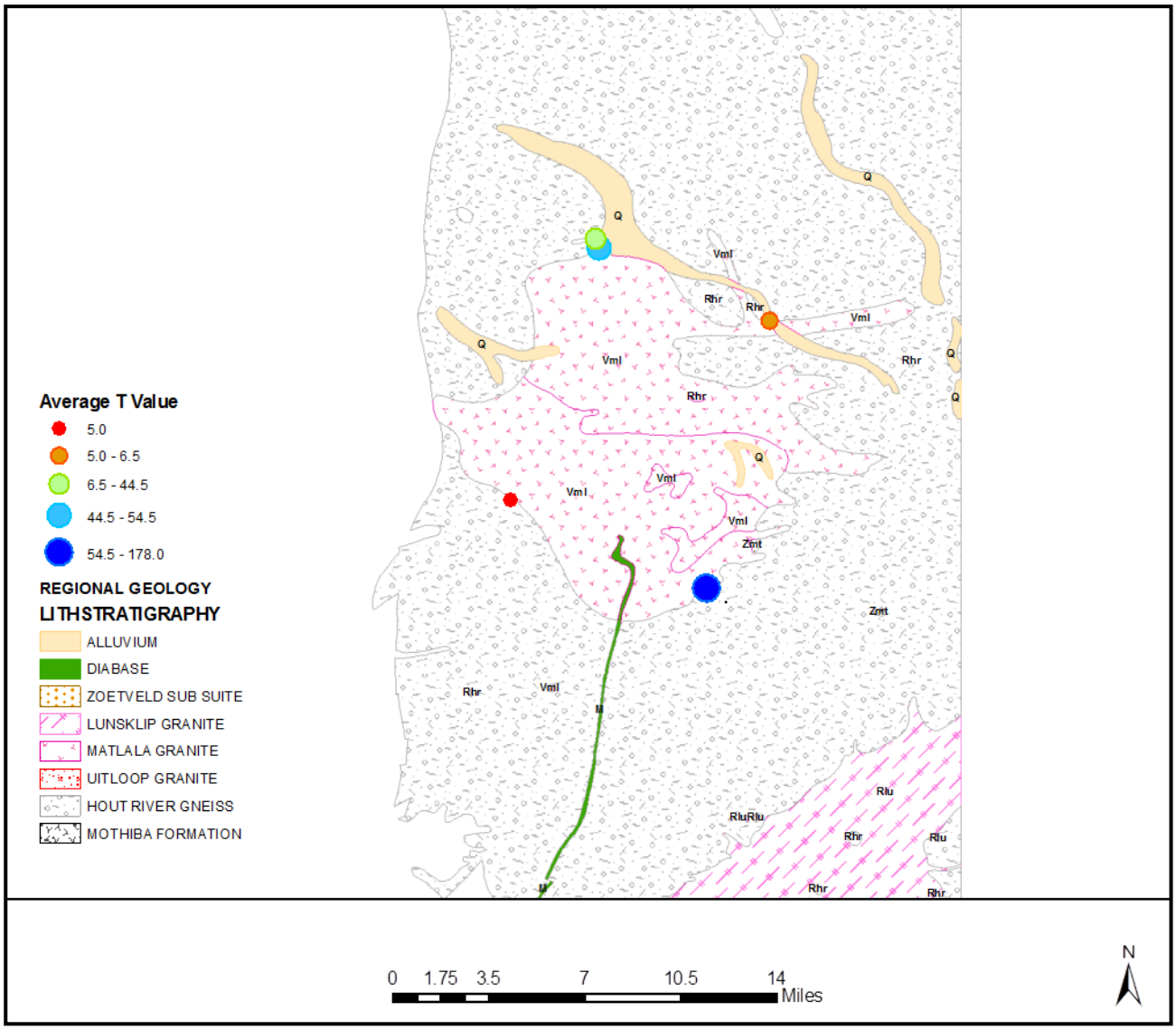

Figure 3.9: Transmissivity values of five boreholes around the Matlala Batholith

Figure 3.11 indicates the yield frequencies in the Matlala Granite; out of 23 boreholes drilled, only 19 were analysed and the remaining four were excluded because the boreholes were dry (yield of <0.1 L/s). From the 19 analysed boreholes, 26% had a yield of >5 L/s, 9% had a yield of between 2 and 5 L/s, and 65% had a yield below 2 L/s. The high-yielding boreholes are generally associated with the remnant fractured and weathered roof section. Du Toit (2001) indicated that the weathered and fractured zones in the study area produced maximum blow yields of >40 L/s.

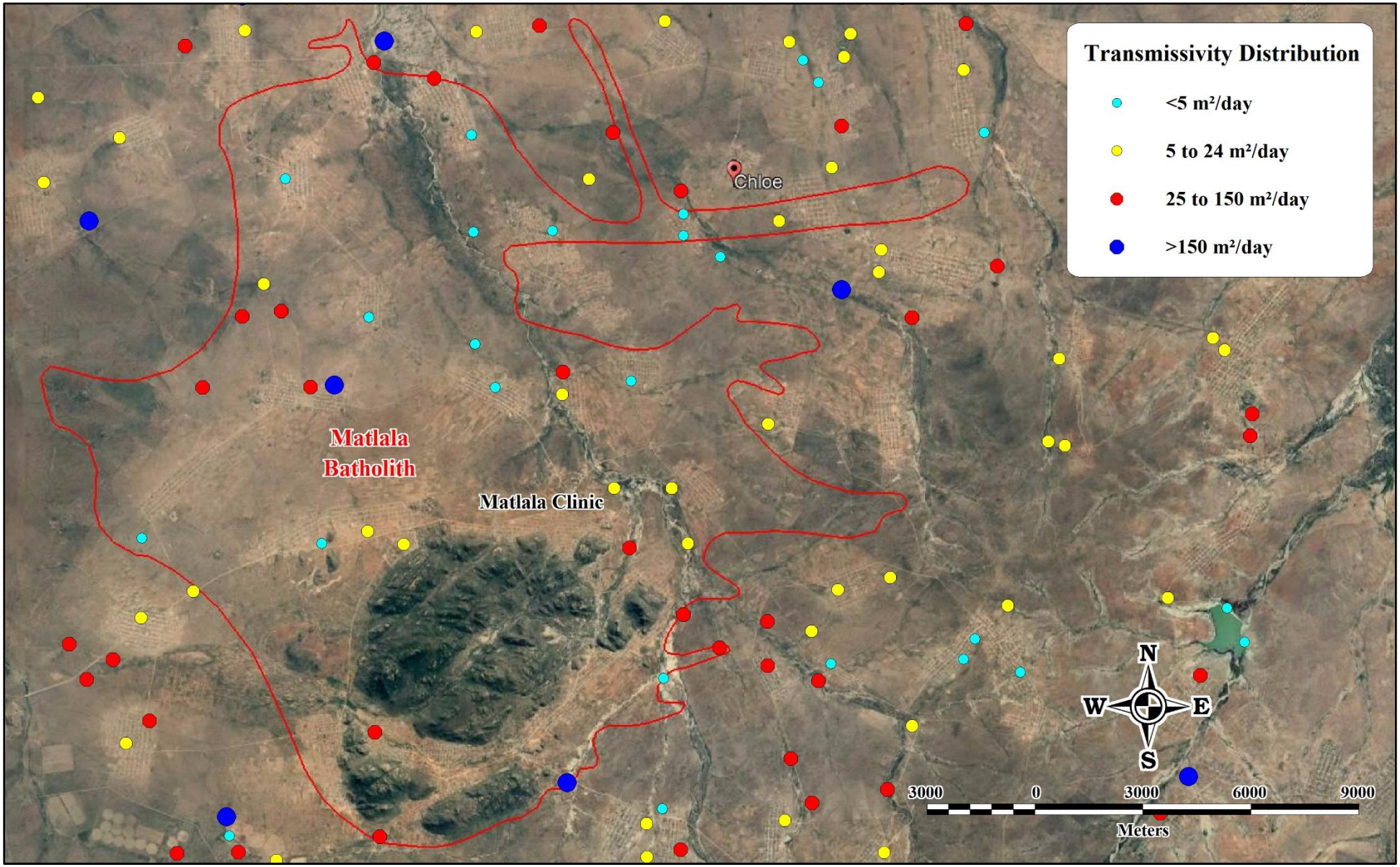

Figure 3.10. Spatial distribution of transmissivities from boreholes on and around the Matlala Batholith as obtained from the GRIP dataset

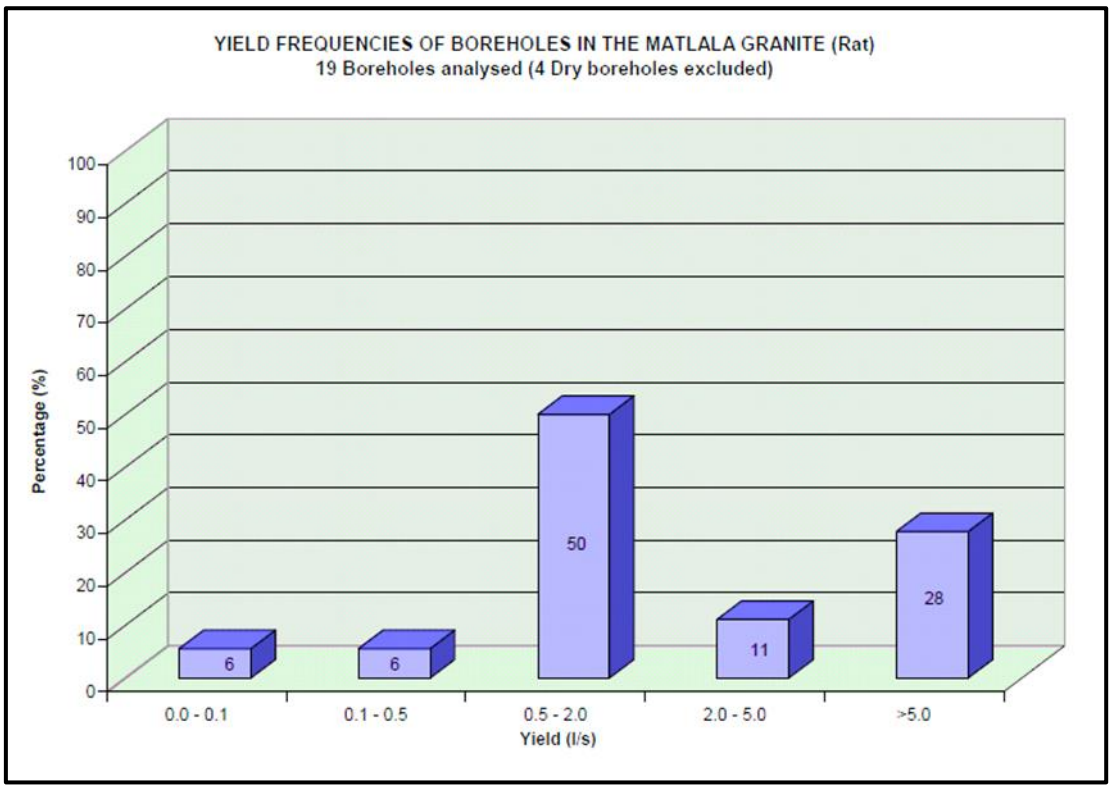

Figure 3.11: Yield frequency for the intergranular and fractured aquifers of the Matlala granite (Du Toit and Sonnekus, 2014)

3.7.4 Groundwater demand and potential

The eastern part of the Matlala Batholith, where the Matlala wellfield is located, falls under the A62E drainage region (refer to Figure 3.8). In 2013, the DWS, which was then called the Department of Water Affairs (DWA), together with EVN Africa Consulting Services (Pty) Ltd., conducted a feasibility study for Aganang Local Municipality's bulk water supply. This study involved determining the water requirements and potential water supply from a groundwater resource of all the villages within a specific drainage area. The water requirements were projected from 2013 to 2030, considering the population, number of villages, and the demand for water.

As shown in Figure 3.12, the groundwater potential in the area could have theoretically met the 2013 high water demand; but the actual surface and groundwater abstractions were insufficient to meet the standard water demand. The study revealed that most of the boreholes used for water supply were low yielding, indicating that there was poor groundwater development and groundwater exploration was unsuccessful in meeting the demand. It is clear that the groundwater potential in the catchment is sufficient to meet the standard demand up to 2025, provided high-potential groundwater areas are identified.

3.7.5 Groundwater quality

Du Toit (2001) showed the distribution of different water classes for domestic use in the area, as per the classification system of the DWS (Table 3.5). An estimated 42% of the water belongs to Class III, 26% to Class II, and the remaining 32% of the water belongs to Classes 0 and Class I, resulting in a low percentage of water that is good and ideal for domestic use in the area without treatment. The result from the chemical analysis revealed the domination of HCO_3^- anion, which suggests recent aquifer recharge, and high concentrations of F^-, which are probably related to the weathering of fluorite (CaF_2)-rich pegmatites and granites. The highest anthropogenic pollution in the area is caused by agricultural activities and on-site sanitation. Boreholes sampled near active pit latrines showed generally high NO_2^-+NO_3^- concentrations. The major water types from the hydrochemistry analysis of the groundwater samples are Na^+-Ca^{2+}-Mg^{2+}-HCO_3^-, Na^+-HCO_3^-, Na^+-Mg^{2+}-HCO_3^-, and Na^+-Ca^{2+}-Mg^{2+}-Cl^--HCO_3^- types (Du Toit, 2001).

Table 3.5: Classification of the groundwater in the study area as per DWS classification (WRC, 1998)

DWS classification	Description	Effects	% of boreholes with this quality
Class 0	Ideal water quality	***Drinking Health:*** No effects, suitable for many generations ***Drinking Aesthetic:*** Water is pleasing ***Food preparation:*** No effects ***Bathing:*** No effects ***Laundry:*** No effects.	0
Class I	Good quality water	***Drinking Health :*** Suitable for lifetime use. Rare instances of sub-clinical effects ***Drinking Aesthetic:*** Some aesthetic effects may be apparent. ***Food preparation:*** Suitable for lifetime use. ***Bathing:*** Minor effects on bathing or on bath fixtures. ***Laundry:*** Minor effects on laundry or on fixtures	32
Class II	Marginal water quality	***Drinking Health :*** Suitable for lifetime use. Rare instances of sub-clinical effects ***Drinking Aesthetic:*** Some aesthetic effects may be apparent. ***Food preparation:*** Suitable for lifetime use. ***Bathing:*** Minor effects on bathing or on bath fixtures ***Laundry:*** Minor effects on laundry or on fixtures	26
Class III	Poor water quality	***Drinking Health :*** Poses a risk of chronic health effects, especially in children and the elderly ***Drinking Aesthetic:*** Bad taste and appearance may lead to rejection of the water ***Food preparation:*** Poses a risk of chronic health effects, especially in children and the elderly ***Bathing:*** Significant effects on bathing or on bath fixtures ***Laundry:*** Significant effects on laundry or on fixtures	42
Class IV	Unacceptable water quality	***Drinking Health:*** Severe acute health effects, even with short-term use. ***Drinking Aesthetic:*** Taste and appearance will lead to rejection of the water ***Food preparation:*** Severe acute health effects, even with short-term use ***Bathing:*** Serious effects on bathing or on bath fixtures ***Laundry:*** Serious effects on laundry or on fixtures	0

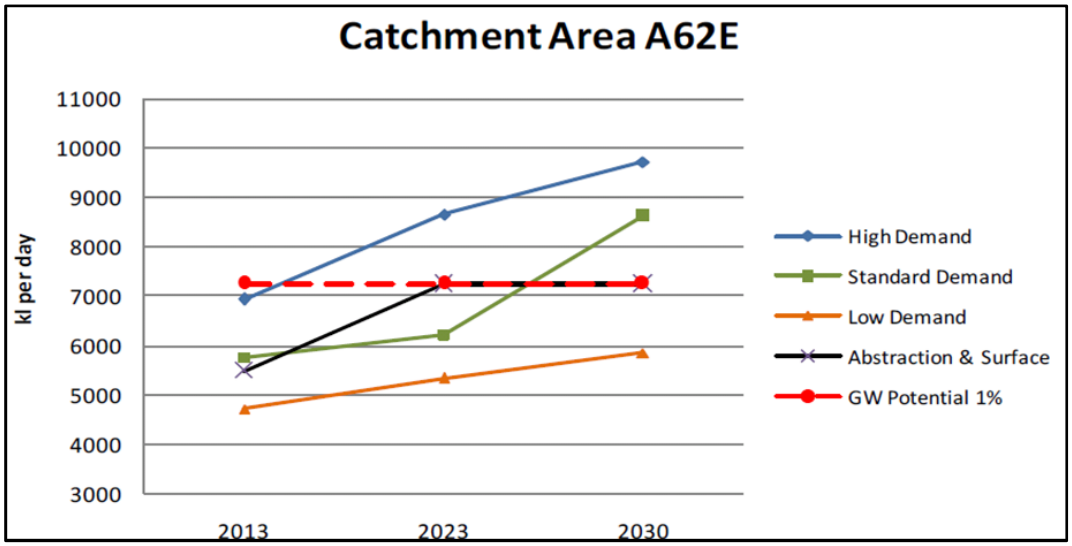

Figure 3.12: Predicted groundwater demand in catchment area A62E (EVN Africa Consulting Services, 2013)

3.8 GEOMORPHOLOGY, VEGETATION AND LAND USE

King (1975) recognised five geomorphic cycles that represent long periods of weathering and erosion. These cycles are Gondwana (190 Ma), Post-Gondwana (135 Ma), African (100 Ma), Post-African (20 Ma), and Pliocene and Quaternary (2 Ma). The study area is situated in the African cycle. McFarlane *et al.* (1992) and Du Toit (2001) suggested that the highly weathered regolith in the area is a good target for groundwater exploration as the pump test revealed high-yielding boreholes associated with this zone. This suggests that the weathering would have created localised zones of deeper weathering with higher storage capacities and conductivities in the area.

The geomorphic features observed in the study area are inselbergs, hills, lowlands, foothills, and valleys. The distribution of vegetation in different areas is largely dependent on local variations in rainfall and soil conditions. The study area is dominated by mixed Bushveld vegetation in the north-west and Pietersburg Plateau Grassveld in the south-east (Figure 3.13).

The main land uses in the area include settlements, agriculture, cultivated land, and grazing land, with the main economic driver being agriculture (Figure 3.14). The main crops produced in the area are cowpeas, maize, and groundnuts.

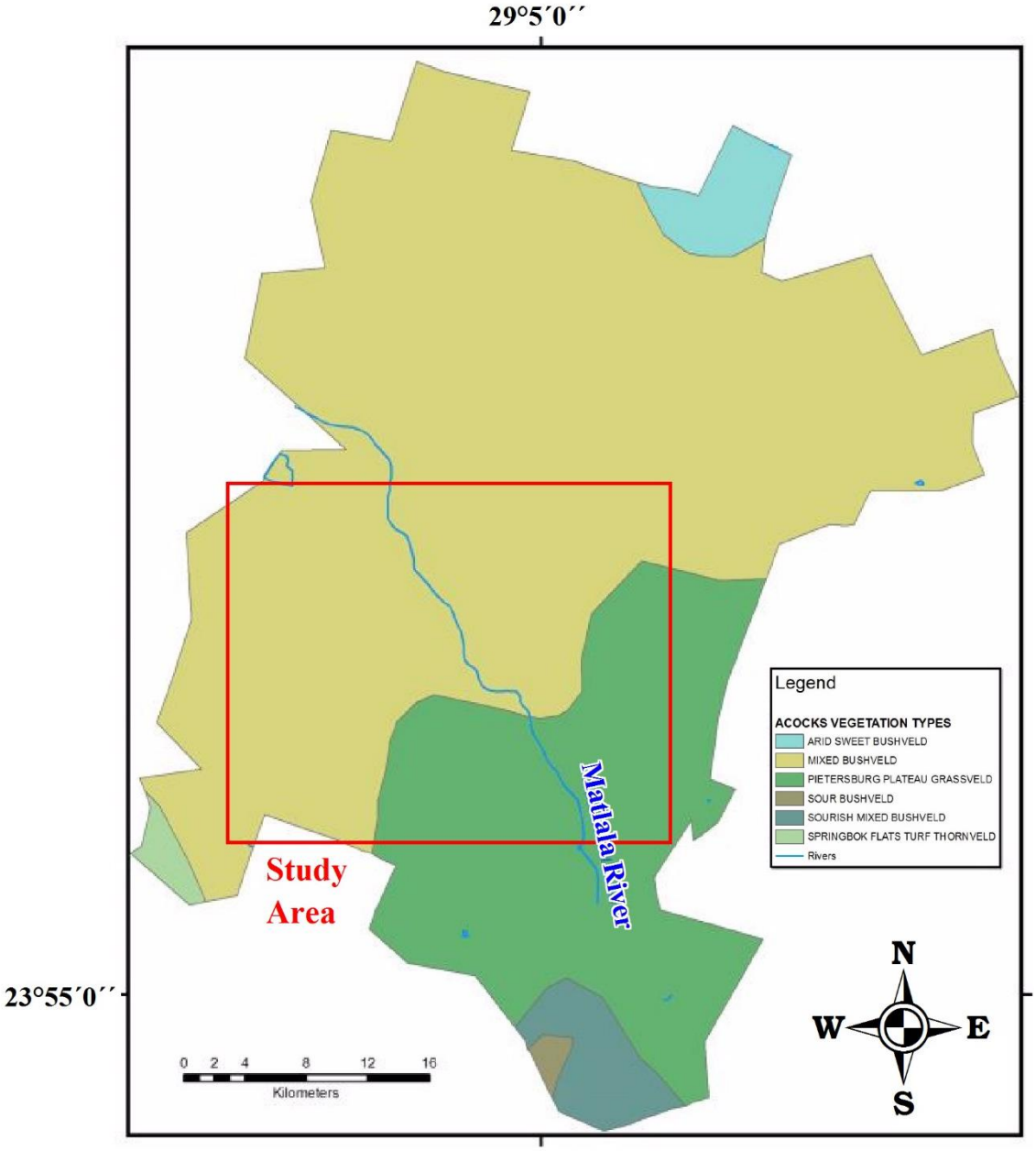

Figure 3.13: Vegetation in the Aganang area (Enviroxcellence, 2009)

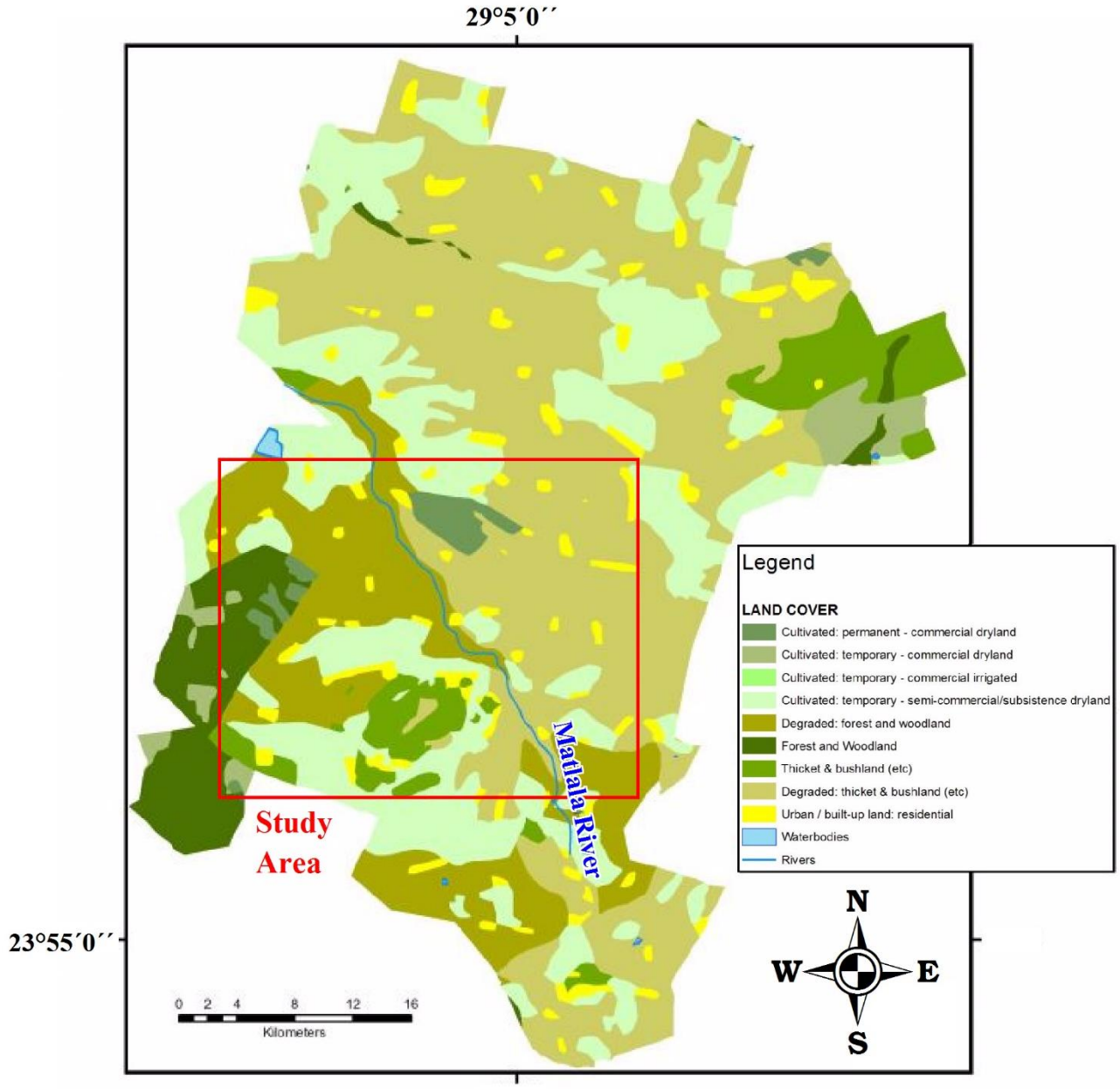

Figure 3.14: Land cover in the Aganang area (Enviroxcellence, 2009)

3.9 WATER RESOURCES

3.9.1 General

In the study area, 95% of the water for domestic and agricultural use comes from the groundwater resource (EVN Africa Consulting Services, 2013). The community, however, faces many problems when they have to utilise the groundwater. Water supply is a challenge because of technical problems, which involve failure of equipment, illegal water connections, and theft of pumps. Another disadvantage is that the community uses water that is not treated and does not necessarily meet drinking water standards as it is pumped using electric and diesel pumps directly to storage tanks. Although the Department of Water and Sanitation (DWS) is intervening, attempting to get consultants and other water entities to conduct tests before handing over boreholes to the community, it is not

sufficient considering that the municipality does not have a functional waste-disposal site. As a result, households use their own dumps to dispose of waste and this practice does not only pose an environmental problem to groundwater (groundwater pollution) and surface water, which affects the health of animals and people, but also degrades the soil, eventually affecting agricultural production.

3.9.2 Surface hydrology

The two main surface water bodies that contribute directly to the water supply of the Aganang Local Municipality are the Hout River and Utjane Dam, located approximately 12 km east of the Matlala Batholith (refer to Figure 3.10). The river close to the study area, however, is the non-perennial Matlala River and its tributaries. These streams carry water only during rainy seasons. Flow is predominantly to the north-east (Figure 3.8).

CHAPTER 4:
RESEARCH METHODS

4.1 INTRODUCTION

The primary objective of this study is to understand the water level response to rainfall, estimate the recharge, and to understand the groundwater flow in the aquifer system in order to develop a general conceptual hydrogeological model of the area. This chapter describes and discusses the methods followed and taken to achieve the aims and objectives of the current research project. The chapter is divided into four sections: borehole selections; recharge estimation; groundwater quality characterisation and development of conceptual geohydrological model.

4.2 BOREHOLE SELECTION

The Groundwater Resource Information Project (GRIP) database lists more than 1 100 boreholes on and around the Matlala Batholith. This database, managed by the DWS, contains the coordinates of the boreholes, as well as the yield, depth, water use, and water quality of some boreholes. To investigate the geohydrological conditions and to estimate the recharge rates, boreholes were selected based on a) the completeness of the information listed in the Grip database, b) whether other geophysical and/or geohydrological studies have been conducted near these boreholes, and c) whether the boreholes occur in a wellfield.

4.3 RECHARGE ESTIMATION

Groundwater recharge was estimated using the CMB, WTF, and CRD methods. These methods where selected based on the availability of data.

4.3.1 CMB Method

To estimate the mean annual recharge in arid and semi-arid regions, it is assumed that the only source of chloride in groundwater comes from rain. The CMB method requires annual rainfall data, and data on chloride concentration in rainwater as well as in groundwater. It is important to note that no rainwater chloride concentration data for the study area were available. The rainwater gauge had been vandalised, which resulted in difficulties with sampling the rainwater. Therefore, for this study, the rainwater chloride concentration used was that proposed by Xu and Van Tonder (2000) with the inland value of 0.2207 mg/L. The average rainfall value and the data for the concentrations of groundwater chloride were obtained from the study conducted by Du Toit (2001) in the study area.

It is important to note that, although the assumption is that the only source of chloride in the groundwater is from rainwater, there are other sources such as fertilizers, irrigation, and pesticides. This could influence the chloride concentration; as a result, the recharge rates should therefore be considered as minimum rates (Nyagwambo, 2006; Banks et al., 2009; Boerner and Weaver, 2012). Equation 1 (Section 2.4.1.1) shows the inverse relationship between the recharge rate and the chloride concentration of the groundwater. This equation was applied to the collected data to estimate recharge in the study area.

4.3.2 WTF Method

The WTF method required groundwater level data, as well as the specific yield of the underlying rocks. Recharge estimation was done using Equation 4, Section 2.4.1.2.2. The following steps were followed in calculating the recharge over the Matlala batholith, using the WTF method:

- Three boreholes for which hydrographs could be compiled were selected to estimate recharge in the Matlala wellfield. These boreholes all intersect the shallow aquifer system. It is important to note that all the boreholes with long-term groundwater level monitoring data were clustered in one area, hence the selection of boreholes in close proximity to one another.
- The main lithology intersected by the boreholes was established from drilling chips and the NGA database. The main lithology that was intersected in all three boreholes was the Goudplaats-Hout River Gneiss. The specific yield value of 0.02 used in this study was obtained from literature, specifically a study conducted in the Hout River Catchment by Tshipala (2018). Water level data were used to determine Δh by subtracting high and low levels for a specific year. The recharge for each year was then calculated.

4.3.3 CRD Method

The following steps were followed to calculate the recharge over the Matlala Batholith using the CRD method:

- The CRD method uses water level data in conjunction with rainfall data to estimate recharge in a given area, based on matching the simulated and observed/measured data. This method was selected based on the availability of data.
- Recharge was simulated using the recharge Excel spreadsheet developed by Xu and Van Tonder (2001).
- The same boreholes used in the WTF method were also simulated using the CRD method. Monthly groundwater level and rainfall data were simulated for a period of 94 months for

Matlala 1. For Matlala 3 and Matlala 12 simulation periods of 76 months and 121 months were used, respectively.

- Specific yield (S_y) values and different lag times were assigned to obtain the best fit between the modelled and observed water level responses.

4.4 GROUNDWATER QUALITY CHARACTERISATION

Based on parameters collected for this study, groundwater quality characterisation is very limited; however, the data are useful for understanding the quality of groundwater in comparison with studies conducted recently in and around the study area. The groundwater quality data were obtained from the analyses of water samples collected during two sampling runs in 1998 and 2017. The data collected in 1998 were also used by Du Toit (2001) to understand the water chemistry along the traverse lines that were used during a geophysical survey to identify the mineralogy of the contact between the host gneissic rocks and intruding granitic rocks. For this study, the same data were used in conjunction with the most recent data (from 2017) to understand the occurrence of recharge and change in water chemistry in the area over the years.

The groundwater chemistry data were captured and organised in Microsoft Excel. The data were then transferred to AqQA, a software program that generates Piper diagrams. These diagrams were then used to group water samples to classify the water types in the study area.

Piper diagrams are developed from two ternary diagrams; one of the major cations on the left and one of the major anions on the right (Bredenkamp *et al.*, 1995; Hounslow, 1995). The points from the two ternary diagrams are then projected towards a diamond-shaped diagram, which is then used to deduce the water type.

4.5 DEVELOPMENT OF CONCEPTUAL GEOHYDROLOGICAL MODEL

A conceptual geohydrological model of the Matlala Batholith in the vicinity of the Matlala wellfield was compiled by using the results of the current study as well as information from previous investigations. These investigations included ground geophysics, geophysical borehole logs, and geological borehole logs (Appendix A). The geophysical data were used to characterise the subsurface geology while the logging results assisted in the identification of potential hydraulically conductive fractures.

4.5.1 Ground geophysics

The data obtained from magnetic and electromagnetic (EM) surveys conducted by Du Toit (2001) across the contact between the batholith and the host rock were correlated with the geological logs to locate the contact zones and to further investigate if the contact zones have groundwater potential. Comparison of the geological cross-section and geophysical profiles along two traverses was done. The two traverse lines were chosen based on the availability of drilling log information and their close proximity to the Matlala well field.

4.5.2 Borehole geophysics

The downhole geophysical logs were used in conjunction with the drilling logs to maximise the understanding of subsurface geology, the lithological change, as well as the location of water strikes (fractures and weathered zones). Due to availability of drilling log information, only three boreholes were investigated.

In groundwater exploration downhole geophysical logging is used to provide the following: 1) borehole construction and design, 2) the characteristics of rocks (i.e., lithology, thickness, and depth of aquifers and confining beds; permeability and porosity of rocks), and 3) fluid in the boreholes. According to Keys (1990), there are several geophysical logging techniques that can be used. These are: acoustic televiewer, acoustic velocity, caliper, conductivity, flow, fluid temperature, gamma-gamma, gamma spectrometry, neutron, spontaneous potential, resistance and resistivity. Keys (1990) and Eastern Research Group and Information (1993) further indicated that to obtain more reliable and accurate results, more than one log should be used and that the local geology should be known. For this study a few logging techniques were selected, as discussed below.

4.5.2.1 Caliper logs

Caliper logging is used to obtain information on borehole construction and for groundwater exploration. Information on the changes in diameter of the borehole may be related to changes in lithology and fracture openings (Keys, 1990). Caliper logging can be conducted in both open and closed boreholes. The rotation of the caliper probe, which may change the direction of the arm, causes different results to be obtained if a caliper log is used as an additional log in a single borehole.

4.5.2.2 Natural gamma logs

Natural gamma logs are used to identify lithology, porosity and permeable zones as well as fractures by measuring the natural radioactivity of rock formation within a selected energy range (Keys, 1990). Similar to caliper logs, they can be conducted on both open and closed boreholes. In groundwater exploration, the most common and significant gamma emitting radioactive isotopes are potassium-40

as well as the uranium- and thorium-decay series (Keys, 1990). However, because uranium is soluble in water, flow and precipitation affects its distribution in boreholes over time, hence its presence may not be detected in gamma logs. In crystalline bedrocks, these radioactive isotopes are abundant in clay that contains decomposed mica and potassium feldspar minerals from gneiss, granites and pegmatitic rocks.

The Gamma log response is affected by materials used during borehole construction. In cased boreholes, both steel and PVC casing can reduce gamma counts; cement with clay may increase/decrease gamma depending on radioactivity of the rock formation; bentonite clay can also increase gamma counts (Keys, 1990). All these factors can negatively affect the interpretation of gamma logs.

4.5.2.3 Neutron logs

In groundwater exploration, neutron logs are used to identify water saturated zones in rock formations by detecting the hydrogen content. They are also used to determine the porosity of these rocks (Keys, 1990). In conjunction with the density tool, neutron logs can also be used to determine lithology. According to (Keys, 1990) there are two types of probes used in neutron logging (1) a small source and short spacing probe largely used for identifying moisture content in the unsaturated zone and (2) large source and long spacing probe used for measuring saturated porosity. Neutron counts decrease as the hydrogen concentration increases (Keys, 1990).

4.5.2.4 Resistivity logs

Resistivity logs measure the resistance of rocks to electrical flow and is expressed in ohm. In groundwater exploration, these logs are used to detect water-bearing fractured zones in the rock formation. In highly resistive crystalline bedrocks, water-bearing fractured zones are associated with zones of decreased resistivity (Williams *et al.*, 2004).

CHAPTER 5:
RESULTS AND DISCUSSION

5.1 INTRODUCTION

This chapter presents and discusses the results obtained in this study. It discusses the selection of boreholes considered for this study, as well as thoroughly interpreting and discussing borehole information obtained during and after borehole drilling and construction. The chapter also discusses the results obtained from the three recharge estimation methods employed in this study (CMB, WTF and CRD method). The chapter incorporates the evaluation of raw groundwater chemistry data; these data were also used in the hydrochemical classification (water types). Understanding the different water types assisted in determining main recharge areas as well as the groundwater flow in the area. Finally, the chapter further evaluates and analyses ground and borehole geophysical surveys. All the results obtained in this chapter are then used in the development of conceptual geohydrological model of the Matlala Batholith.

5.2 BOREHOLE SELECTION

Boreholes used in this study were selected from the boreholes that appear in the Groundwater Resource Information Project (GRIP) database (Figure 5.1). To investigate the geohydrological conditions and to estimate the recharge rates, boreholes were selected based on a) the completeness of the information listed in the Grip database, b) whether other geophysical and/or geohydrological studies have been conducted near these boreholes, and c) whether the boreholes occur in a wellfield. The positions of the 42 selected boreholes around the Matlala Batholith are shown in Figure 5.2. Since numerous boreholes occur in and near the Matlala wellfield near the south-eastern perimeter of the batholith (demarcated by a dashed black line), the borehole numbers of these boreholes are indicated in Figure 5.3 and Figure 5.4. Information on the selected boreholes was retrieved from the GRIP database and is listed in Table 5.1 and Table 5.2.

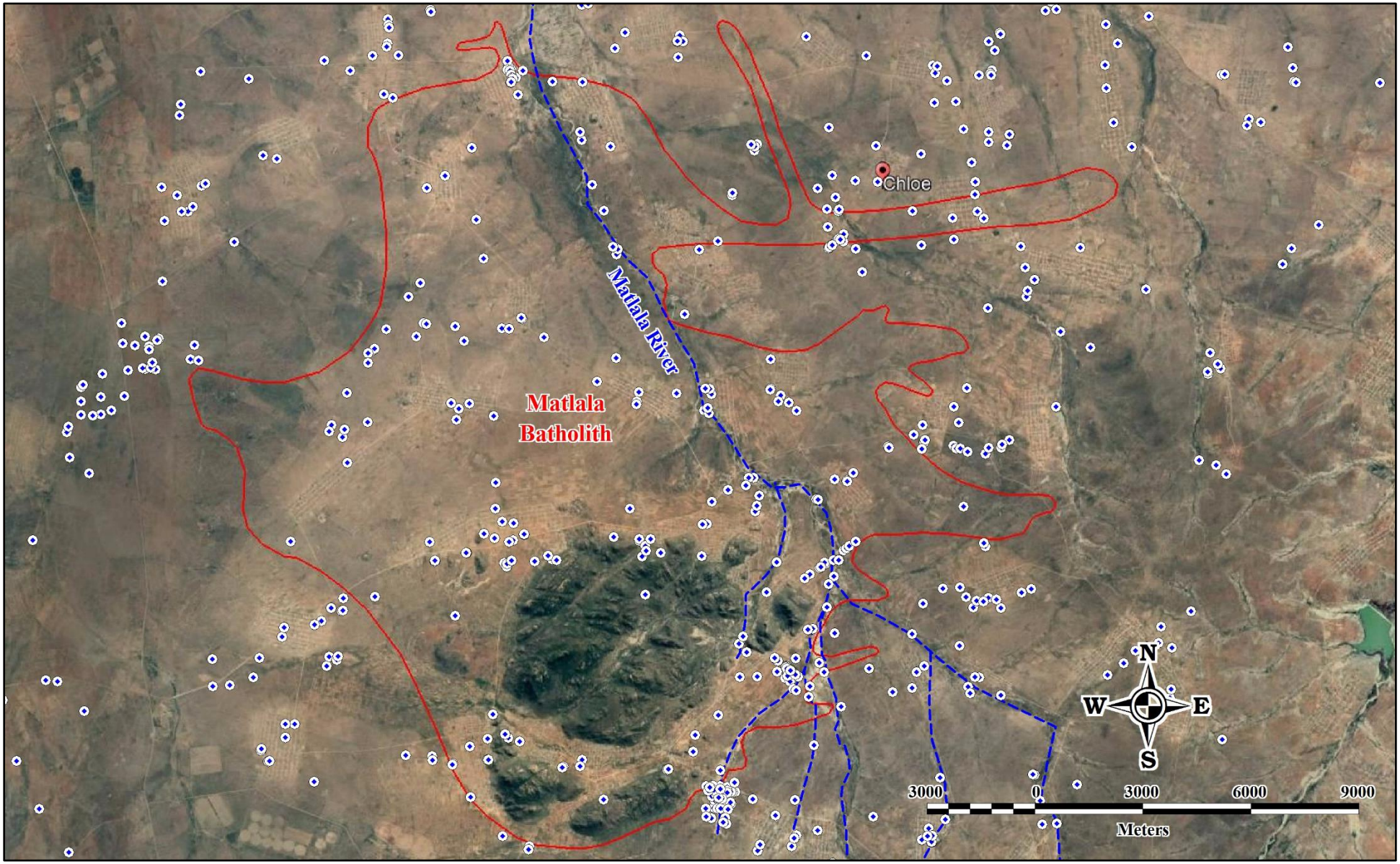

Figure 5.1: Boreholes on and in the vicinity of the Matlala Batholith (from the GRIP database)

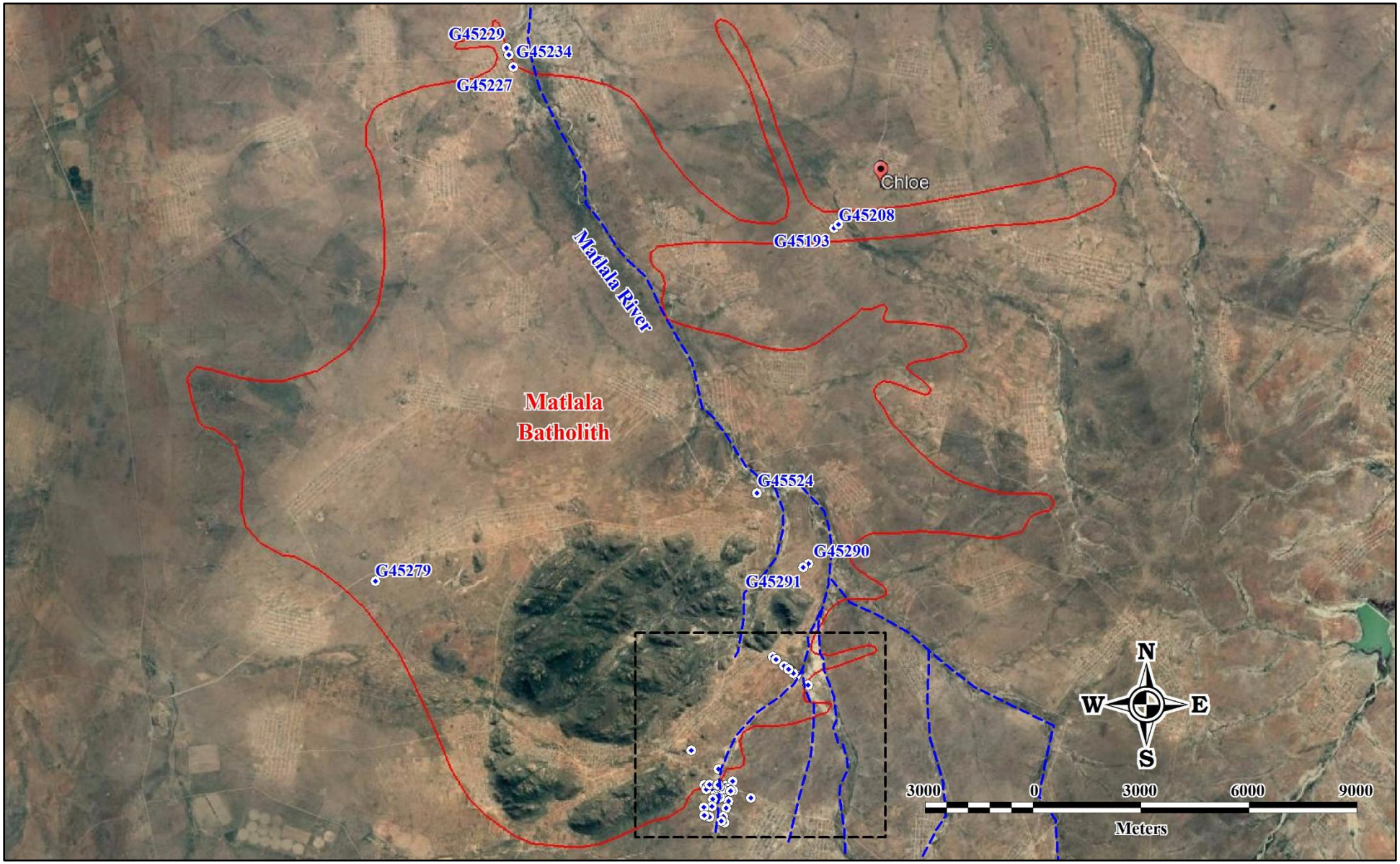

Figure 5.2: Boreholes included in the recharge investigations (boreholes within the dashed rectangular area are numbered in Figure 5.3 and Figure 5.4)

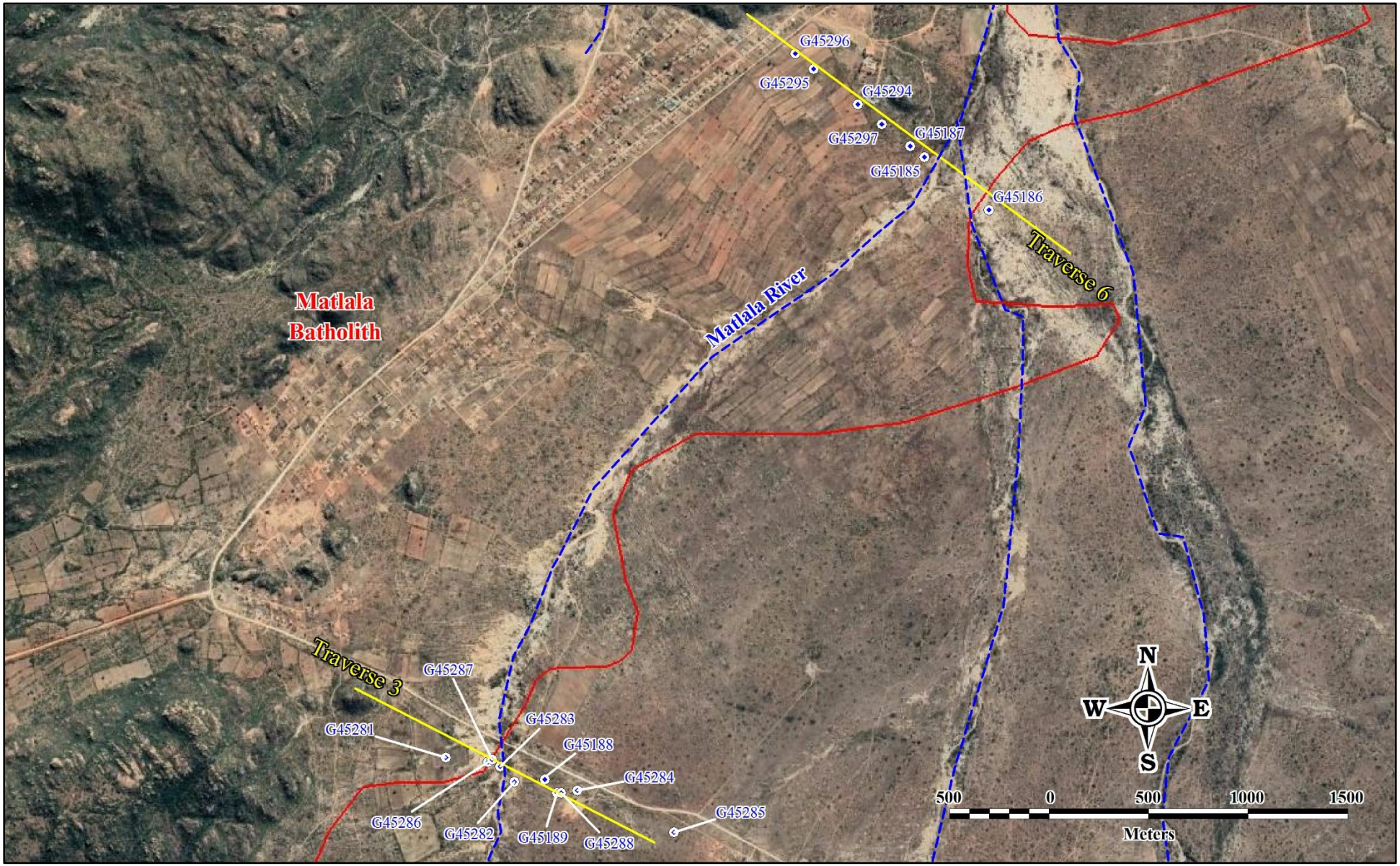

Figure 5.3: Boreholes along two geophysical traverses across the south-eastern boundary of the Matlala Batholith outcrop

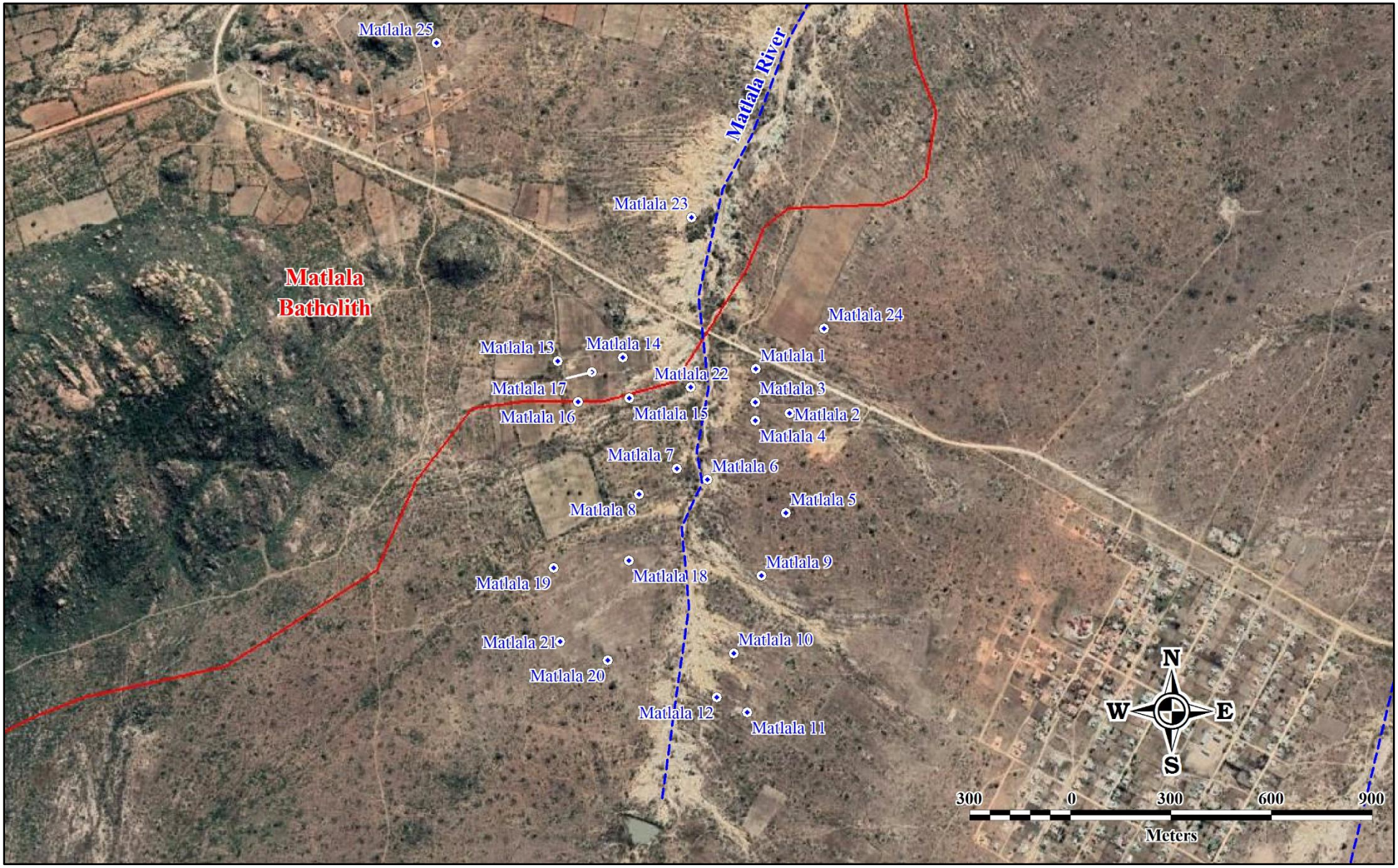

Figure 5.4: Boreholes in the Matlala wellfield near the south-eastern perimeter of the Matlala Batholith

Table 5.1: Information on the boreholes selected for the recharge investigations (borehole along geophysical traverses)

Longitude (^{o}E)	Latitude (^{o}S)	Site name	Borehole number	Elevation (mamsl)	Static water level (mbgl)	Static water level (mamsl)	Borehole depth (m)	Water strike (mbgl)	Date drilled	Yield (L/s)
29.0695	-23.7873	G45185	H04 1047	1230	5.54	1224.46	144	39	05/08/1997	<0.1
29.0727	-23.7897	G45186	H04 1048	1225	5.48	1219.52	156	13, 16, 62	08/08/1997	2.0
29.0688	-23.7868	G45187	H04 1046	1238	7.29	1230.71	150	None	19/08/1997	Dry
29.0509	-23.8156	G45188	H04 0984	1268	14.40	1253.60	120	31, 39, 43, 60	18/11/1997	7.7
29.0515	-23.8162	G45189	H04 1049	1271	16.59	1254.41	138	33, 60, 75	04/02/1998	5.75
29.0460	-23.8146	G45281	H04 0991	1265	10.84	1254.16	150	31	20/06/1997	3
29.0494	-23.8157	G45282	H04 0986	1262	12.12	1249.88	150	30, 56-57, 108-110	25/06/1997	6
29.0487	-23.8150	G45283	H04 0989	1259	6.92	1252.08	126	24, 46, 60, 72	01/07/1997	40
29.0525	-23.8161	G45284	N/A	1274	16.32	1257.68	138	33, 59, 62, 68, 115	11/07/1997	20
29.0573	-23.8180	G45285	H04 0987	1291	34.51	1256.49	156	36, 60, 108	15/07/1997	4,0
29.0481	-23.8148	G45286	H04 0990	1261	6.34	1254.66	78	14, 32, 56	16/07/1997	8
29.0483	-23.8147	G45287	N/A	1261	6.51	1254.49	150	8, 21-24, 33, 40, 42, 46	31/07/1997	40-60
29.0517	-23.8162	G45288	H04 0985	1271	16.74	1254.26	72	30, 52, 62	06/08/1997	8
29.0662	-23.7849	G45294	H04 1044	1235	11.35	1223.65	144	31, 43	09/10/1997	1
29.0640	-23.7833	G45295	H04 0982	1232	19.17	1212.83	126	30, 122	17/10/1997	3
29.0631	-23.7826	G45296	H04 0986	1232	19.50	1212.50	120	24	21/10/1997	0.6
29.0674	-23.7858	G45297	H04 1045	1242	16.50	1225.50	120	None	23/10/1997	Dry

Note: mbgl – metre below ground level; mamsl – metre above mean sea level

Table 5.2: Information on the boreholes selected for the recharge investigations (borehole in the Matlala wellfield)

Longitude (°E)	Latitude (°S)	Site name	Borehole number	Elevation (mamsl)	Static water level (mbgl)	Static water level (mamsl)	Borehole depth (m)	Water strike (mbgl)	Date drilled	Yield (L/s)
29.0503	-23.8149	Matlala 1	H04-1457	1269	9.59	1259.41	84	6, 23, 35, 41, 68	N/A	N/A
29.0513	-23.8161	Matlala 2	H04-1049	1275	22.49	1252.51	138	33, 60, 75	N/A	N/A
29.0503	-23.8158	Matlala 3	H04-0986	1272	12.12	1259.88	150	30, 55, 108	N/A	N/A
29.0503	-23.8163	Matlala 4	H04-2281	1273	12.82	1260.18	102	12, 31, 65, 74	08/06/2006	>10
29.0512	-23.8188	Matlala 5	H04-2264	1280	20.14	1259.86	72	10, 25, 34	09/03/2006	Dry
29.0489	-23.8179	Matlala 6	H04-1459	1270	21.86	1248.14	54	11, 21, 34, 39, 45	N/A	N/A
29.0480	-23.8176	Matlala 7	H04-1456	1270	21.84	1248.16	24	3, 6, 16	N/A	N/A
29.0469	-23.8183	Matlala 8	H04-2280	1271	12.65	1258.35	102	24, 37, 68	05/06/2006	>8
29.0505	-23.8205	Matlala 9	H04-2265	1278	15.44	1262.56	72	10, 17, 29, 49	10/03/2006	Dry
29.0497	-23.8226	Matlala 10	H04-2266	1278	12.35	1265.65	102	18, 25	15/03/2006	Dry
29.0501	-23.8242	Matlala 11	H04-2267	1282	16.62	1265.38	102	7, 28, 52	16/03/2006	Dry
29.0492	-23.8238	Matlala 12	H04-2268	1281	14.14	1266.86	72	15, 21, 36, 52	21/03/2006	Dry
29.0445	-23.8147	Matlala 13	H04-2277	1276	9.76	1266.24	102	5,16	15/05/2006	Dry
29.0464	-23.8146	Matlala 14	H04-2274	1273	10.61	1262.39	102	40	03/05/2006	1.5
29.0466	-23.8157	Matlala 15	H04-2278	1271	11.38	1259.62	102	8, 16, 26, 31	17/05/2006	Dry
29.0451	-23.8158	Matlala 16	H04-2275	1276	14.7	1261.3	102	N/A	17/05/2006	Dry
29.0455	-23.8150	Matlala 17	H04-2276	1277	13.6	1263.4	102	16, 24, 29, 94	09/05/2006	0.5
29.0466	-23.8201	Matlala 18	H04-2271	1280	15.57	1264.43	102	13, 27, 37, 46, 61, 77	06/04/2006	7
29.0444	-23.8203	Matlala 19	H04-2273	1283	21.83	1261.17	102	43, 54, 79, 82	11/04/2006	4
29.0460	-23.8228	Matlala 20	H04-2269	1278	15.24	1262.76	102	7, 19, 32, 45	24/03/2006	0.3
29.0446	-23.8223	Matlala 21	H04-2270	1280	22.24	1257.76	112	31, 35, 45	06/04/2006	3
29.0484	-23.8154	Matlala 22	H04-0988	1265	21.78	1243.22	150	8, 22, 33, 40, 46	N/A	N/A
29.0484	-23.8108	Matlala 23	H04-1460	1258	21.83	1236.17	102	N/A	N/A	N/A
29.0523	-23.8138	Matlala 24	H04-1461	1269	13.014	1255.986	72	6, 18, 39, 63	N/A	N/A
29.0409	-23.8061	Matlala 25	H04-1458	1291	18.53	1272.47	102	24, 46, 60, 72	N/A	N/A

Note: mbgl – metre below ground level; mamsl – metre above mean sea level

5.2.1 Borehole and groundwater information

The depths of the selected boreholes vary from shallow (<25 mbgl) to very deep (156 mbgl) (see Table 5.1 and Table 5.2), and depend on the geological setting in which the boreholes were drilled. The depth follows a bimodal distribution (see Figure 5.5), with 78% of the boreholes drilled to depths >100 mbgl, and 28% of them drilled to depths of between 100 and 109 mbgl. Nineteen per cent of the boreholes represent the deep boreholes drilled to depths of between 150 and 160 mbgl. This frequency distribution graph is markedly similar to that of depth to first water strike (see Figure 5.6), although fewer boreholes were used to construct the distribution graph. This gives an indication that for some of the boreholes, drilling was stopped once a sufficient water strike was reached.

Eighty-eight per cent of the boreholes encountered their first water strike at a depth below 40 m (Figure 5.6), with an average depth of 13 m. Most boreholes had multiple water strikes with depths ranging between 3 and 115 mbgl, indicating that multiple aquifers were intersected during drilling. The static water levels measured in the boreholes may therefore represent the maximum hydraulic head of the different aquifers intersected, and not the water table of the shallow unconfined aquifer. Figure 5.7 illustrates the distribution of groundwater levels; it is clear that majority of the boreholes have shallow groundwater levels less than 21 mbgl.

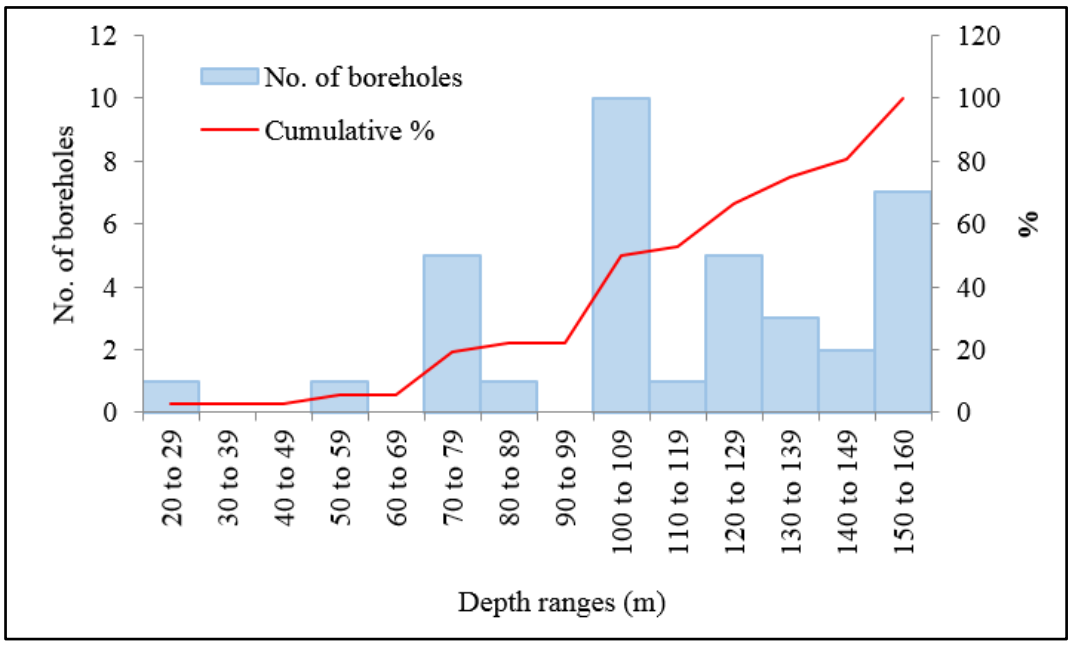

Figure 5.5: Depth distribution of boreholes selected for recharge estimation

Groundwater level data in the selected boreholes were collected and evaluated on a quarterly basis by the DWS. Automatic data loggers were used to record groundwater level data and were set to record a reading on an hourly basis and corrected using hand measurement data, if any drift was identified. The monitoring data was collected from 2007 to 2013 by the groundwater monitoring team

from DWS as part of the Matlala Groundwater Monitoring Project. The results are displayed in Figure 5.7.

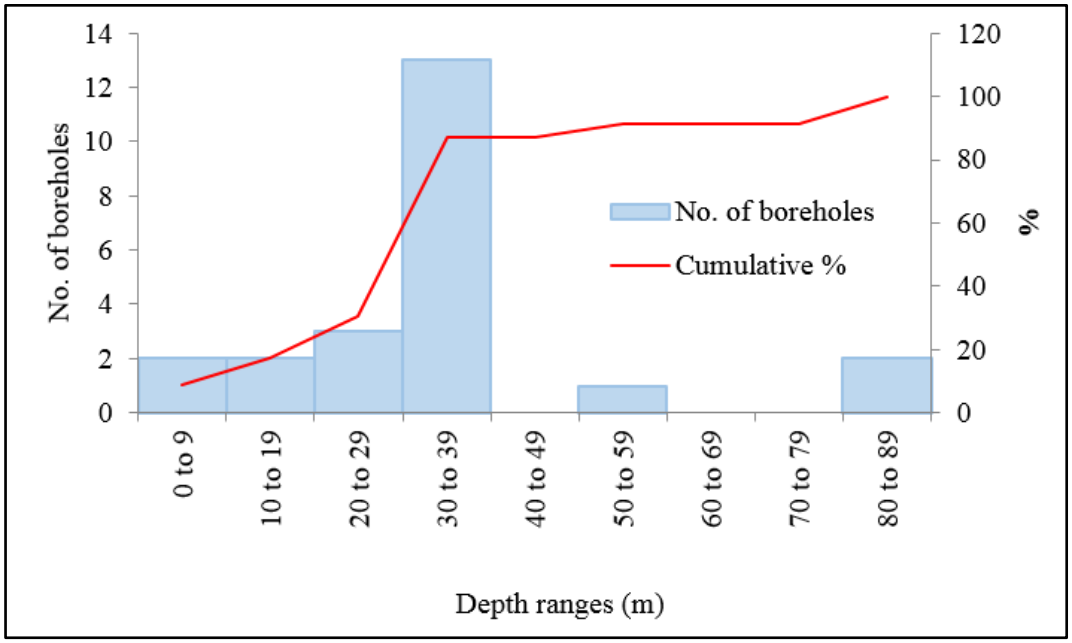

Figure 5.6: Depth distribution of first water strikes in boreholes selected for recharge estimation

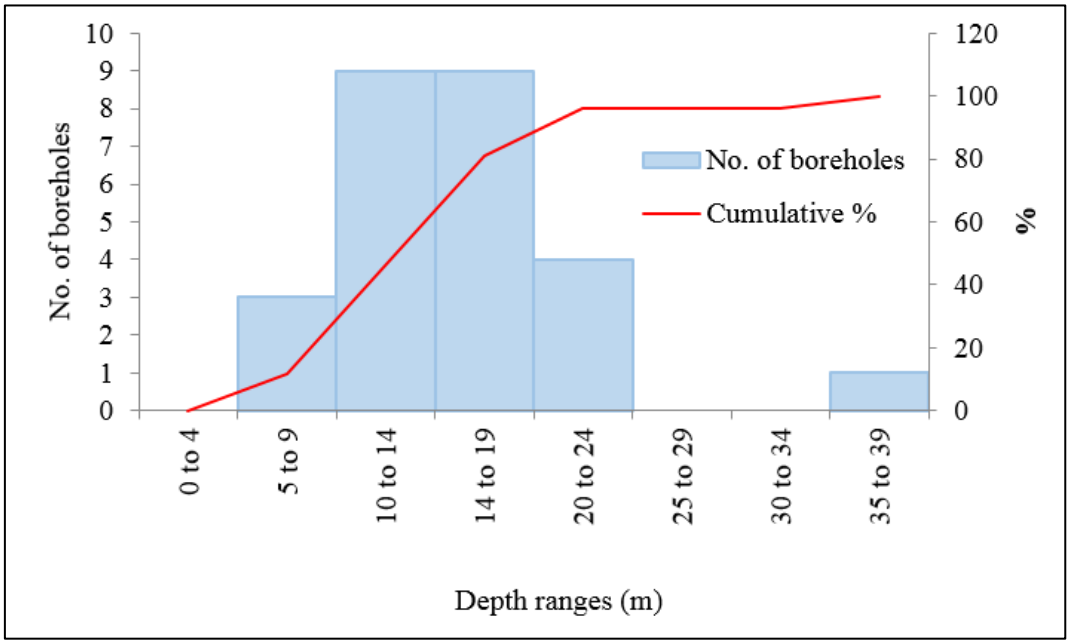

Figure 5.7: Distribution of groundwater levels in Ga-Matlala

Trends in the annual average groundwater levels in selected boreholes are shown in Figure 5.8. It is seen that the most prominent increases in the groundwater levels occurred in 2010 while the lowest levels were observed in 2007. The trends observed in Figure 5.8 indicate that the average groundwater level was increasing over the monitoring period. The increase in groundwater level may be due to the overall increasing trend in the annual precipitation between 2007 and 2013, as seen in Figure 3.6. As

an example, Figure 5.9 shows the relationship between rainfall and water level in Matlala 3. The graph shows that when there is cumulative rainfall over a certain period, there is a positive response in the water level as a result of the field capacity of the unsaturated zone being exceeded, thereby causing recharge. The fact that the water level trends shown in Figure 5.8 all emulate one another shows that all these boreholes were similarly affected by rainfall. This observation strongly suggests that water levels in these boreholes represent the hydraulic heads of the same aquifer system.

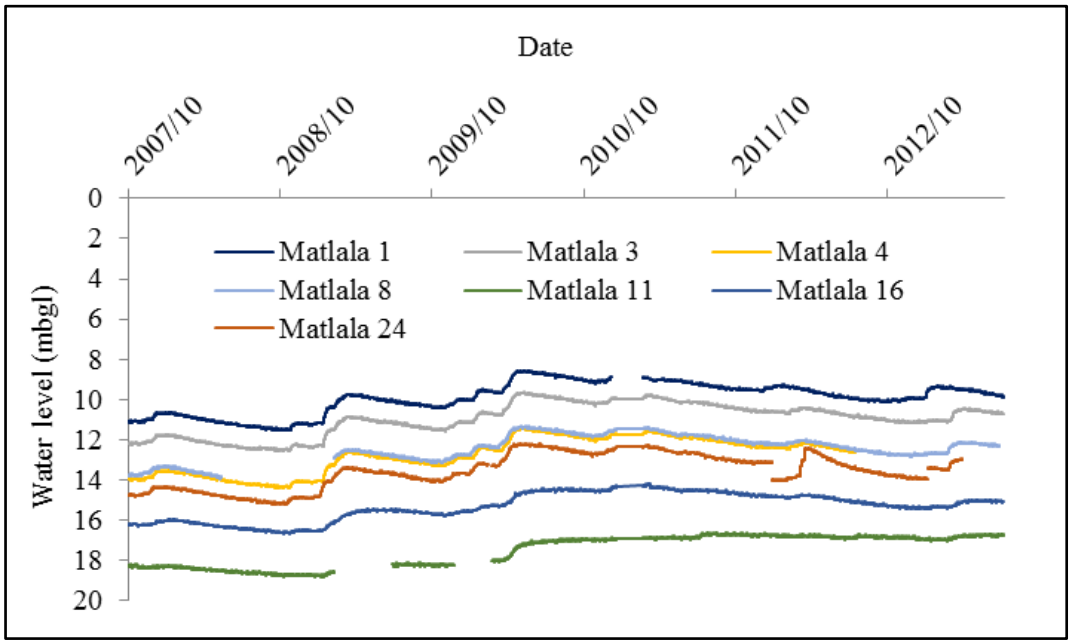

Figure 5.8: Trends in the average annual groundwater levels for selected boreholes

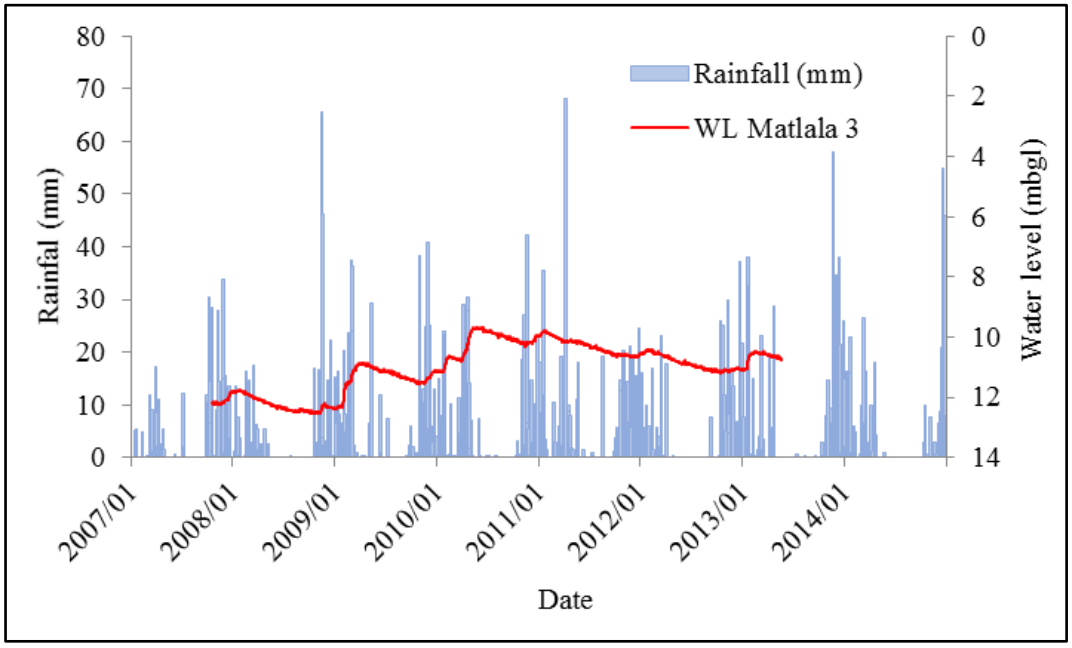

Figure 5.9: Daily rainfall data for the Matlala area and the corresponding groundwater level data recorded in borehole Malala 3.

Figure 5.10 shows the groundwater elevations in the boreholes selected for recharge estimation plotted against the topographic elevations of these boreholes. Some boreholes were drilled along straight lines across the contact of the batholith with the host rocks (refer to Figure 5.3) in order to locate and investigate the contact. Boreholes in the wellfield are located at high elevations in the south and lower elevations along the flow direction of the non-perennial Matlala River (refer to Figure 5.4). The static water levels measured in 2013 and the elevation data for the respective boreholes were used to construct a correlation plot (Figure 5.10). The graph shows a strong linear correlation between surface elevation and static water level ($R^2 = 0.88$). This indicates that the groundwater table in the study area generally emulates the surface topography, and that groundwater flow generally follows the local topographic gradient. The generally small deviation of the boreholes from the linear regression line also suggests that the boreholes intersect the same aquifer system.

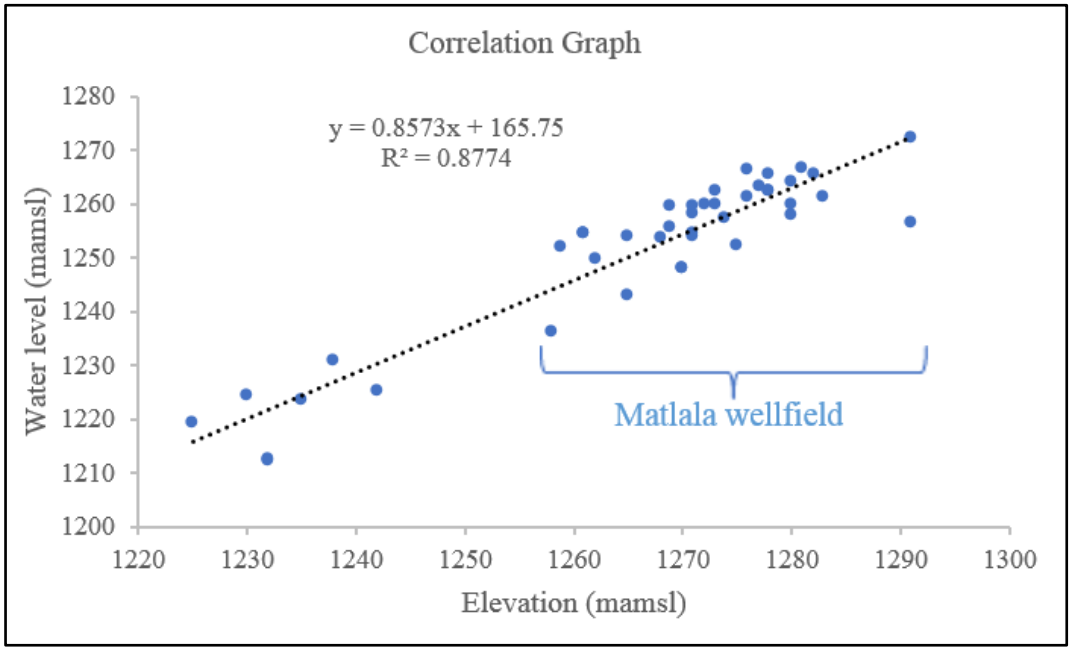

Figure 5.10: Graph showing the correlation be the observed groundwater levels and the borehole elevation

Groundwater elevation data from the dry season of 2013 were used to generate a contour map illustrating the distribution of the groundwater elevations in the Matlala wellfield (Figure 5.11). The groundwater elevation ranges from 1236 to 1272 mamsl and displays a regional gradient to the north-east. Locally, gradients are observed towards the non-perennial Matlala River along which the groundwater elevations are notable lower. The lower groundwater elevations along the river are most likely due to the lower surface topography associated with the river, since there is a good correlation between topographic elevation and groundwater elevation (Figure 5.10).

It should be noted that the groundwater contours shown in Figure 5.11 represent conditions during the dry season. No data were available to construct contours for the rainy season. However, during

times that the Matlala River carries water, groundwater recharge from the river can be expected. During these times the groundwater elevations in the vicinity of the river are expected to exceed the elevations at positions displaced from the river, so that the hydraulic gradient will then be away from the river at positions along its banks.

5.3 GROUNDWATER QUALITY CHARACTERISATION

5.3.1 Groundwater sampling

A trailer-mounted submersible-type sampling pump was used for the sampling of boreholes. Sampling was done at the main water strike. Purging was done to remove all the stagnant water in the hole and to ensure a clean and representative sample. A volume equal to three times the volume of the borehole was abstracted during purging.

5.3.2 Results of the 1998 sampling event

The results of the chemical analyses performed on a total of 13 boreholes sampled during 1998 are listed in Table 5.3. This table lists the major ion, SiO_2 and TDS concentrations, as well as the EC and pH values of the groundwater samples from the various boreholes. The listed data can be used to evaluate the water chemistry within the weathered and fractured aquifer system in the study area.

5.3.3 Evaluation of the 1998 data

The major cations in the 13 boreholes with data from 1998 expressed one order of abundance. The order moved from $Na^+ > Ca^{2+} > Mg^{2+} > K^+$. The average order of cations for all boreholes showed $Na^+ > Ca^{2+} > Mg^{2+} > K^+$, with concentrations of 192.8 mg/L, 51.8 mg/L 39.5 mg/L and 8.1 mg/L, respectively. The major anions also showed consistency in one order of abundance in 12 boreholes. The order moved from $Cl^- > HCO_3^- > SO_4^{2-} > NO_3^-$. Borehole G45208 had a slightly different order of abundance. The order moved from $Cl^- > HCO_3^- > NO_3^- > SO_4^{2-}$. The average values for anions did not match the order $Cl^- > HCO_3^- > SO_4^{2-} > NO_3^-$. HCO_3- had higher concentration than Cl^-, which changed the average order to $HCO_3^- > Cl^- > SO_4^{2-} > NO_3^-$, with concentrations of 376.6 mg/L, 203.1 mg/L, 59.7 mg/L, and 18.6 mg/L, respectively. Nevertheless, NO_3- is the least abundant anion in all the samples.

Table 5.3 shows the recommended water quality standards according to SANS 241:2006 for drinking water. Based on the analysis, the following is observed:

- The pH values of all boreholes fall within the recommended limits for drinking water.

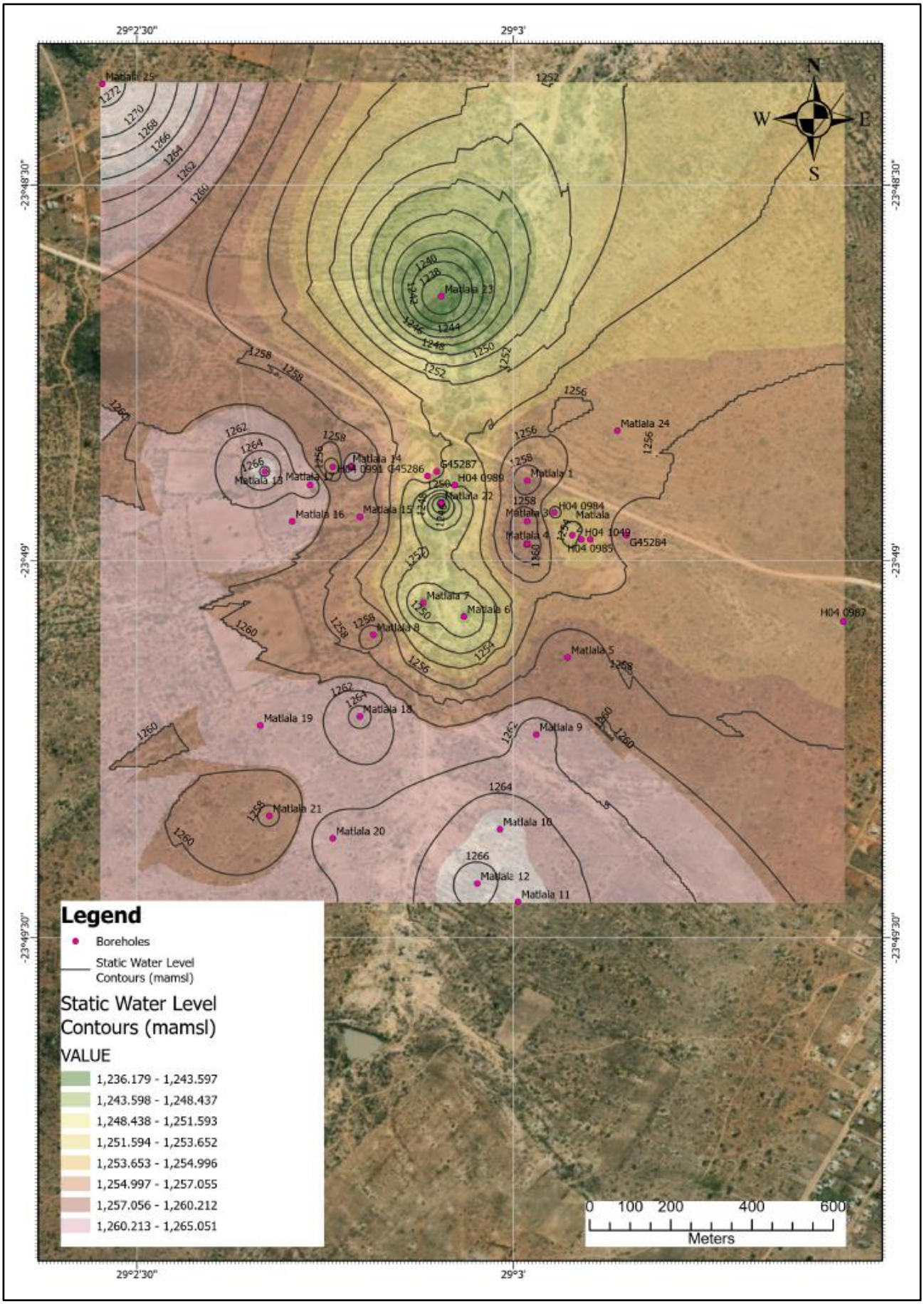

Figure 5.11: Contour map of the 2013 groundwater levels at the Matlala wellfield

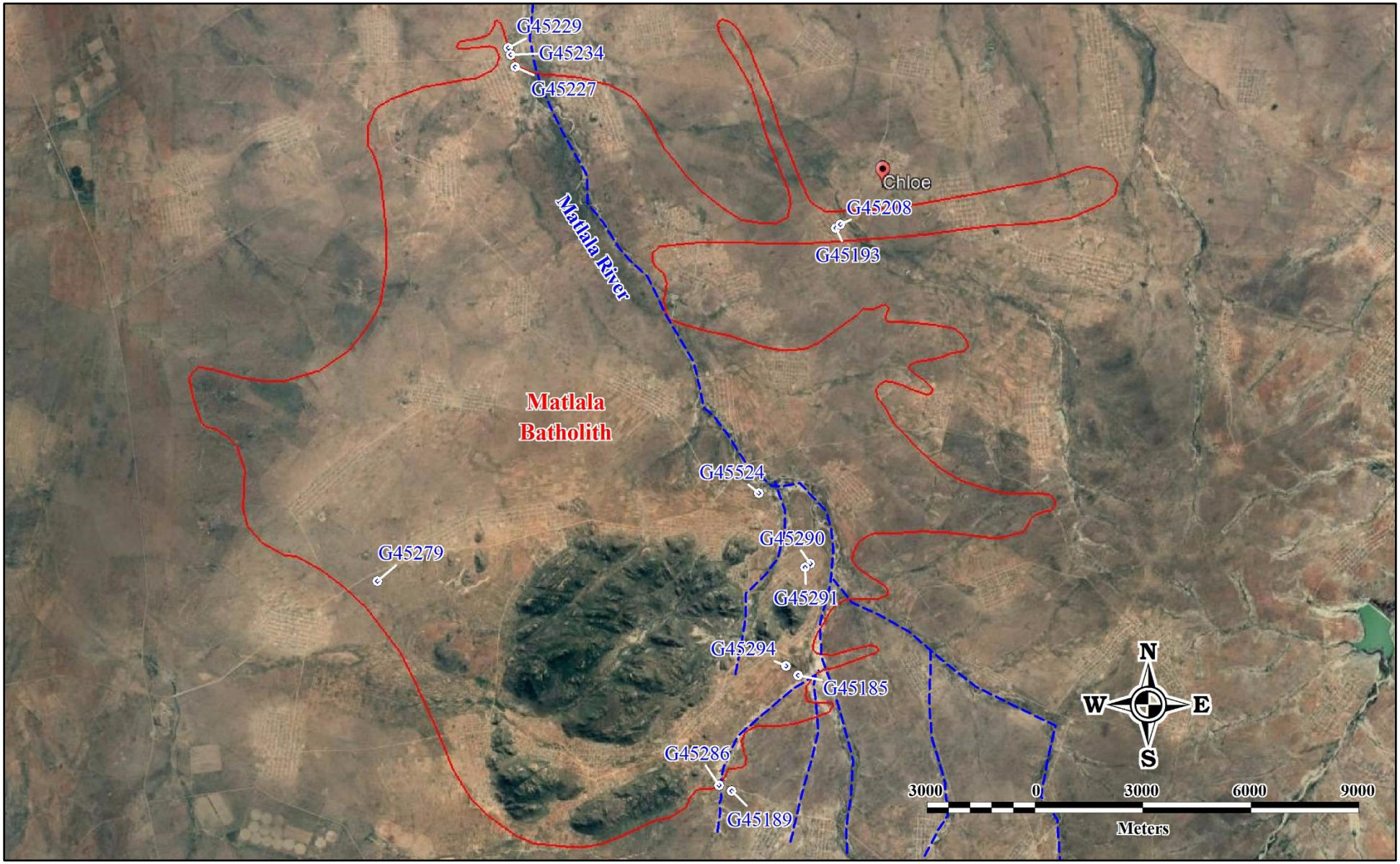

Figure 5.12. Boreholes sampled during the 1998 sampling run

Table 5.3: Results of the chemical analyses performed on the groundwater samples from the study area (1998)

	Determinants	pH	EC	TDS	Na	Ca	Mg	K	HCO_3	Cl	SO_4	NO_3	SiO_2	F
Standards (SANS 241:2006)	**Recommended limits**	5.0-9.5	<150	<1000	<200	<150	<70	<50	-	<200	<400	<10	-	<1.0
	Maximum limits	4-10	150-370	1000-2400	200-400	150-300	70-100	50-100	-	200-600	400-600	10-20	-	1.0-1.5
	Above maximum limits	>10	>370	>2400	>400	>300	>100	>100	-	>600	>600	>20	-	>1.5
Borehole number	**G45279**	7.70	511	3022	547	206	195	18.8	399	1555	84	2.4	17.1	2.2
	G45286	8.20	75.4	565	82	32	32	5.5	291	65	10	9.3	30.3	0.5
	G45189	7.97	37.0	275	39	12	15	5.0	159	18	6	4.2	27.9	0.5
	G45227	8.30	165	1536	406	15	14	7.7	712	170	82	23.2	35.0	3.4
	G45229	8.22	72.0	585	270	17	14	6.1	706	60	16	0.9	34.5	1.2
	G45234	8.31	64.4	566	120	16	12	3.2	376	9	17	0.8	31.9	1.0
	G45291	8.40	113	890	182	32	25	6.5	362	71	52	32.6	14.9	3.1
	G45524	8.10	63.4	478	50	42	25	4.2	233	3	25	14.3	31.9	4.6
	G45290	8.50	106	861	195	27	24	5.8	376	54	40	36.1	29.9	3.1
	G45294	8.20	39.2	314	36	25	13	6.5	153	10	14	11.9	18.4	0.8
	G45185	8.00	59.9	488	67	36	20	7.7	299	45	8	0	20.2	1.4
	G45208	8.11	165	1113	177	83	50	7.9	401	223	24	31.3	15.6	0.4
	G45193	8.00	268	2084	336	131	74	21	429	357	398	74.8	33.9	0.4

- The TDS values for Boreholes G45279, G45286, G45189, G45227, G45229, G45234, G45291, G45524, and G45290 ranged from 275 to 890 mg/L. The geochemical constituents fall below the recommended limits, except for Boreholes G45227, G45208, and G45193 which have TDS values above the recommended limit but still fall below the maximum limit. Borehole G45279 has a value above the maximum limits. If the TDS value is <1 000 mg/L, the water is suitable for domestic use. These TDS values also suggest that some of the boreholes might have interactions with meteoric water. Boreholes with TDS values ranging from 1 113 to 3 022 mg/L give an indication of groundwater mineralisation taking place. The high TDS concentrations are attributed to long-term groundwater circulation within the aquifer and/or agricultural activities.
- Boreholes G45227, G45291, G45524, G45290, G45294, G45208, and G45193 show high concentration of F^- and NO_3^-. The latter is due to pollution of the groundwater. Borehole G45279 showed values above the maximum limit in Na, Ca, Mg, and Cl.

Hydrochemical (water type) classification

A Piper diagram (see Figure 5.13) was constructed using the groundwater chemistry data. This was done to determine the main water types in the study area based on how certain ions were expressed in the water. Deductions on the water type were then made from the distribution of the samples on the Piper diagram.

From the Piper diagram, the following water types can be identified:

- The water type for boreholes G45227, G45229, and G45234 is Na-HCO_3. This water type was likely formed as a result of the evolvement of Ca-HCO_3 rainwater produced during the weathering of clay in the area.
- Boreholes G45291 and G45290 show a mixed water type of Ca-Na HCO_3.
- Boreholes G45189, G45185, G45294, and G45524 show a water type of Mg-HCO_3, which could be as a result of ion exchange in the ferromagnesium rocks, evident in the drilling log (see **Appendix A**).
- Boreholes G45279 and G45208 have a mixed water type of Ca-Mg-Cl.
- Lastly, Borehole G45193 has a Na-Cl water type, formed as a result of a lengthened groundwater resident time and low recharge. This borehole had a low estimated recharge of 0.06% of the MAP (Table 5.5). The dominating cations in most of the boreholes are Na and K and the dominant anion is HCO_3.

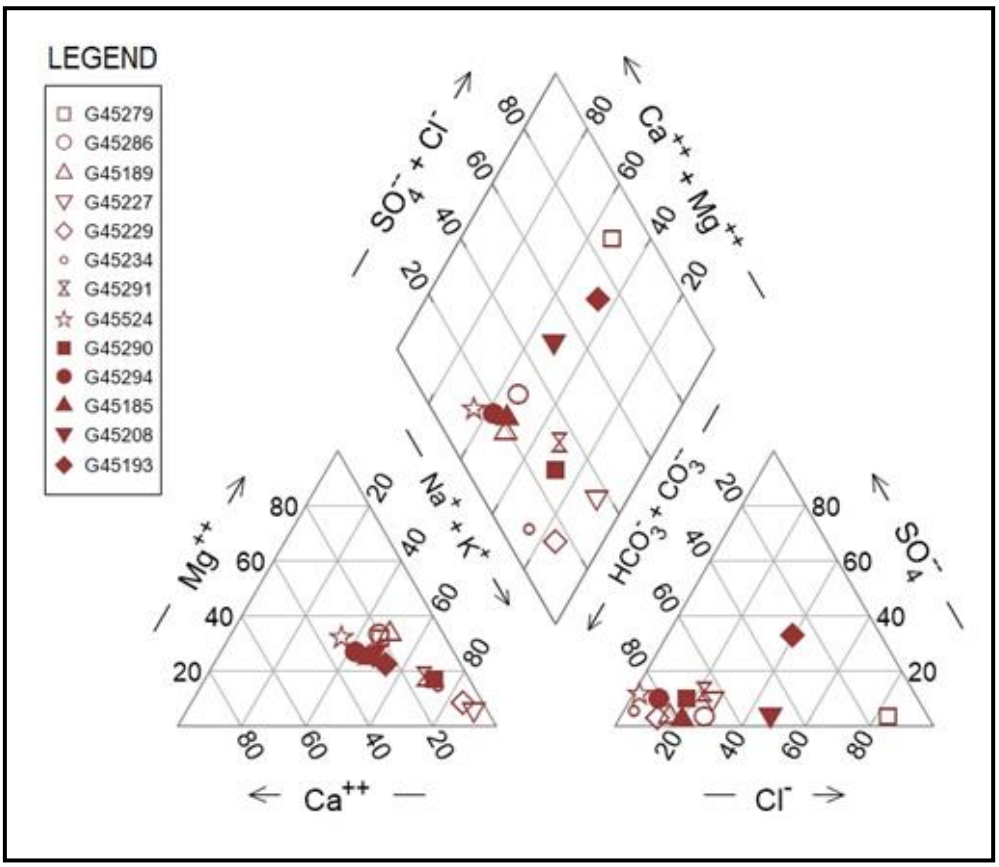

Figure 5.13 Piper diagram showing water types for boreholes drilled around the Matlala Batholith

5.3.4 Results of the 2017 sampling events

The results of the chemical analyses performed on groundwater samples collected during the two sampling events of 2017 are listed in Table 5.4. Unfortunately, the 2017 sampling runs were very limited and only three boreholes along the non-perennial Matlala River were sampled. These boreholes were different from those of the 1998 sampling event. In addition, one of the boreholes was located approximately 16 km north-west of the Matlala Batholith, outside the current study area. The three boreholes were, however, sampled twice in 2017: once in the spring season and once in autumn. The data from these two sampling events allow some insight into the seasonal changes in the groundwater quality.

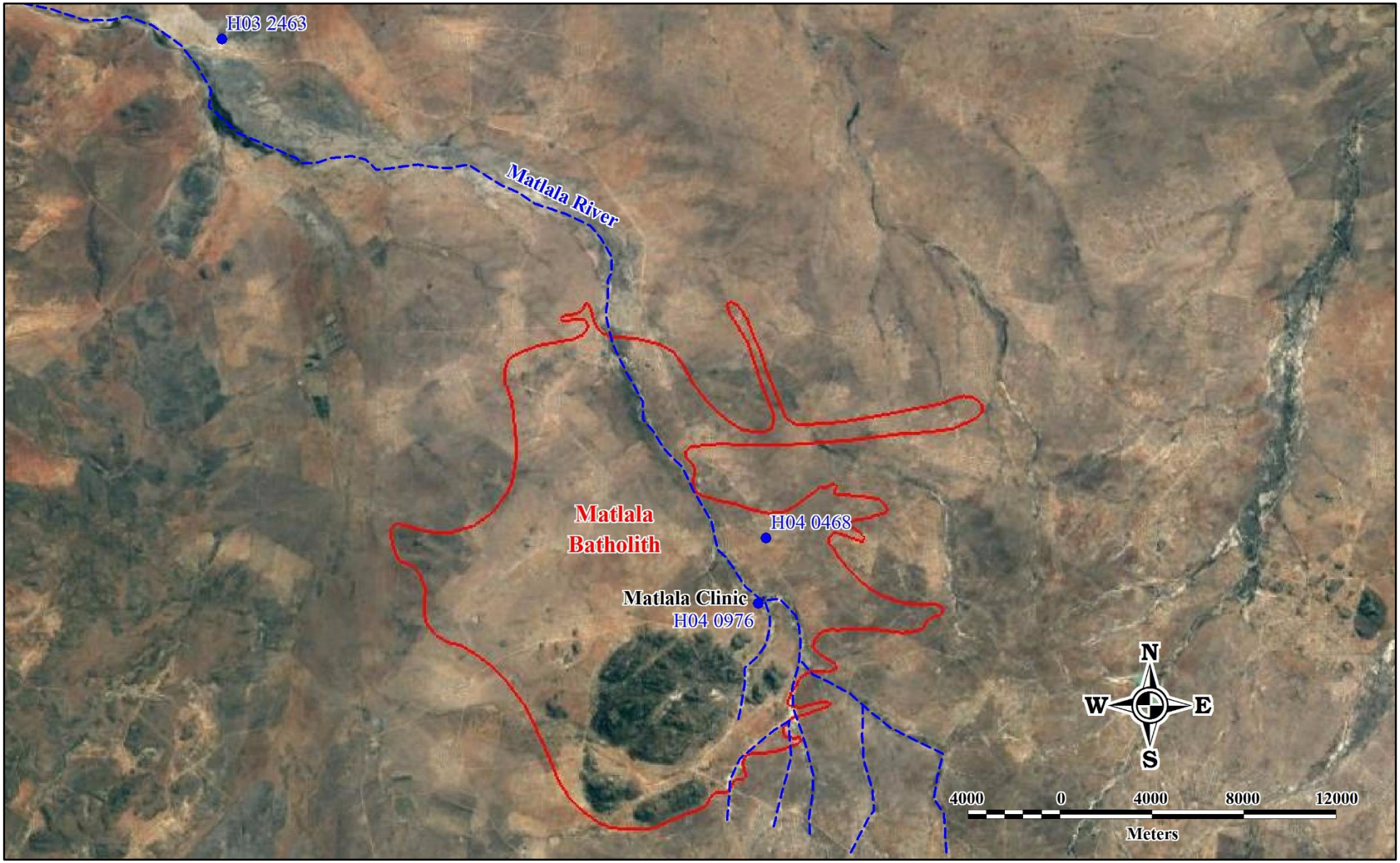

Figure 5.14. Boreholes sampled during the 2017 sampling run

Table 5.4: Results of the chemical analyses performed on the groundwater samples from the study area (2017)

	Determinants	pH	EC	TDS	Na	Ca	Mg	K	HCO_3	Cl	SO_4	NO_3	SiO_2	F
Standards (SANS 241:2006)	**Recommended limits**	5.0-9.5	<150	<1000	<200	<150	<70	<50	-	<200	<400	<10	-	<1.0
	Maximum limits	4-10	150-370	1000-2400	200-400	150-300	70-100	50-100	-	200-600	400-600	10-20	-	1.0-1.5
	Above maximum limits	>10	>370	>2400	>400	>300	>100	>100	-	>600	>600	>20	-	>1.5
Spring 2017														
Borehole number	**H04 0976**	8.90	93.1	758	155	27.8	23.7	4.60	431	47.3	6.7	5.83	39.2	1.88
	H04 0468	8.70	118	-	139	27	44.1	9.50	260	200.4	34	16.92	36.1	0.52
	H03 2463	8.70	339	2320	589	36.1	69.2	24.9	654	688	145	18.2	38.0	1.15
Autumn 2017														
Borehole number	**H04 0976**	8.90	92.1	758	172	13.5	22.3	5.60	431	49.8	10.5	3.87	39.0	1.80
	H04 0468	7.20	113.7	776	127	32.6	42.7	10.50	306	179.3	21.6	12.60	32.2	0.34
	H03 2463	8.90	331	2081	531	12.1	74.6	26.7	451	656	224	15.7	40.4	0.89

5.3.5 Evaluation of the 2017 data

5.3.5.1 Spring season

The major cations in Borehole H04 0976 showed the same order of abundance as the results from 1998. The order moved from $Na^+ > Ca^{2+} > Mg^{2+} > K^+$; however, Borehole H03 2463 exhibited a slight change in the above order of abundance as it moved from $Na^+ > Mg^{2+} > Ca^{2+} > K^+$.

For the major anions, there is consistency in one order of abundance for Boreholes H03 2463 and H04 0468: their order moves from $Cl^- > SO_4^{2-} > HCO_3^- > NO_3^-$. Borehole H04 0976 shows a slight difference as it moves from $Cl^- > HCO_3^- > SO_4^{2-} > NO_3^-$.

Table 5.4 shows the recommended water quality standards according to SANS 241: 2006 for drinking water. Based on the analysis, the following is observed:

- The pH values of all three boreholes fall within the recommended limits for drinking water.
- EC values of boreholes located upstream (H04 0976 and H04 0468) fall within the recommended limit; however, Borehole H03 2463, which is downstream, has a higher EC value that falls within the maximum limit.
- The TDS value for Borehole H04 0976 is 758.046 mg/L. The geochemical constituents fall below the recommended limits, except for Borehole H03 2463 that has a TDS value above the recommended limit but still falls below the maximum limit. If the TDS value is <1 000 mg/L, the water is suitable for domestic use. These TDS values also suggest that some of the boreholes might have interactions with meteoric water. Borehole H03 2463, located downstream, with TDS values >2 000 mg/L gives an indication of groundwater mineralisation taking place, which is attributed to long-term groundwater circulation within the aquifer and/or agricultural activities.
- The Cl concentration differs in all three boreholes. The Cl concentrations for boreholes upstream (H04 0976 and H04 0468) fall within the maximum recommended limits, while Borehole H03 2463, which is located downstream, has a Cl value above the recommended maximum limit.
- Lastly, Borehole H04 0976 has a high concentration of F^-. The latter is due to pollution of the groundwater.

Hydrochemical (water type) classification: spring season

A Piper diagram (see Figure 5.15) for the spring season was constructed using the groundwater chemistry data for the three boreholes. Deductions of the water type were made from the distribution of the samples on the Piper diagram.

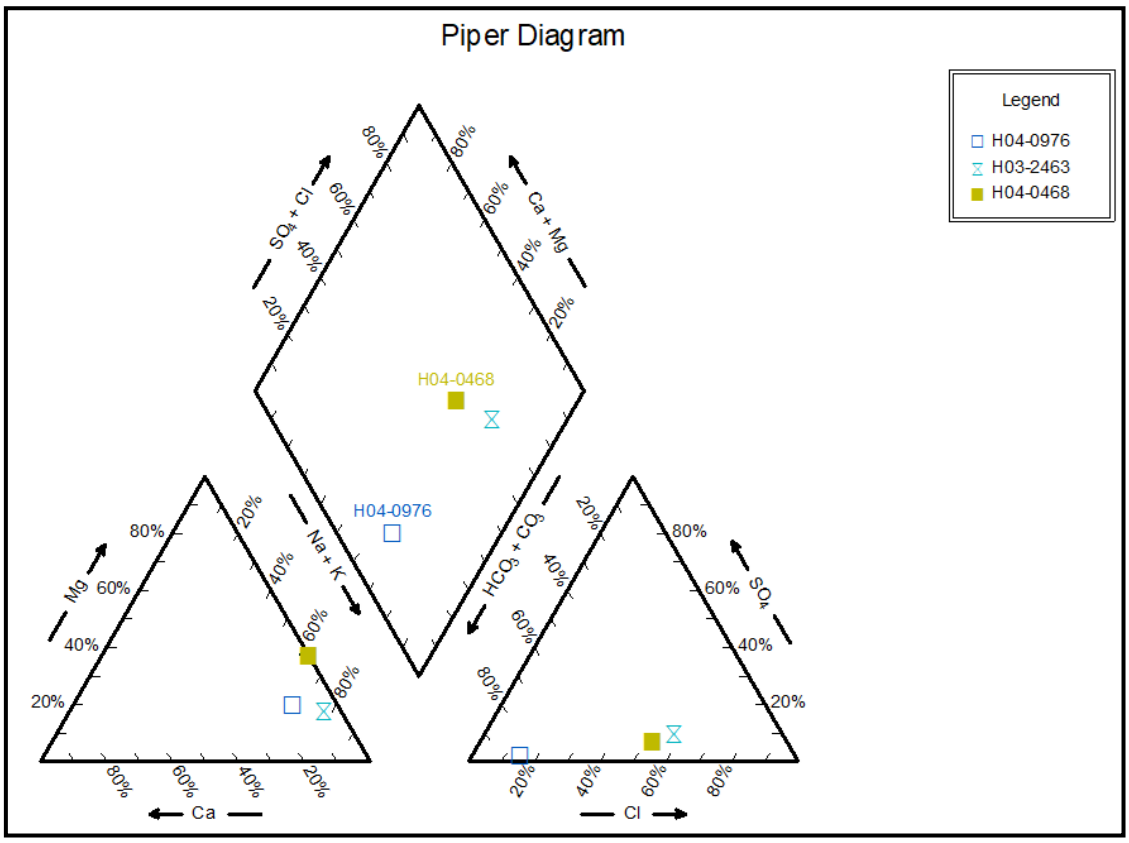

Figure 5.15 Piper diagram generated using the spring season results (a total of three samples were plotted)

Sodium bicarbonate water type

This water type is represented by Borehole H04 0976, which is located upstream in the study area. Based on results obtained from the recharge estimation methods, boreholes upstream receive fairly higher recharge as compared to those located midstream and downstream. This water type was probably formed as a result of the evolvement of Ca-HCO_3 rainwater. During cation exchange, the Ca-rich recharge water exchanges the Ca for Na and K and produces the Na-HCO_3 water type.

Sodium chloride water

This water type is represented by Boreholes H03 2463 and H04 0468, which are located midstream and downstream. This water type represents stagnant water or possibly old groundwater. Both boreholes followed the same order of cation and anion abundance as discussed above for Borehole H03 2463, which is located downstream and shows an excess of ions Na^+, Cl^-, HCO_3^-, SO_4^{2-}, EC, and TDS in solution through mineralisation. The CMB method indicated that boreholes in a semiconfined aquifer system that have high chloride content receive little recharge

5.3.5.2 Autumn season

The difference in the order of ions for spring and autumn season is discussed in this section. The major cations for all three boreholes exhibit the same order of abundance similar to that of Borehole

H03 2463 in the spring season (refer to Table 5.4). The order moved from $Na^+ > Mg^{2+} > Ca^{2+} > K^+$. The dominant order of abundance of the anion in autumn differ to that of the spring season, where it moves from $HCO_3^- > Cl^- > SO_4^{2-} > NO_3^-$; however, Borehole H03 2463 exhibits a similar order of abundance as the spring season. The order moves from $Cl^- > HCO_3^- > SO_4^{2-} > NO_3^-$. As compared to spring, the pH values of all three boreholes fall within the recommended limits for drinking water. Borehole H03 2463, which is located downstream, has EC, Na, and Cl values above the maximum limits, while in spring the EC value was within the recommended maximum limit. Similar to the spring season, Borehole H04 0976 has an F^- value above the maximum limit.

Hydrochemical (water type) classification: autumn season

A Piper diagram (see Figure 5.16) for the autumn season was also constructed using the groundwater chemistry data for the three sampled boreholes. Deductions of the water type were then made from the distribution of the samples on the Piper diagrams.

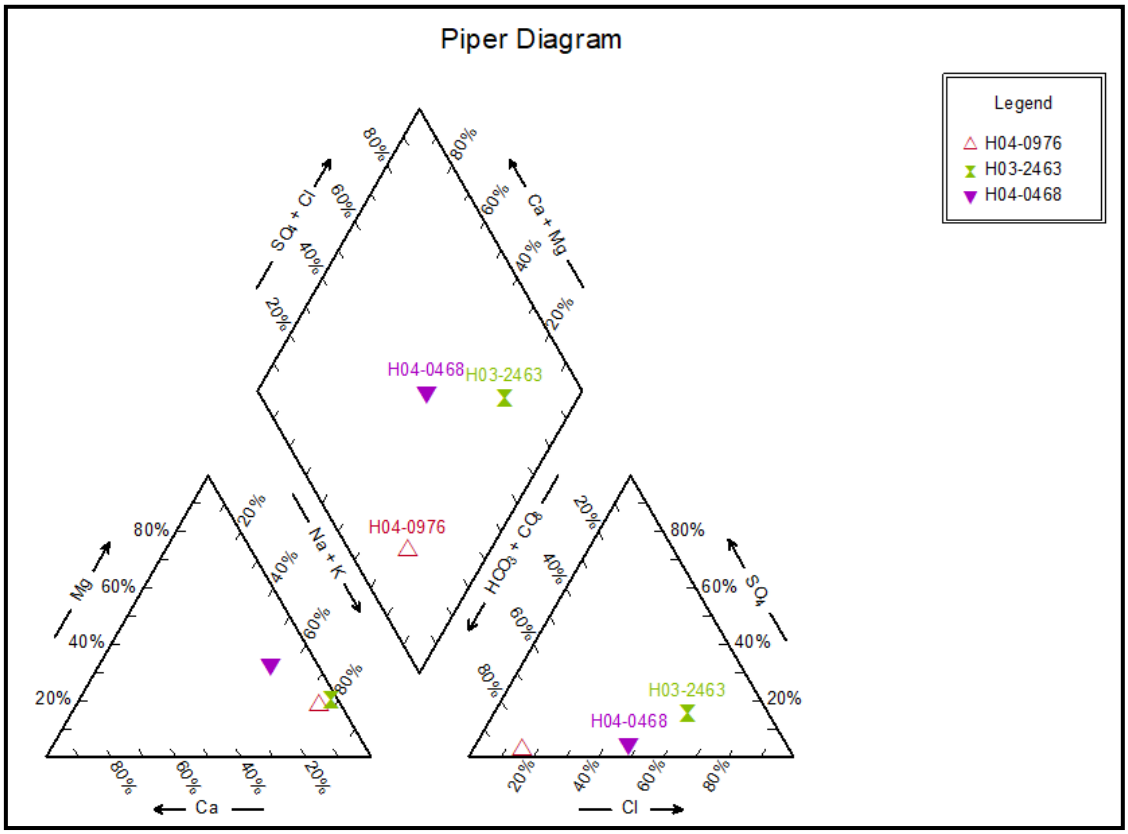

Figure 5.16 Piper diagram generated using the spring season results (a total of three samples were plotted)

Sodium bicarbonate water type

This water type is represented by Boreholes H04 0976 and H04 0468, which are located upstream and midstream respectively. In spring, Borehole H03 2463 represents the sodium chloride water type.

The change in water type is as a result of sample collection just after the rainy period. This borehole shows HCO_3^- as the highest ion (see Figure 5.16).

Sodium chloride water

In autumn, this water type was represented by Borehole H03 2463, which is located downstream.

The general conclusion regarding the classifications of water types is that little change occurred due to seasonal influences. However, Borehole H03 2463 showed a decrease in TDS from spring to autumn, while the pH of Borehole H04 0468 also decreased significantly. Since only two sampling events were available to evaluate temporal trends, it is not possible to state with certainty that these observed changes in the water chemistry represent real changes in the groundwater conditions. For example, it is possible that the lower pH-value observed in Borehole H04 0468 during the autumn season was an outlier that would have been revealed had more sampling events taken place. Water types identified included: sodium bicarbonate, sodium chloride, and mixed water.

5.4 RECHARGE ESTIMATION

5.4.1 Recharge Estimation Using the CMB Method

The groundwater chloride concentration was measured in 13 boreholes situated on six traverses along which geophysical data had previously been recorded (Figure 5.17, Figure 5.18). The ground geophysics for two of these traverses (Traverses 3 and 6) is discussed in Section 4.5.1. The chloride concentration recorded in these 13 boreholes were used for recharge estimation (Figure 5.19).

For all 13 boreholes, the long-term mean annual rainfall in the study area was taken as 484 mm, the average for the period 2007 to 2014, while the mean chloride concentration in rainwater for inland areas used was 0.2207 mg/L, as obtained from Xu and Van Tonder (2000). It is important to note that there was no long-term mean dry chloride deposition data in the study area. The mean chloride concentrations in groundwater for the 13 boreholes are listed in Table 5.5. This table also shows the estimated recharge rates calculated for each borehole.

The recharge estimation with the CMB method indicates that the study area experienced recharge ranging between 0.07 and 36.0 mm/year, representing 0.01% to 7.44% of the total precipitation received in the area. The highest recharge value was obtained at borehole G45524, which was drilled at the Matlala Clinic (Figure 5.17). Most of the boreholes on the eastern side of the study area intersect highly weathered and fractured rock. They occur along the non-perennial Matlala River. During periods of rainfall and flow, the permeable rocks allow recharge to take place, which suggests that there is an interaction between the surface and groundwater. Borehole G45279 near the western perimeter of the Matlala Batholith has a low estimated recharge of 0.07 mm/year, even though the geological log shows a fractured and weathered regolith (see **Appendix A**). The low calculated recharge rate is due to the high chloride value of 1 555 mg/L recorded in this borehole. Since all boreholes were purged prior to sampling (Du Toit, 2011), the high chloride value cannot be due to the presence of stagnant water in the borehole. The reason for the anomalously high chloride concentration in this borehole is currently unknown, and should be further investigated.

The average annual groundwater recharge of the study area was estimated to be 5.81 mm, which represents 1.20% of the MAP (484 mm). Although the chloride concentration in the rainwater was not measured and the long-term mean chloride deposition was unknown, the recharge estimate of this study is in line with that of other studies conducted in and around the Matlala area. A similarly low recharge value of 0.5% of the MAP (365 mm) was obtained by Holland (2011) using the CMB method in Chloe, which occurs near the north-eastern perimeter of the Matlala Batholith outcrop (Figure 5.2). Bredenkamp *et al*. (1995) applied the CMB method in the Limpopo Mogwadi aquifer, where a recharge estimate of 0.7-8.0% of the MAP (440 mm/year) was obtained.

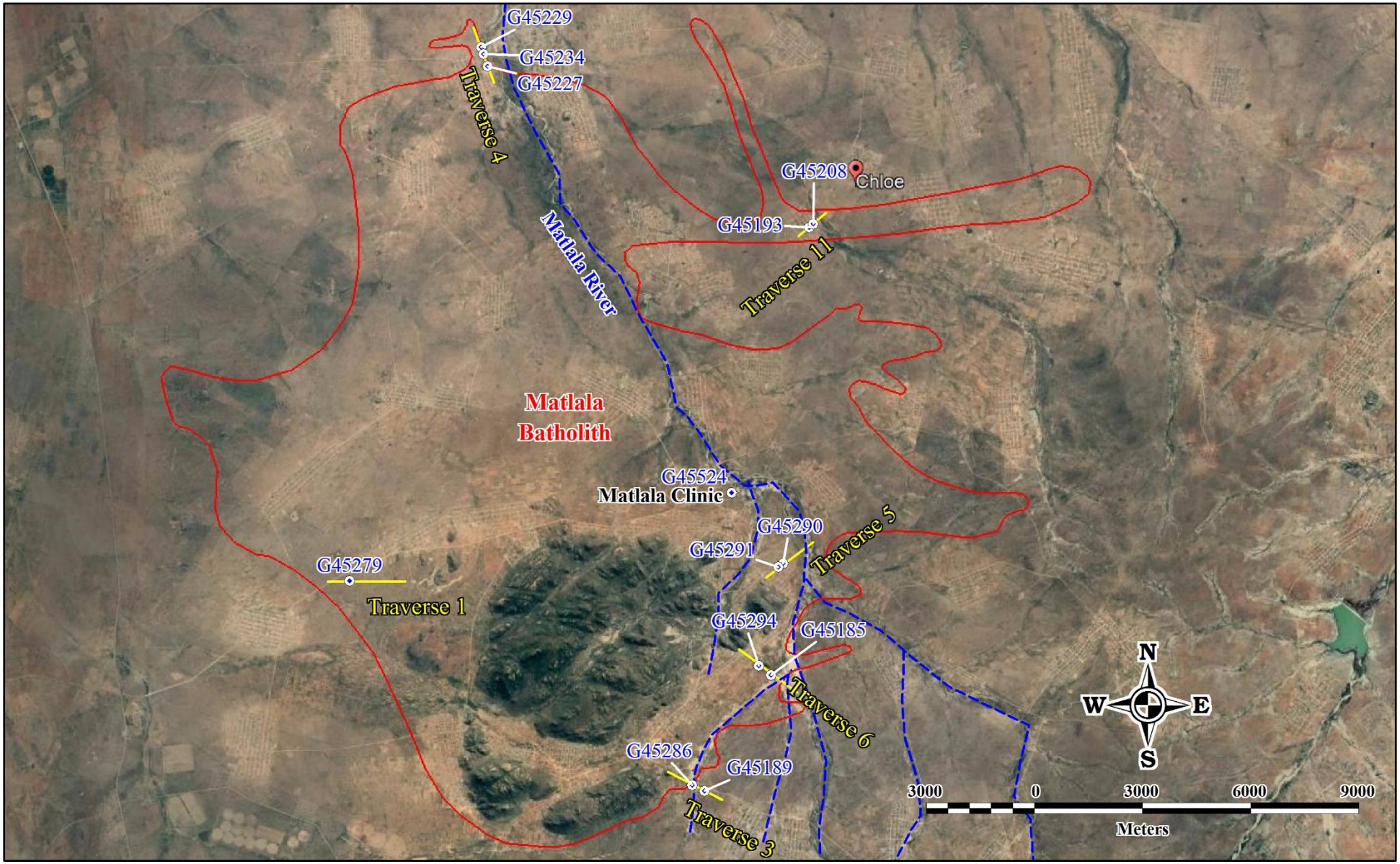

Figure 5.17. Locations and orientations of the geophysical traverses and boreholes used for the recharge estimation using the CMB method

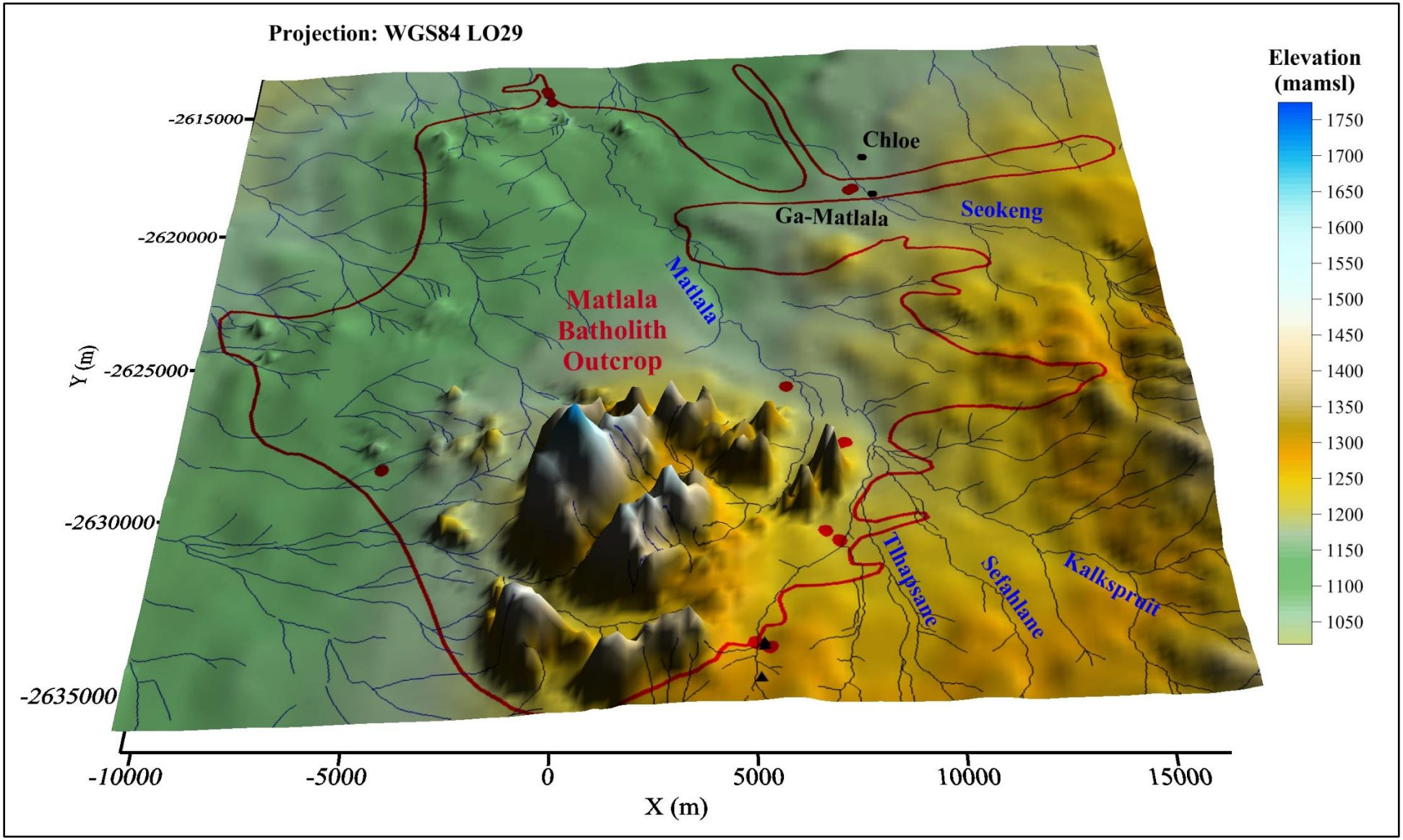

Figure 5.18. Locations of the boreholes used for the recharge estimation using the CMB method (red circles) and WTF and CRD methods (black triangles) relative to the site topography

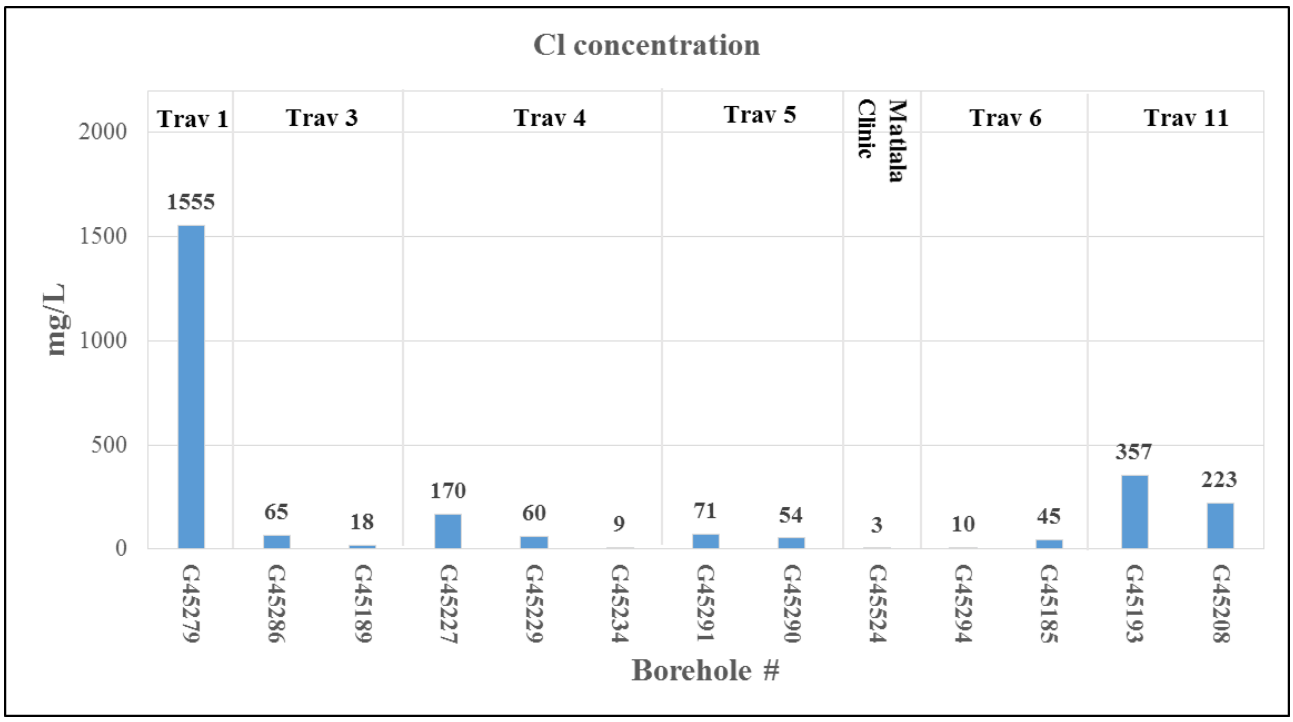

Figure 5.19 Groundwater chloride concentrations in the boreholes along Traverses 1, 3, 4, 5, 6, and 11 and at the Matlala Clinic

Table 5.5: Average groundwater recharge estimates from chloride mass balance

Traverse	Borehole	Lithology intersected	Annual precipitation (mm/year)	Precipitation Cl^{-1} concentration (mg/L)	Groundwater Cl^{-1} concentration (mg/L)	Groundwater recharge (mm/year)	Groundwater recharge (% of MAP)
Traverse 1	G45279	Granite	484	0.2207	1555	0.07	0.01
Traverse 3	G45286	Gneiss			65	1.66	0.34
	G45189				18	5.98	1.24
Traverse 4	G45227	Granite			170	0.63	0.13
	G45229				60	1.80	0.37
	G45234				9	12.0	2.47
Traverse 5	G45291	Granite			71	1.52	0.31
	G45290				54	1.99	0.41
Matlala Clinic	G45524	Granite			3	36.0	7.44
Traverse 6	G45294	Granite			10	10.8	2.23
	G45185				45	2.39	0.49
Traverse 11	G45193	Granite			357	0.30	0.06
	G45208				223	0.48	0.10

5.4.2 Recharge Estimation using the WTF and CRD Methods

5.4.2.1 Available data

The time series groundwater level monitoring dataset is from 2007 to 2019 and was obtained from the DWS Polokwane regional office. Predetermined specific yield values of the encountered lithology were obtained from literature (Tshipala, 2018), and the yearly rainfall data were obtained from the South African Weather Services (SAWS) station in Polokwane (677802bx). The datasets obtained had enough data to a create hydrographs for selected boreholes.

Three boreholes (Matlala 1, Matlala 3 and Matlala 12, Figure 5.21) within the wellfield were selected for recharge estimation using the WTF and CRD methods. These boreholes were selected because they had long-term and recent groundwater level data as opposed to many of the other boreholes in the wellfield. All three these boreholes occur within the gneiss host rock adjacent to the batholith.

5.4.2.2 Rainfall

The rainfall station used for this study is located in Polokwane, which is 45 km from the current study area. Data from the station were plotted to determine the rainfall trends over the period of the study. The highest rainfall was recorded in 2015 at 199 mm, as shown in Figure 5.20.

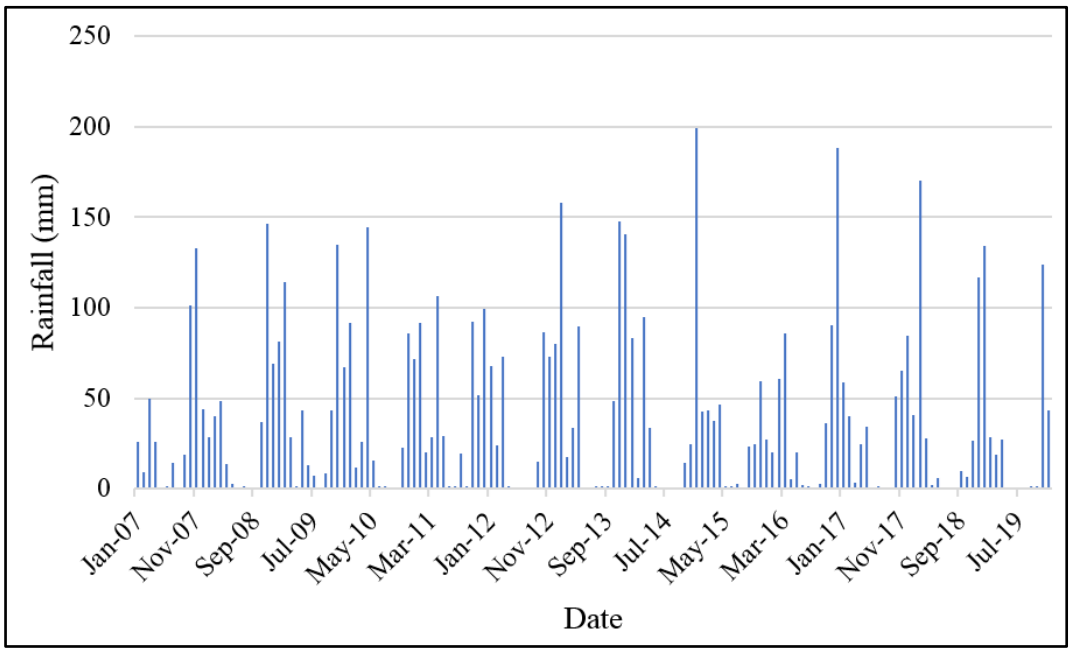

Figure 5.20 Rainfall trends from 2007 to 2019 from Polokwane (Station 677802bx)

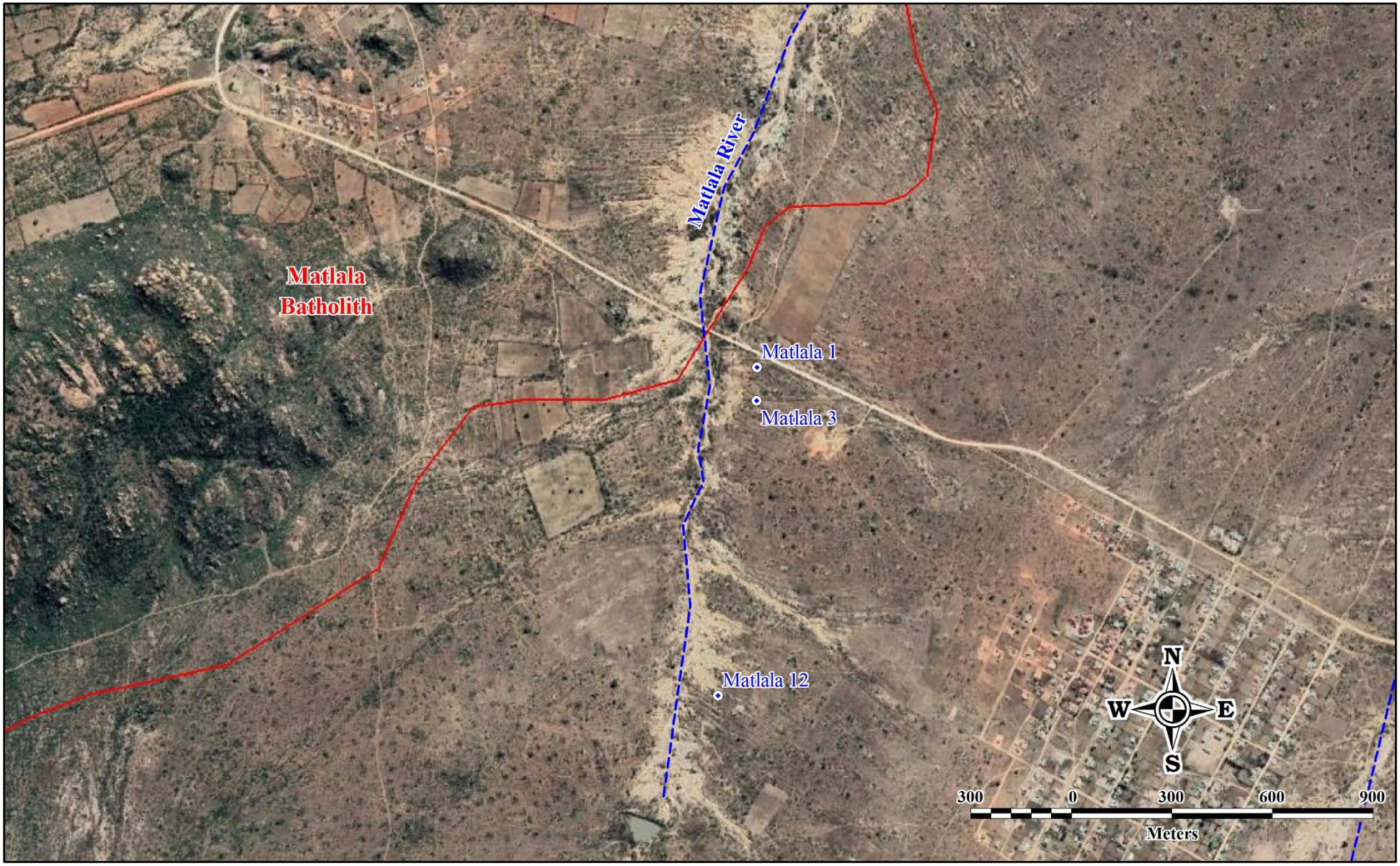

Figure 5.21. Locations of the boreholes used for recharge estimation using the WTF and CRD methods

5.4.2.3 Response of groundwater levels to rainfall

According to Moon *et al.* (2004), groundwater level fluctuation can be influenced by hydrogeological variables (i.e. topography), as well as the characteristics of the precipitation (i.e. its amount, intensity, and duration). In this study, it is assumed that the rise in groundwater level is due to the interaction between rainfall and groundwater, as adopted from Van Wyk *et al.* (2011). The hydrographs for boreholes Matlala 1, Matlala 3, and Matlala 12 were plotted using an Excel spreadsheet. The groundwater level and rainfall interaction were assessed and used to determine the response of groundwater levels to rainfall, either slow, intermediate, or rapid. For Matlala 3, the hydrograph was analysed from 2007 to 2013, while for Matlala 1 and Matlala 12 it was from 2007 to 2019 (see Figure 5.22). The water level data gaps in boreholes Matlala 1 and Matlala 12 are the result of malfunctioning water level loggers.

The following general observations are made:

- There is periodic groundwater fluctuation in all three boreholes during and after the wet season.
- The three hydrographs do not always show a positive correlation between rainfall and groundwater level. For example, in 2008 from April to August, rainfall decreased but the groundwater level increased. Similarly, between December 2009 and May 2010, the groundwater level decreased, with increased rainfall.
- When there is cumulative rainfall over a certain period, there is a positive response in the water level as a result of the field capacity of the unsaturated zone being exceeded, thereby causing recharge.
- The overall groundwater level for Matlala 12 increased (became shallower) by approximately 2.5 m, over the period 2007-2019, while Matlala 1 decreased (became deeper) by approximately 1.5 m. This suggests that the response to rainfall is different at the two boreholes and that the recharge mechanisms may differ.
- The overall groundwater level response to rainfall is intermediate, i.e., the groundwater levels respond to rainfall events in a timeframe of months.

The hydrographs in Figure 5.22 suggest that (1) there is a threshold annual rainfall below which water table changes are not pronounced, (2) once the threshold has been overcome, the water table response to rainfall becomes evident, (3) sharp and short duration rises occur in the water table in response to large rainfall events, and (4) the groundwater response to rainfall is delayed.

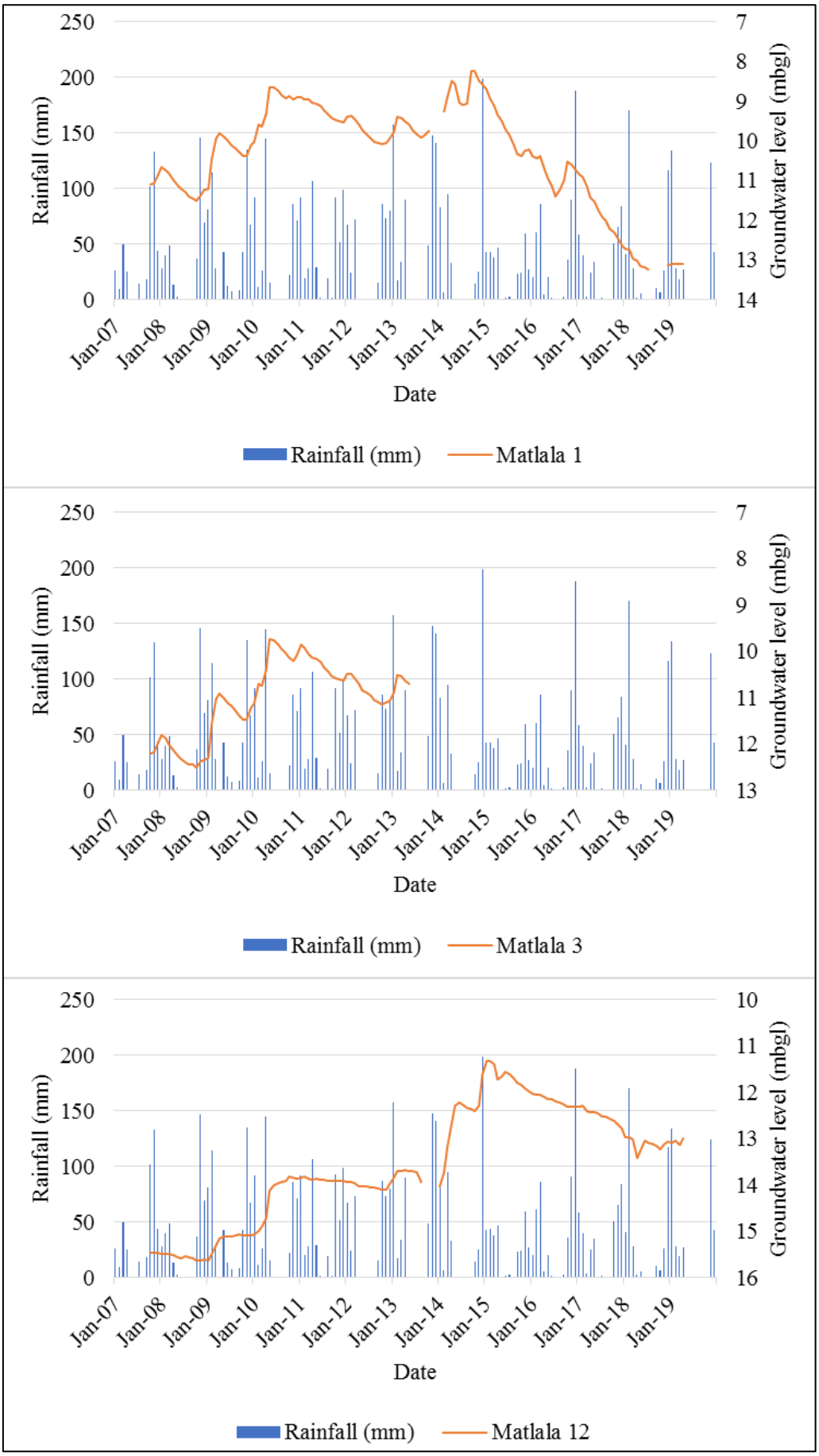

Figure 5.22 Hydrographs of averaged groundwater levels from the boreholes Matlala 1 (top), Matlala 3 (middle), and Matlala 12 (bottom) from 2007 to 2019 and rainfall record from the Polokwane (677802bx) rainfall station

5.4.2.4 Recharge estimation using the WTF method

The three boreholes for which hydrographs could be compiled (Matlala 1, Matlala 3, Matlala 12; see Figure 5.21) all intersect the shallow aquifer system and were chosen to estimate recharge in the Matlala wellfield. It is important to note that all the boreholes with long-term groundwater level monitoring data were clustered in one area; hence the selection of boreholes in close proximity to one another.

5.4.2.4.1 Results and discussion

The results of the recharge estimation using the WTF method are listed in Table 5.6. This table shows the recharge estimating from boreholes located within the gneiss host in the Matlala Batholith intruded. The lowest estimated recharge rate for Matlala 1 was in the year 2013 with a value of 4.60 mm, which represented 1.65% of the rainfall received during that year, while the highest estimated recharge was in 2015 with a value of 10.9% of the rainfall received. The lowest estimated rate at Matlala 3 was 1.16% in 2013 while the highest recharge rate was 5.89% in 2010. Finally, for Matlala 12, the lowest estimated recharge rate was 0.79%, with the highest estimate equal to 10.52% of the received rainfall. The average estimated recharge rates for Matlala 1, 2 and 3 were 4.33%, 3.34% and 2.50%, respectively.

Tshipala (2018) obtained a value of 5.42% of the MAP using the WTF method in Mogwadi. Masiyandima *et al*. (2002) used the rainfall model calculations provided by DWAF (Tshipala, 2018) and obtained recharge rates of 3-5% of MAP. Although the boreholes are drilled in the same lithology with the specific yield of 0.02, there is a variation in the recharge estimate. It is clear that the different depth of fracturing and weathering of the regolith influenced the flow and recharge. It is important to note that data gaps in 2007, 2013, and 2019 would have affected the average recharge in the water years and the calculated recharge; hence there is less discussion around these years.

Figure 5.23 shows little positive correlation between groundwater recharge estimates and rainfall. In all the boreholes, the highest recharge estimate peaks are not associated with high rainfall years but rather periods of cumulative rainfall. This gives an indication that there is a lag period before groundwater recharge takes place. The lag in response of groundwater level to rainfall is affected by the highly fractured and weathered regolith, which needs to be saturated with water for water to flow farther down to the underlying aquifer.

Table 5.6: Average groundwater recharge estimates from the WTF method

Borehole	Year	Total precipitation (mm)	Mean Δh (m)	Lithology	Specific yield (S_y)	Recharge (mm/year)	Recharge (%)
Matlala 1	2007	278.5	0.23	Gneiss	0.02	4.60	1.65
	2008	386.0	0.84			16.9	4.37
	2009	541.0	1.40			28.0	5.17
	2010	469.2	1.37			27.3	5.83
	2011	541.7	0.63			12.6	2.32
	2012	419.4	0.73			14.6	3.49
	2013	636.3	0.53			10.5	1.66
	2014	456.5	1.00			20.0	4.39
	2015	309.5	1.68			33.6	10.9
	2016	511.2	1.02			20.3	3.98
	2017	363.2	1.78			35.6	9.81
	2018	407.4	0.53			10.6	2.60
	2019	208.5	0.02			0.40	0.19
Matlala 3	2007	278.5	0.22			4.42	1.59
	2008	386.0	0.70			14.1	3.64
	2009	541.0	1.40			27.9	5.16
	2010	469.2	1.38			27.6	5.89
	2011	541.7	0.77			15.5	2.86
	2012	419.4	0.65			12.9	3.08
	2013	636.3	0.37			7.40	1.16
Matlala 12	2007	278.5	0.02			0.37	0.13
	2008	386.0	0.15			3.03	0.79
	2009	541.0	0.55			11.1	2.05
	2010	469.2	1.23			24.5	5.23
	2011	541.7	0.09			1.90	0.35
	2012	419.4	0.18			3.55	0.85
	2013	636.3	0.25			5.03	0.79
	2014	456.5	2.40			48.0	10.5
	2015	309.5	0.66			13.2	4.25
	2016	511.2	0.29			5.81	1.14
	2017	363.2	0.49			9.88	2.72
	2018	407.4	0.46			9.20	2.26
	2019	208.5	0.15			2.90	1.39

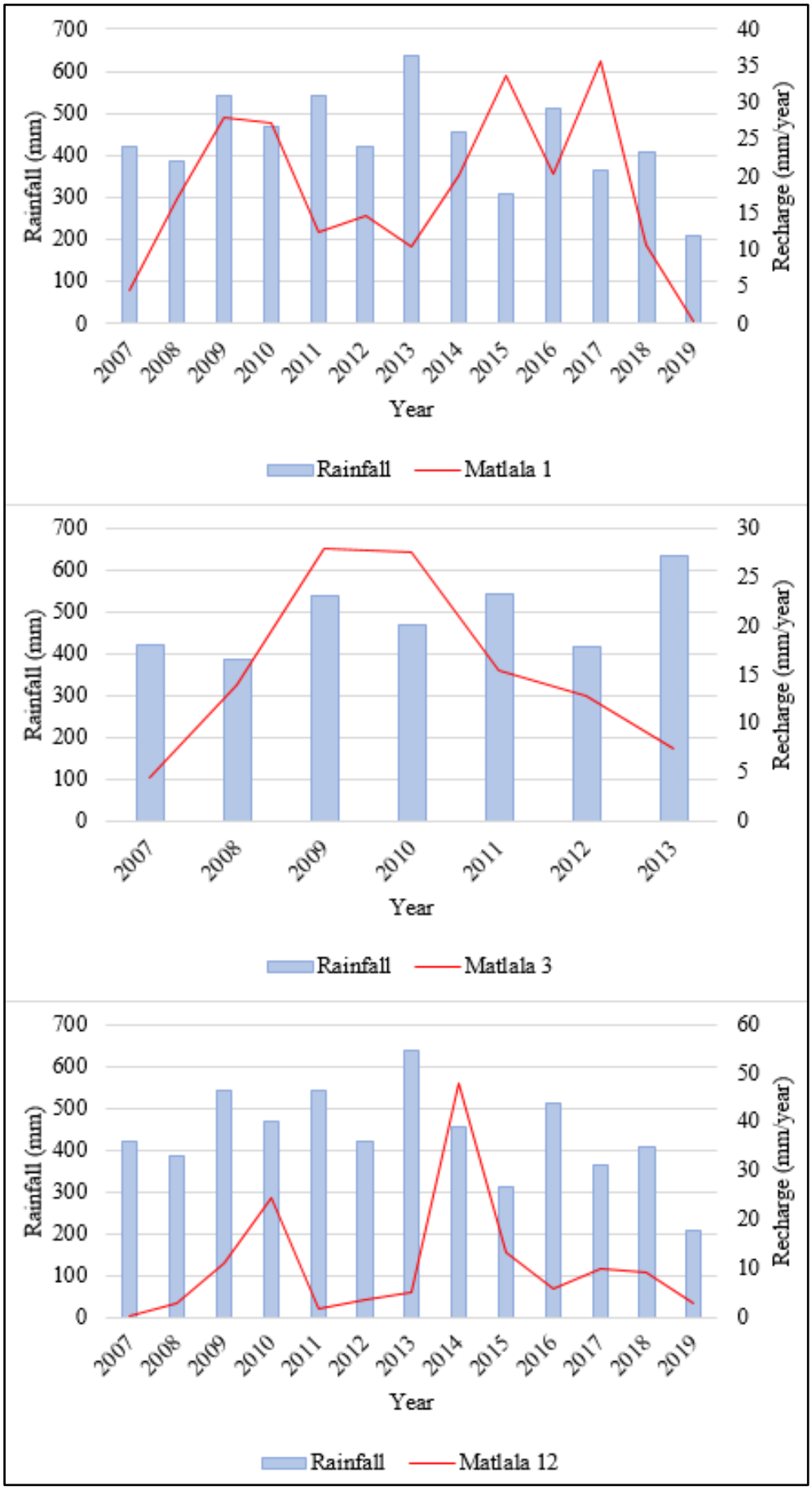

Figure 5.23 Groundwater recharge rates calculated for boreholes Matlala 1 (top), Matlala 3 (middle) and Matlala 12 (bottom) using the WTF method

5.4.2.5 Recharge estimation using the CRD method

The time series groundwater level monitoring dataset is from 2007 to 2013 and was obtained from the DWS Polokwane regional office. Predetermined specific yield values of the encountered lithology were obtained from literature (Tshipala, 2018), and the yearly rainfall data were obtained from the South African Weather Services (SAWA) station in Polokwane (677802BX). The datasets obtained had enough data to a create hydrograph.

5.4.2.5.1 Results and discussion

After calibrating the observed and simulated CRD time lag and specific yield parameters the best fit graphs for all three boreholes were obtained. The simulation results are shown in Figure 5.24 and listed in Table 5.7. For comparison, Table 5.7 also lists the recharge estimates obtained with the WTF method.

Table 5.7 Recharge estimations based on the CRD method

Borehole number	Specific yield (S_y)	CRD recharge (%)	Lag (months)	WTF recharge (%)
Matlala 1	0.02	3.90	1	4.33
Matlala 3	0.02	4.85	2	3.34
Matlala 12	0.02	2.54	1	2.50

Monthly rainfall for the simulated period was above average. This is evident from the water level fluctuation in all three boreholes. It is also observed that fluctuations are seen during the period with cumulative rainfall. The simulation for all three boreholes shows a correlation between the observed and simulated CRD. However, a deviation is seen when the simulated water level is higher than the observed water level due to outflow (abstraction), and when the observed water level is higher than the simulated water level as a result of lateral flow and surface inflow from an intermittent stream outside the recharge area.

All three boreholes were assigned a *Sy* value of 0.02, which is similar to the value used in the WTF method. The averaged estimated recharge values ranged from 2.54% to 4.85%. Although these boreholes are drilled in the same lithology, the depth of weathering and fracturing of the regolith influence the different depth in water level in all three boreholes, as well as a variation of recharge estimates and lag time. Borehole Matlala 12 is located upstream and the weathered zone is only 9 m thick. This borehole has a deeper water level as compared to boreholes Matlala 1 and Matlala 3, which are drilled in the highly weathered regolith with a thickness of 35 m.

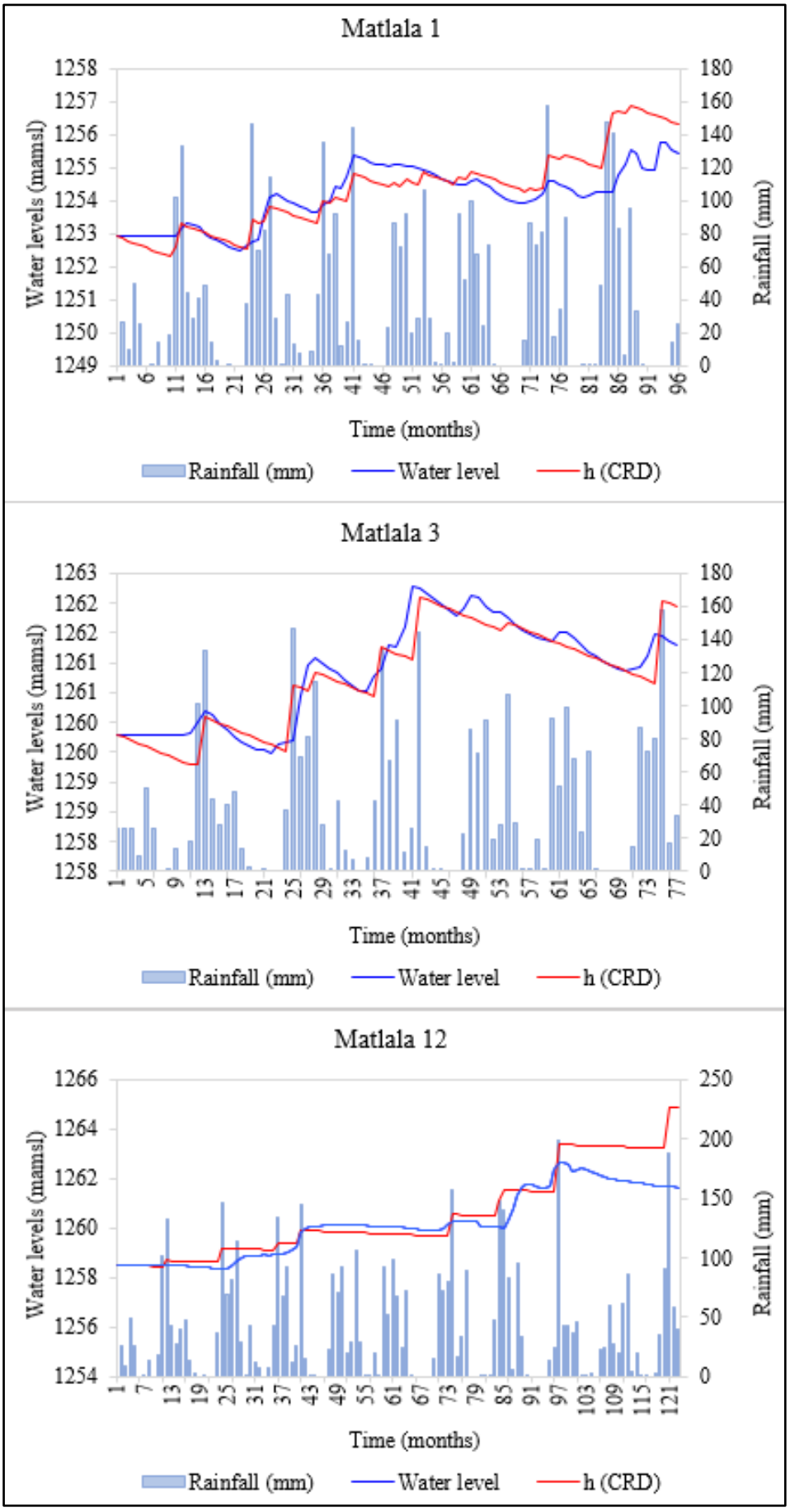

Figure 5.24 Observed and simulated CRD graph for boreholes Matlala 1 (top), Matlala 3 (middle) and Matlala 12 (bottom)

The estimated recharge values from both physical methods indicate that recharge is not uniform in the study area, which is expected because recharge is a function of aquifer properties, rainfall, and the geomorphology of the area. The CRD and WTF recharge estimates vary despite the use of data from the same period; however, the difference is not significant. The CRD method gives an average recharge for the whole simulated period, while the obtained WTF estimates are also averaged over the simulated period for the CRD method. Although the estimates from the CRD and WTF differ, other authors obtained estimates ranging from 1% to 6% using the CRD and WTF methods. Using the CRD method, Holland (2011) obtained a recharge estimate of 1.4%, whereas Tshipala (2018) obtained a value of 5.7 % using the WTF method.

5.5 DEVELOPMENT OF CONCEPTUAL GEOHYDROLOGICAL MODEL

5.5.1 Ground Geophysics

The data obtained from magnetic and electromagnetic (EM) surveys conducted by Du Toit (2001) across the contact between the batholith and the host rock (refer to Figure 5.3) were correlated with the geological logs to locate the contact zones and to further investigate if the contact zones have groundwater potential.

The results of the geophysical surveys on Traverse 3 across the Matlala wellfield are show in Figure 5.25. This figure also shows a geological cross-section compiled from drilling logs and the geophysical data. Both the magnetic and EM survey results indicated variation in the subsurface lithology. From 0 to 700 m, the two techniques do not reveal significant lateral changes in the physical properties of the subsurface. However, the EM readings are not entirely smooth and this may be due to local conductivity changes associated with fracturing and weathering of the regolith. Variations can be seen from 750 m onwards where the traverse extends above the batholith, as revealed by drilling. The EM data indicate that the subsurface is more conductive where the batholith occurs as compared to the gneiss host rock. The magnetic profile indicated the presence of a magnetic body (most likely a dolerite dyke) between 1 100 and 1 200 m. Numerous water strikes were noted in the boreholes intersecting the roof contact with the batholith. In most of the boreholes in Traverse 3, the first water strikes were encountered at depths ranging from 10 to 40 m.

Figure 5.26 shows the results of the geophysical surveys conducted on Traverse 6 to the north of the Matlala wellfield. As on Traverse 3, the geophysical methods successfully located the contact between the batholith and its host rock and revealed the presence of magnetic intrusives (dolerite dykes).

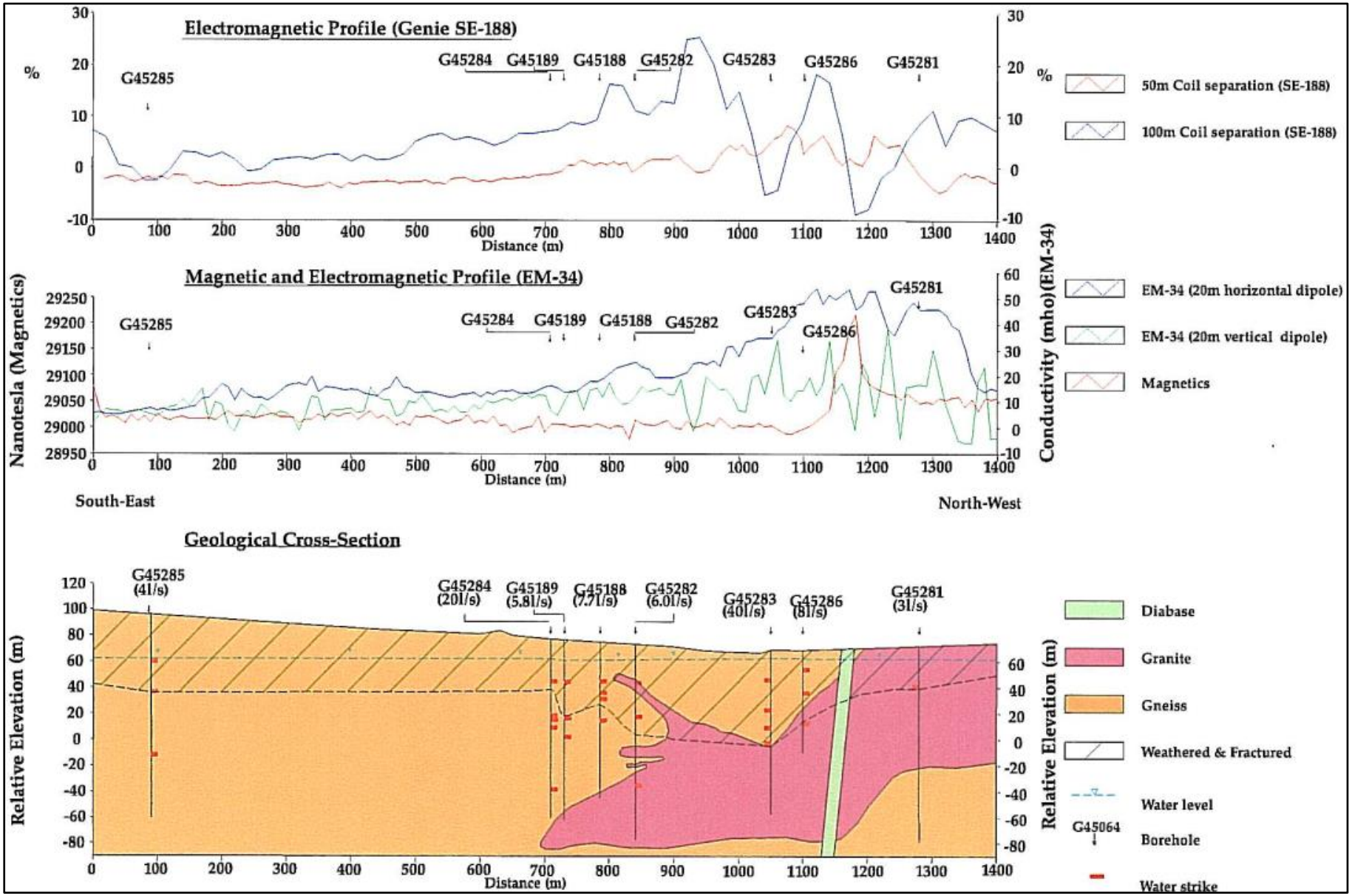

Figure 5.25. Comparison of the geological cross-section (ESE-WNW) and geophysical profiles along Traverse 3 (Du Toit, 2001)

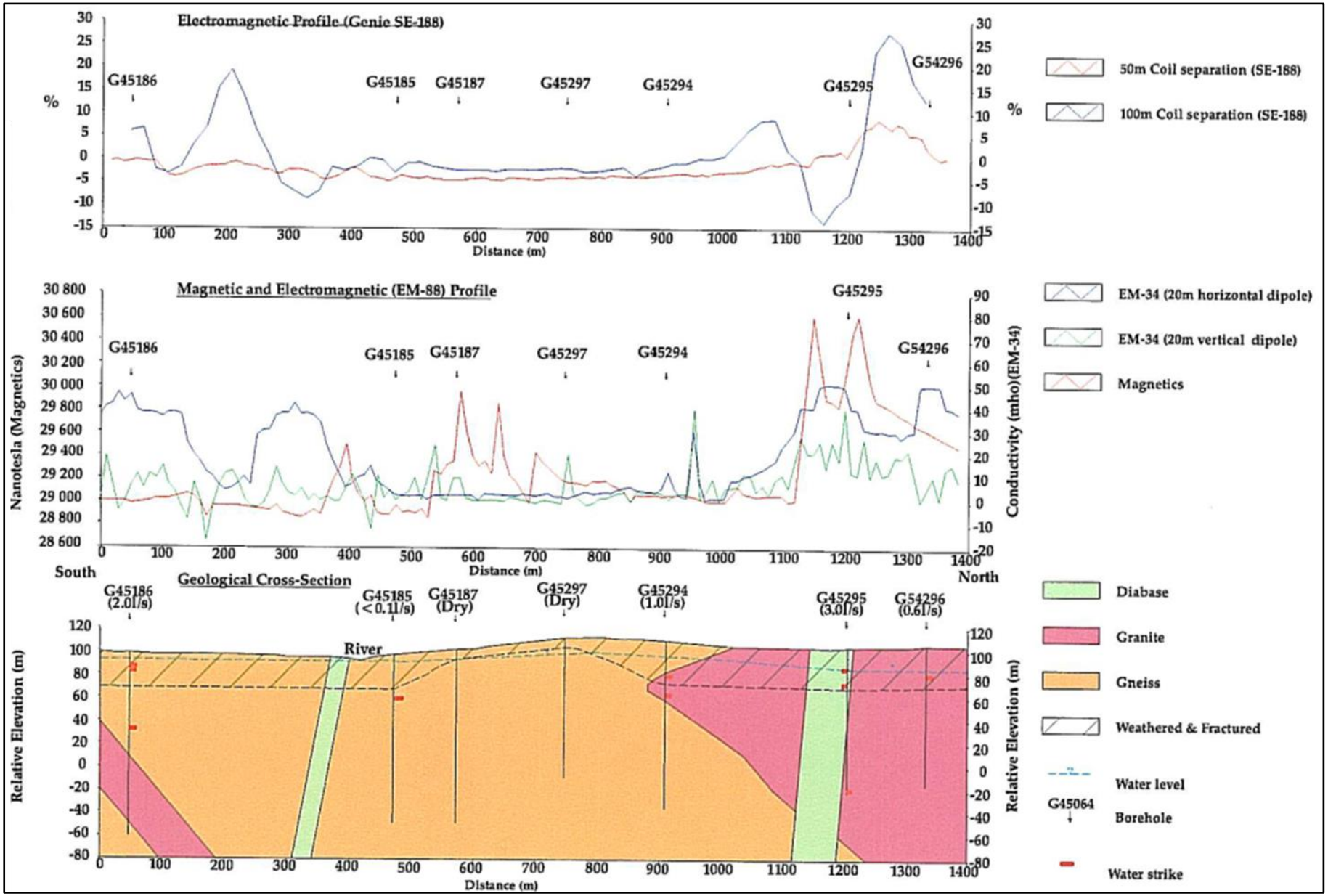

Figure 5.26. Comparison of the geological cross-section (ESE-WNW) and geophysical profiles along Traverse 6 (Du Toit, 2001)

5.5.2 Borehole Geophysics

The borehole geological log data show different geologic units in the area. The logs show interlayering of permeable and less permeable material (gneiss, granite, and dolerite). The main water-bearing geological unit is the weathered and fractured section. The dolerite dykes encountered show low permeability.

The downhole geophysical logs were used in conjunction with the lithological logs to maximise the understanding of subsurface geology, the lithological change, as well as the location of water strikes (fractures and weathered zones). The data showed heterogeneity in the geological units in both the vertical and lateral extent, with the host rocks (gneiss) and the granitic batholith intruded by dykes, which is clear in a number of lithological logs. The results for both logs show a highly fractured and weathered regolith with multiple water strikes.

Borehole geophysical logging was performed by the DWS on eight boreholes along the non-perennial Matlala River (Figure 5.27). Due to availability of drilling log information, the results from only three boreholes (Matlala 1, Matlala 8 and Matlala 12) are discussed in this section.

5.5.2.1 Geophysical logging of Matlala 1

Figure 5.28 shows the results of the geophysical borehole logging performed on Matlala 1. The depths of the water strikes are indicated by red markers. Due to the caliper logging tool malfunctioning, it is not possible to identify the breakout zones and the change in diameter along the borehole wall.

The gamma log shows localised zones of higher natural radiation, particularly near 38 mbgl, 50 mbgl, and at depths greater than 73 mbgl. These zones probably indicate changes in the lithology and do not appear to be directly related to the water strikes in the borehole. As expected, the neutron log displays a rapid decrease below the depth of the water table (9.59 mbgl) due to the increased hydrogen concentration. Below this depth, the neutron log exhibits a gradually increasing trend, most likely indicating a generally decreasing porosity with depth. Several zones of locally decreased cps values indicate zones of increased hydrogen content which may be related to fracturing. Prominent zones of deceased cps occur at depths of approximately 60 mbgl and 75 mbgl. The zone near 75 mbgl corresponds to the depth of a major water strike.

As expected, the resistivity log displays a rapid decrease below the depth of the water table. Similar to the neutron log, the resistivities show an increasing trend with depth below the water table. This again suggests decreasing bulk porosity with depth. Localised zones of lower resistivity could indicate either changes in the subsurface lithology or increased water content. One such a zone occurs near 60 mbgl, where the neutron log also indicated the presence of increased hydrogen concentrations.

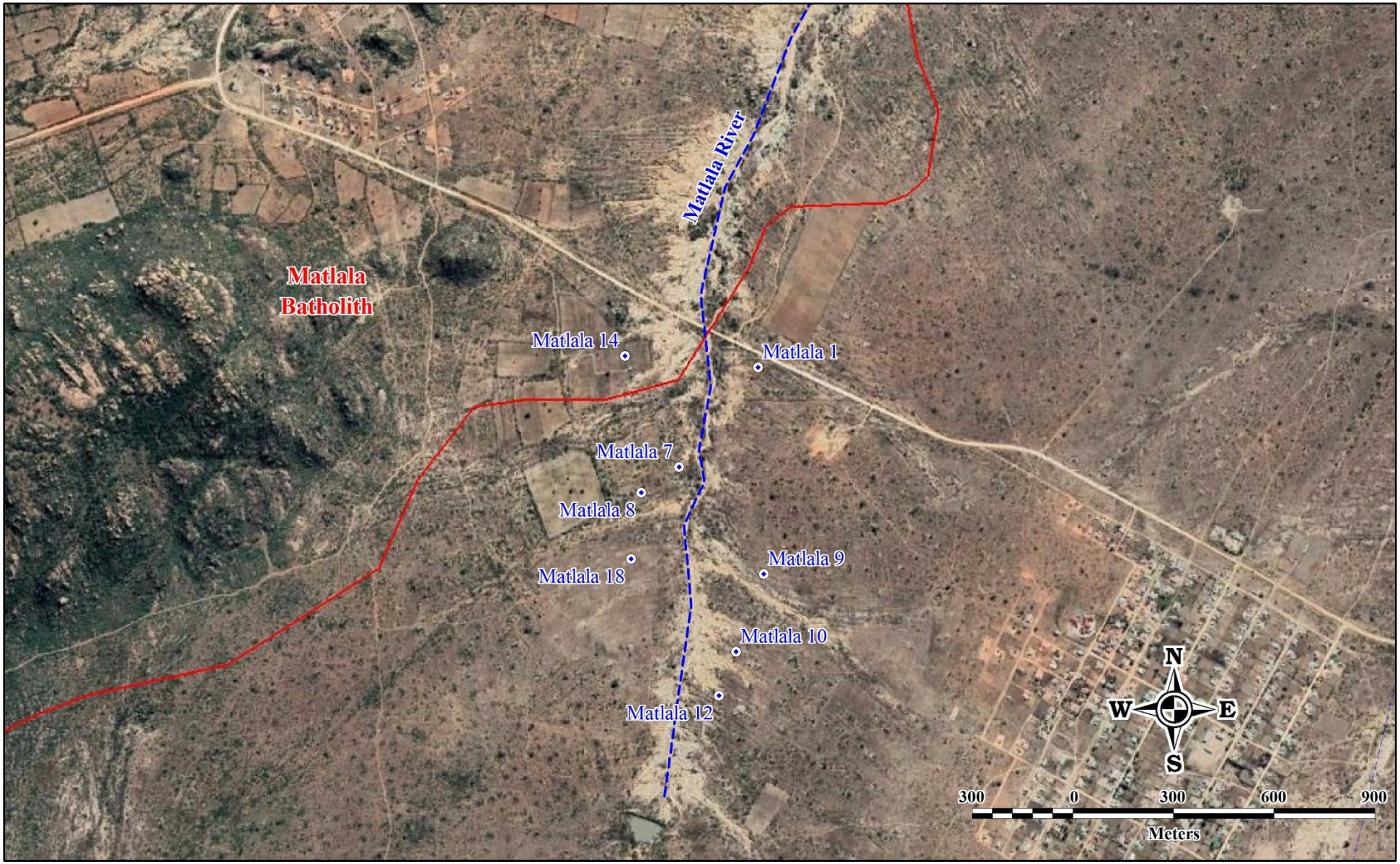

Figure 5.27. Locations of the boreholes used for geophysical logging

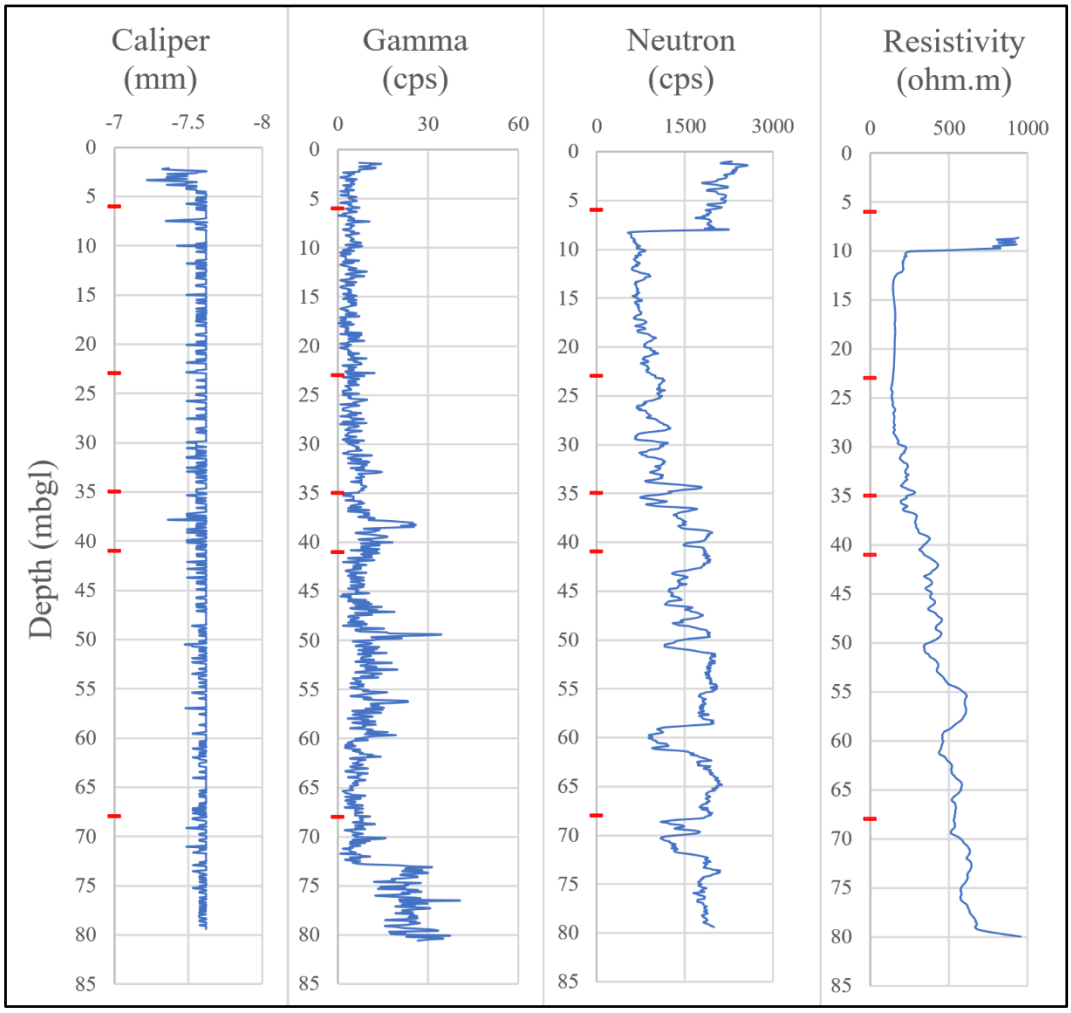

Figure 5.28 Geophysical logging results of Matlala 1 (red markers indicate depths of water strikes)

5.5.2.2 Geophysical logging of Matlala 8

The results of the geophysical borehole logging performed on Matlala 8 are shown in Figure 5.29. The caliper log shows a gradually decreasing wall diameter with increasing borehole depth. This change may reflect the increasing competence of the subsurface rock materials. The five sharp negative peaks in the caliper log between 21 mbgl and 61 mbgl correspond to unrealistic decreases in the borehole diameter and are most likely due to measurement errors. Below 70 mbgl the borehole diameter decreases and displays irregularities in the wall of the borehole. This is the approximate depth of a major water strike and could indicate fracturing at the contact between different lithological units.

The gamma log shows zones of increased natural radiation, particularly between 41 mbgl and 46 mbgl, and near 67.5 mbgl and 76 mbgl. These zones could indicate different lithological units in the subsurface.

Similar to the log of Matlala 1, the neutron log displays a rapid decrease at the depth of the water table and then a gradually increasing trend which may reflect a decreasing bulk porosity with

increasing depth. Local zones of decreased cps counts are again observed. These zones are due to increased hydrogen concentrations and may indicate changes in the subsurface lithology or increases in porosity and water content. A prominent step in the cps count is observed below the depth of the water strike at 68 mbgl.

The resistivity log indicates a low resistivity below the water table and up to a depth of approximately 71 mbgl. A localised resistivity high near 43 mbgl is probably due to the presence of a denser rock unit with lower porosity. Below 71 mbgl there is an abrupt increase in the resistivity, possibly indicating the presence of a contact between different lithologies.

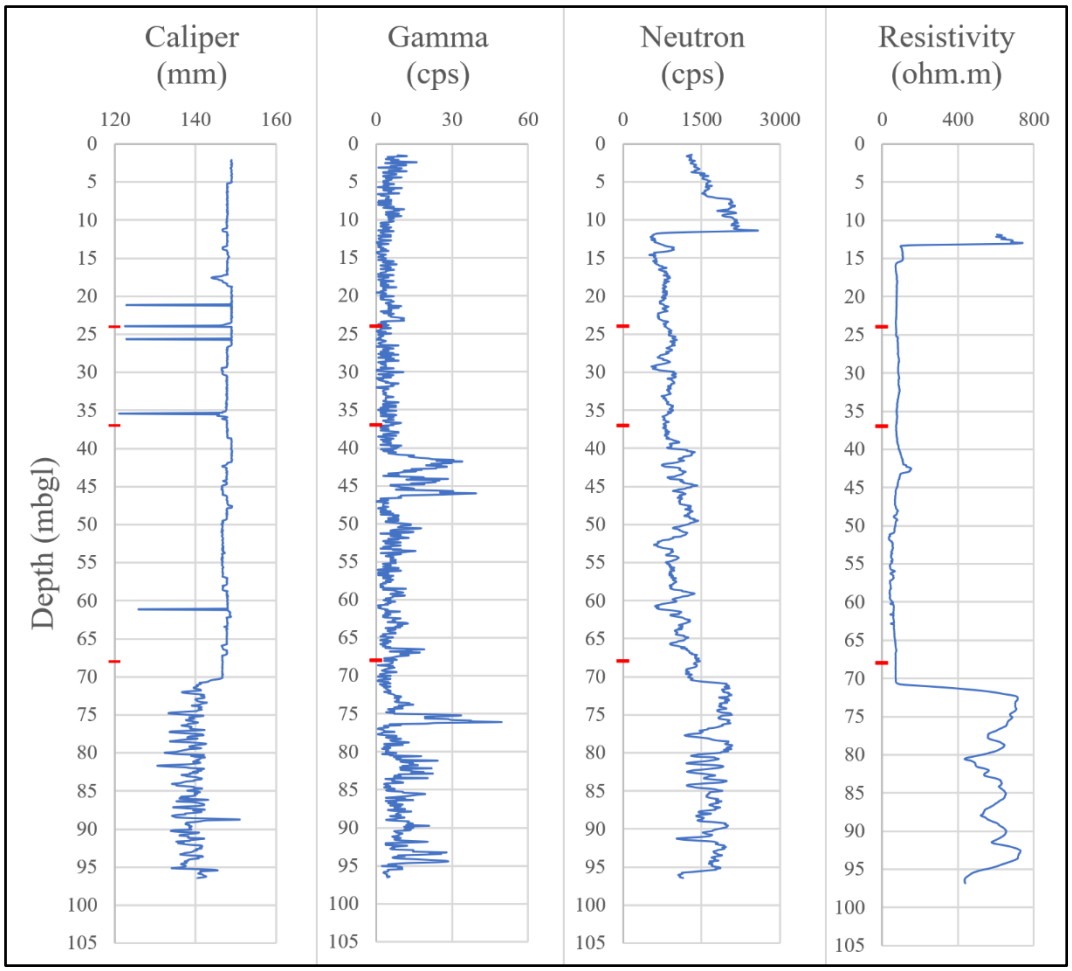

Figure 5.29 Geophysical logging results of Matlala 8 (red markers indicate depths of water strikes)

5.5.2.3 Geophysical logging of Matlala 12

The results of the geophysical borehole logging performed on Matlala 12 are shown in Figure 5.30. The different logs for Matlala 12 correspond to each other and indicate the presence of fractures. Increases in the borehole diameter are noted at depths of approximately 20 mbgl, 34 mbgl and 51 mbgl in the caliper log. These depths correspond to zones of low cps in the neutron log and decreased resistivity in the resistivity log. These observations suggest the presence of a water-bearing

fractures at these depths. Major water strikes were indeed recorded at depths of 21 mbgl, 36 mbgl and 52 mbgl.

Other apparent fracture zones are observed at depths of approximately 62 mbgl and 77 mbgl. However, no water strikes were recorded at these depths.

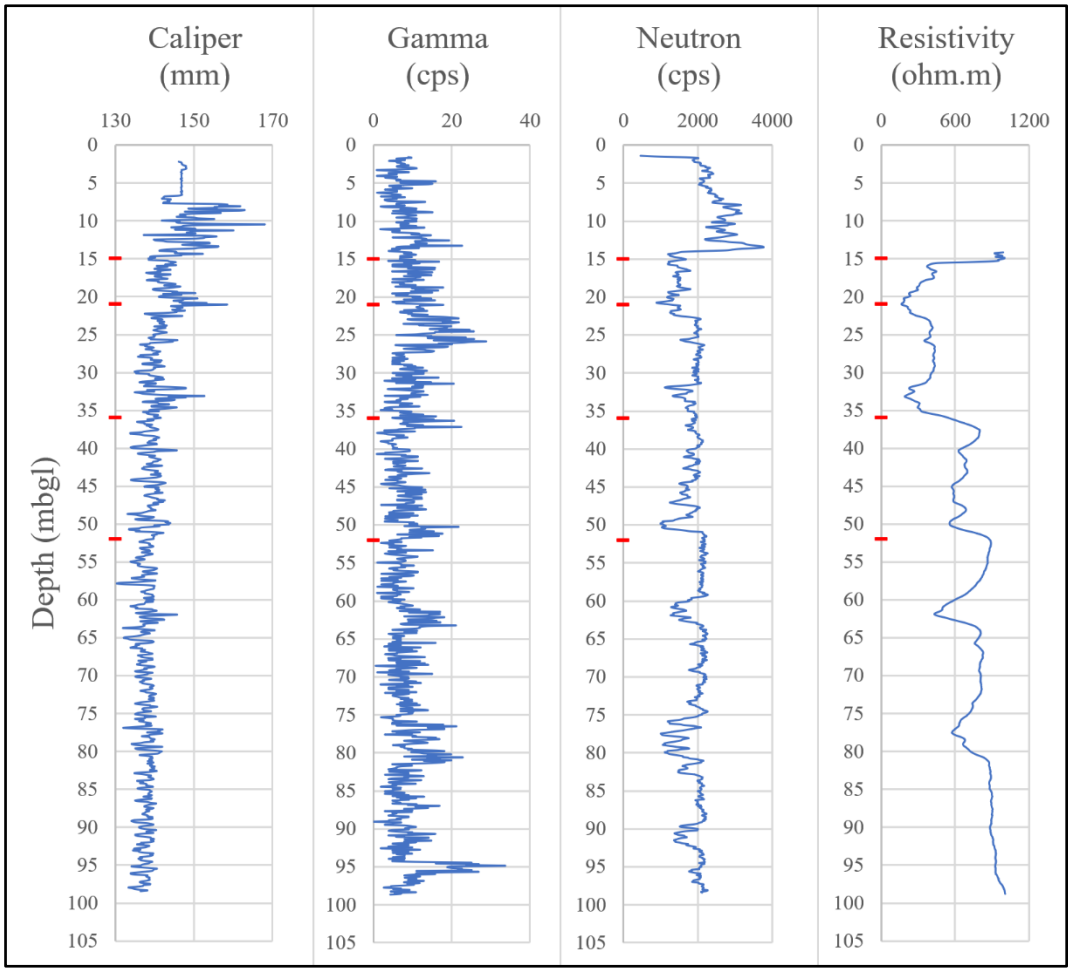

Figure 5.30 Geophysical logging results of Matlala 12 (red markers indicate depths of water strikes)

The geological borehole logs were used to calibrate the resistivity logs in terms of the intersected lithologies, and to estimate the lithological distributions and layer thicknesses. A total of 42 borehole data sets around the Matlala Batholith were used for this task (**Appendix B**). The lithologies in the Matlala Batholith were grouped into three zones: (1) the weathered and fractured regolith zone, (2) the fractured zone, and (3) the fresh rock zone (Table 5.8). Previous geological mapping and geophysical investigations conducted by Du Toit (2001) assisted to understand and develop a geohydrological model for the Matlala Batholith in the vicinity of the Matlala wellfield.

Table 5.8 Geological zones of the Matlala Batholith

Structural/geological zone	Lithology	Resistivity (Ohm.m)	Average depth (mbgl)
Weathered and fractured regolith	Gneiss, granite, diabase, silty clay	5 - 250	0.5 - 7
Fractured zone	Gneiss, granite, diabase	250 - 500	7 - 35
Unaltered bedrock	Gneiss, granite	500 - 1500	35 - 40

5.5.3 Conceptual Model

The results obtained from the geophysical surveys were used to identify the three geological zones in the area. These zones are (1) the weathered and fractured regolith zone, (2) the fractured zone, and (3) the unaltered bedrock zone. These zones are composed of the following lithologies: Goudplaats-Hout River Gneiss, Matlala Granite, diabase, and some quaternary deposits (alluvium).

The Matlala Batholith shows no strong magnetic signature, but magnetic diabase dykes cut through it. These dykes have south-west/north-east, west-south-west/east-north-east and west-north-west/east-south-east strikes.

The aquifer system of the Matlala Batholith can be divided into two, namely: the regolith (weathered and fractured) zone, and (2) the fractured bedrock. The interface between the two zones is delineated based on the results obtained from the downhole geophysical logs and lithology data form Du Toit (2001). Du Toit (2001) further recorded that the transmissivities of the weathered and fractured regolith varies from 151 to 205 m^2/d while that of the fractured bedrock varies from 3 to 57 m^2/d.

One main stream, the non-perennial Matlala River, is represented in the conceptual model (Figure 5.31). This stream is mostly dry during dry seasons, but it is evident that it has a positive influence on the recharge mechanism in the area, probably due to surface and groundwater interaction. Boreholes G45524 located near the stream has a higher recharge estimate, followed by G5189 on the southern side of the batholith. Borehole G45193 located on the eastern side of the batholith and farther away from the stream has a low recharge estimate.

Borehole and groundwater information shows that boreholes with shallower groundwater levels are mostly encountered in the weathered and fractured regolith and along the Matlala River. These boreholes have groundwater levels less than 21 mbgl. Boreholes with deeper groundwater levels are associated with the fractured bedrock. The groundwater level data were used to determine the hydraulic gradient and flow direction in the vicinity of the wellfield. Based on the water level results, groundwater flows from south to north and south-south-east to north-north-west.

Groundwater quality characterisation for this study is limited, however the information is useful in understanding the influence of recharge on water quality. Boreholes G45193 located on the eastern side of the batholith has higher EC and TDS; these values suggest groundwater mineralisation. Boreholes G45189 in the south and G45524 located along the stream have lower EC and TDS values. The overall water quality results display an increase in mineralisation and dissolved solids from the south to the north.

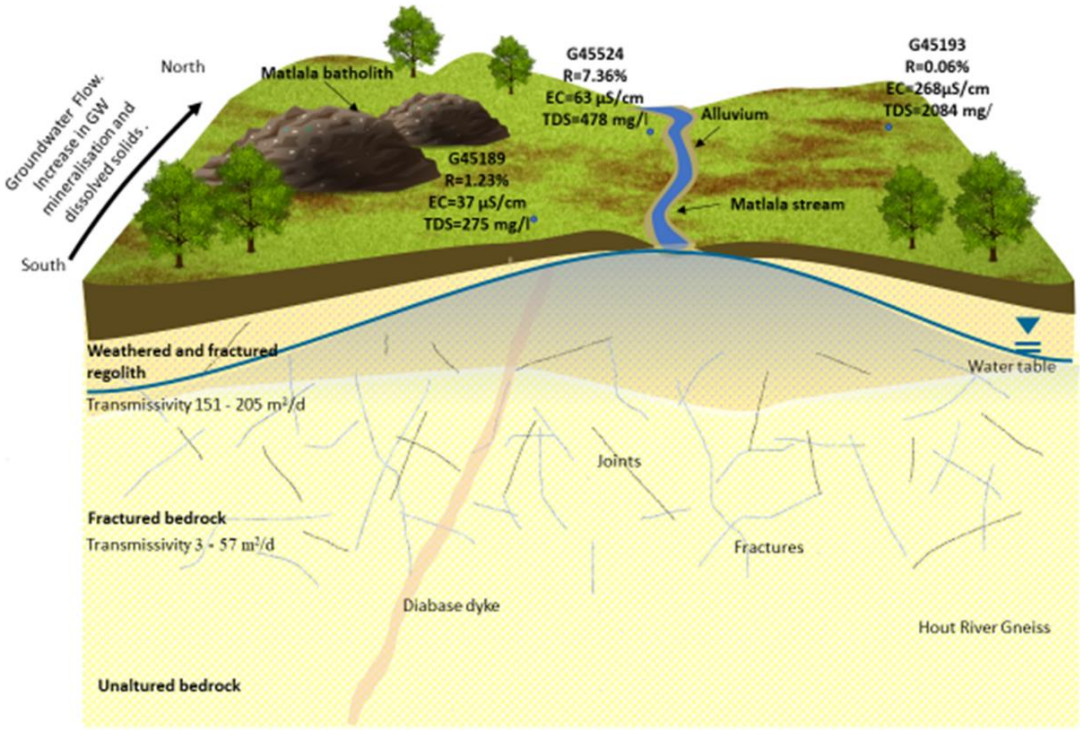

Figure 5.31 Conceptual geohydrological model of the Matlala Batholith in the vicinity of the Matlala wellfield during the rainy season when groundwater recharge occurs from the river

CHAPTER 6:
CONCLUSIONS AND WAY FORWARD

6.1 CONCLUSIONS

This study aimed to understand the water level response to rainfall and to estimate the groundwater recharge to the Matlala Batholith and surrounding gneissic host rock by evaluating historical groundwater level and chemistry data. Specific focus was placed on an area near the south-eastern boundary of the batholith where a wellfield occurs. Groundwater from this wellfield may in future supply the local community with water to meet their drinking and domestic water needs. However, no sustainable yield has yet been calculated for the boreholes in the wellfield, and the risk therefore exists that over-abstraction from these boreholes could cause permanent damage to the aquifer system. As a first step towards determining a sustainable yield for the wellfield, information on the recharge of the aquifer system is required.

The available historical data are sparse and contain large temporal and spatial gaps. This lack of complete, comprehensive, and recent data was a severe limitation to the current recharge investigation. Despite this shortcoming, three methods were used to estimate the groundwater recharge in the study area from the available data, namely the CMB, WTF and CRD methods.

The investigations into the groundwater recharge mechanisms and rates allowed the development of a conceptual geohydrological model for the Matlala Batholith. According to this model the aquifer system can be divided into two main aquifers, namely: the regolith (weathered and fractured) zone, and (2) the fractured bedrock. From an analysis of the water level response to rainfall it is clear that there is a lag period of one to two months between rainfall events and groundwater recharge. The lag in response of groundwater level to rainfall is affected by the highly fractured and weathered regolith, which needs to be saturated for water to flow farther down to the underlying fractured bedrock aquifer.

The recharge rate estimated with the CMB method varied between 0.01% and 7.44% of the MAP for different boreholes with an average value of 1.20% of the MAP. Applying the WTF method to different boreholes in the study area, the recharge was estimated to be between 0.13% and 10.9% of the received rainfall, with an average value of 3.39%. The recharge rates estimated with the CRD method varied between 2.54% and 4.85%, with an average value of 3.76% of the received rainfall.

The average recharge rates estimated with the physical methods were very similar (3.39% and 3.76% of the rainfall received) but differed from the estimate obtained with the CMB method (1.20% of the MAP). However, all three methods indicate low average recharge rates of well below 5%, in line with

the results obtained by other scholars. These low recharge estimates should be used when calculating the sustainable abstraction rate from the aquifer system.

For all three methods, the recharge values were not uniform for boreholes drilled around the Matlala Batholith. The large variations in the estimated recharge rates for the different boreholes indicate that different recharge conditions occur at these boreholes. The recharge rates are most likely affected by the depth of weathering and fracturing of the regolith in the vicinity of the different boreholes.

Boreholes drilled along the non-perennial Matlala River indicated higher recharge rates compared to those farther away from the stream, and boreholes downstream showed little recharge compared to those along the midstream and upstream towards the contact of the batholith. Results from the CMB method indicated higher recharge values for boreholes located on the eastern side of the batholith towards the Matlala River, where deeper weathering occurs.

The groundwater quality investigations revealed that boreholes located downstream on the northern side of the batholith had higher EC and TDS values with NaCl water types, and those on the southern side of the batholith had lower EC and TDS values with $MgHCO_3$ water types. The water quality results displayed an increase in mineralisation and dissolved solids from the south to the north. The distribution of the water types is in line with the results obtained from the recharge estimations: boreholes located upstream indicate higher recharge rates than those located downstream.

From the recharge investigation it is clear that there is no straightforward method to estimate recharge in fractured and weathered crystalline terrain. However, the use of different methods can assist in obtaining a more reliable recharge estimate. Recharge in crystalline aquifers is influenced by multiple factors, including: the intensity, frequency and duration of rainfall events; the topographic gradient; the state of weathering and fracturing of the regolith; and the clay content of weathering products. Reliable recharge estimates require long-term groundwater chemistry and elevation data of good quality.

The study has improved the understanding of the groundwater recharge mechanisms and recharge rates at the Matlala Batholith. While estimates of the recharge rate to the aquifer system were obtained, this information alone is not enough to determine a sustainable abstraction rate from the boreholes in the Matlala wellfield. Further investigations, outlined in Section 6.2, should be carried out before handing over the boreholes to the community for water supply.

6.2 WAY FORWARD

Based on the findings of this study, the following way forward is proposed for future investigations at the Matlala Batholith, and more specifically at the Matlala wellfield to ensure that the aquifer system is not overexploited:

- Pumping tests should be performed on the high-yielding boreholes in the wellfield to investigate the flow regimes in the aquifers and to determine the aquifer hydraulic parameters.
- Based on the results of the pumping tests, sustainable abstraction rates should be calculated using the Flow Characteristic (FC) method.
- Isotope analyses should be performed on groundwater samples from the different boreholes on and adjacent to the batholith to investigate groundwater origins, ages and mixing.
- The hydraulic connection between the regolith and the underlying fractured bedrock should be investigated. Depending on their construction, the boreholes in the Matlala wellfield may be suitable for such investigations.
- A numerical model should be developed for the Matlala wellfield, based on the conceptual geohydrological model developed in this study, to investigate different pumping scenarios for future water supply purposes. The recharge rates estimated in this study should be used as an input to the numerical model.

REFERENCES

ACWORTH, R. 1987. The development of crystalline basement aquifers in a tropical environment. Quarterly Journal of Engineering Geology and Hydrogeology, 20**,** 265-272.

ADAMS, S., TITUS, R. AND XU, Y. 2003. Groundwater recharge assessment of the basement aquifers of central Namaqualand. University of the Western Cape.

ADAMS, S., TITUS, R. AND XU, Y. 2009. A methodological approach to recharge estimation of semi-arid basement aquifers–the central Namaqualand case. The Basement Aquifers of Southern Africa**,** 45.

ALLISON, G., GEE, G. AND TYLER, S. 1994. Vadose-zone techniques for estimating groundwater recharge in arid and semiarid regions. Soil Science Society of America Journal, 58**,** 6-14.

ALLISON, G. AND HUGHES, M. 1978. The use of environmental chloride and tritium to estimate total recharge to an unconfined aquifer. Soil Research, 16**,** 181-195.

ALLISON, G., STONE, W. AND HUGHES, M. 1985. Recharge in karst and dune elements of a semi-arid landscape as indicated by natural isotopes and chloride. Journal of Hydrology, 76**,** 1-25.

BALOOCHESTANI, F. 2008. Estimation of hydraulic properties of the shallow aquifer system for selected basins in the Blue Ridge and the Piedmont physiographic provinces of the southeastern US using streamflow recession and baseflow data.

BANKS, E. W., SIMMONS, C. T., LOVE, A. J., CRANSWICK, R., WERNER, A. D., BESTLAND, E. A., WOOD, M. AND WILSON, T. 2009. Fractured bedrock and saprolite hydrogeologic controls on groundwater/surface-water interaction: a conceptual model (Australia). Hydrogeology Journal, 17**,** 1969-1989.

BAZUHAIR, A. S. AND WOOD, W. W. 1996. Chloride mass-balance method for estimating ground water recharge in arid areas: examples from western Saudi Arabia. Journal of Hydrology, 186**,** 153-159.

BEEKMAN, H., GIESKE, A. AND SELAOLO, E. 1996. GRES: Groundwater recharge studies in Botswana 1987-1996. Botswana J. Earth Sci, 3**,** 1-17.

BEEKMAN, H. AND XU, Y. 2003. Review of groundwater recharge estimation in arid and semi-arid Southern Africa. Council for Scientific and Industrial Research (South Africa) and University of the Western Cape Report.

BISSON, R. A. AND LEHR, J. H. 2017. Modern groundwater exploration: discovering new water resources in consolidated rocks using innovative hydrogeologic concepts, exploration, drilling, aquifer testing and management methods, John Wiley AND Sons.

BOERNER, A. AND WEAVER, C. 2012. Nebraska recharge estimation from chloride mass balance. Nebraska.

BOWEN, N. 1922. The reaction principle in petrogenesis. The Journal of Geology, 30**,** 177-198.

BRANDL, G. 1986. The Geology of the Pietersburg Area: Explanation of Sheet 2328, Scale 1: 250 000, Republic of South Africa, Department of Mineral and Energy Affairs ….

BREDENKAMP, D., BOTHA, L., VAN TONDER, G. AND JANSE VAN RENSBURG, H. 1995. Manual on Quantitive Estimation of Groundwater Recharge and Aquifer Storativity: based on practical hydro-logical methods. Pretoria: Water Research Commision.

CHILTON, P. AND SMITH-CARINGTON, A. 1984. Characteristics of the weathered basement aquifer in Malawi in relation to rural water supplies, IAHS Press.

CHILTON, P. J. AND FOSTER, S. 1995. Hydrogeological characterisation and water-supply potential of basement aquifers in tropical Africa. Hydrogeology journal, 3**,** 36-49.

CHIMPHAMBA, J., NGONGONDO, C. AND MLETA, P. 2009. Groundwater chemistry of basement aquifers: A case study of Malawi. The Basement Aquifers of Southern Africa, 39.

CLARK, L. 1985. Groundwater abstraction from Basement Complex areas of Africa. Quarterly Journal of Engineering Geology and Hydrogeology, 18**,** 25-34.

COOK, P. G. 2003. A guide to regional groundwater flow in fractured rock aquifers, Citeseer.

COOK, P. G., MCEWAN, K. AND HERCZEG, A. 2001. Groundwater recharge and stream baseflow, Atherton Tablelands, Queensland, CSIRO Land and Water.

Department of Water Affairs and Forestry (DWAF). 2004. Limpopo Water Management Area: Internal strategic perspective version 1: Report no. P WMA 01/000/00/0304. Pretoria: DWAF.

Department of Water Affairs and Forestry (DWAF). 2006. Groundwater resource assessment II – Task 3-recharge. Pretoria: DWAF.

DETTINGER, M. D. 1989. Reconnaissance estimates of natural recharge to desert basins in Nevada, USA, by using chloride-balance calculations. Journal of Hydrology, 106**,** 55-78.

DIPPENAAR, M. A., WITTHÜSER, K. T. AND VAN ROOY, J. L. 2009. Groundwater occurrence in Basement aquifers in Limpopo Province, South Africa: model-setting-scenario approach. Environmental Earth Sciences, 59**,** 459.

DU TOIT, W. 2001. An investigation into the occurrence of groundwater in the contact aureole of large granite intrusions (batholiths) located west and northwest of Pietersburg. Dept. of Water Affairs and Forestry, Pretoria, South Africa.

DU TOIT W.H AND SONNEKUS C.J. 2014. Explanation of the 1:500 000 hydrogeological map 2326 Polokwane. Pretoria: Directorate Geohydrology.

DUKE, H. R. 1972. Capillary properties of soils-influence upon specific yield. Transactions of the ASAE, 15**,** 688-0691.

EASTERN RESEARCH GROUP, I. AND INFORMATION, C. F. E. R. 1993. Use of airborne, surface, and borehole geophysical techniques at contaminated sites: A reference guide, US Environmental Protection Agency.

ENVIROXCELLENCE. 2009. Environmental management plan - Aganang Local Municipality. Ref. No. 1514_Exs.2009. December 2009.

ERIKSSON, E. 1960. The yearly circulation of chloride and sulfur in nature; meteorological, geochemical and pedological implications. Part II. Tellus, 12**,** 64-109.

EVN AFRICA CONSULTING SERVICES (PTY) LTD,2013. DWA – Feasibility Study for Aganang Mun. BWS. Project No. 1302A0.

GEE, G. W. AND HILLEL, D. 1988. Groundwater recharge in arid regions: review and critique of estimation methods. Hydrological processes, 2**,** 255-266.

GUSTAFSON, G. AND KRÁSNÝ, J. 1994. Crystalline rock aquifers: their occurrence, use and importance. Applied Hydrogeology, 2**,** 64-75.

HARTE, P. T. AND WINTER, T. C. Factors affecting recharge to crystalline rock in the Mirror Lake area, Grafton County, New Hampshire. USGS Toxic Substances Hydrology Program–Proceedings of the Technical Meeting, Colorado Springs, Colorado, 1993.

HEALY, R. W. AND COOK, P. G. 2002. Using groundwater levels to estimate recharge. Hydrogeology journal, 10**,** 91-109.

HEATH, R. C. 1983. Basic Groundwater Hydrology: US Geological Survey Water Supply Paper 2220; prepared in cooperation with the North Carolina Department of Natural Resources and Community Development.

HOLLAND, M. 2011. Hydrogeological characterisation of crystalline basement aquifers within the Limpopo Province, South Africa. University of Pretoria.

HOUNSLOW, A. 1995. Water quality data: analysis and interpretation, CRC press.

HOUSTON, J. 1992. Rural water supplies: comparative case histories from Nigeria and Zimbabwe. Geological Society, London, Special Publications, 66**,** 243-257.

HUDAK, P. F., 2000. Principles of Hydrogeology. 2 Ed. Lewis Publishers. 200pp.

JARAWAZA, M. 1999. Estimation of groundwater recharge - Grasslands research catchment, Marondera, Zimbabwe. MSc. Thesis, University of Zimbabwe, Harare, pp. 91

JONES, M. 1985. The weathered zone aquifers of the basement complex areas of Africa. Quarterly Journal of Engineering Geology and Hydrogeology, 18**,** 35-46.

KELLETT, R. AND BAUMAN, P. 2004. Mapping groundwater in regolith and fractured bedrock using ground geophysics: a case study from Mal. CSEG, 28.

KEYS, W. 1990. Borehole geophysics applied to ground-water investigations: US Geological Survey Techniques of Water-Resources Investigations, book 2, chap. E2.

KING, L.C. 1975. Geomorphology: A basic study for civil engineers. Proceedings of the 6th Regional Conference for Africa on Soil Mechanics and Foundation Engineering, Durban, Volume 2: 259 - 263.

KINZELBACH, W. AND AESCHBACH, W. 2002. A survey of methods for analysing groundwater recharge in arid and semi-arid regions, Division of Early Warning and Assessment, United Nations Environment Programme.

KIRCHNER, J. 2009. Basement aquifers Groundwater recharge, storage and flow. The Basement Aquifers of Southern Africa**,** 58.

KRÁSNÝ, J. AND SHARP, J. 2007. Groundwater in Fractured Rocks, selected papers from the Groundwater in Fractured Rocks Internat. Conf., Prague, 2003. International Association of Hydrogeologists, London.

KRUSEMAN, G. AND DE RIDDER, N. 1990. Analysis and evaluation of pumping test data, ILRI publication 47. International Institute for Land Reclamation and Improvement, The Netherlands.

LERNER, D. N., ISSAR, A. S. AND SIMMERS, I. 1990. Groundwater recharge: a guide to understanding and estimating natural recharge, Heise Hannover.

MACDONALD, A. AND DAVIES, J. 2000. A brief review of groundwater for rural water supply in sub-Saharan Africa.

MASIYANDIMA, M., VAN DER STOEP, I., MWANASAWANI, T. AND PFUPAJENA, S. C. 2002. Groundwater management strategies and their implications on irrigated agriculture: the case of Dendron aquifer in Northern Province, South Africa. Physics and Chemistry of the Earth, Parts A/B/C, 27**,** 935-940.

MCCARTNEY, M. P. 1998. The hydrology of a headwater catchment containing a dambo. University of Reading.

MCFARLANE, M. 1991. Some sedimentary aspects of lateritic weathering profile development in the major bioclimatic zones of tropical Africa. Journal of African Earth Sciences (and the Middle East), 12**,** 267-282.

MCFARLANE, M.J., CHILTON, P.J. AND LEWIS, M.A. 1992. Geomorphological controls on borehole yields: a statistical study in an area of basement rocks in central Malawi. In: Wright, E.P. and Burgess, W.G. (eds.) Hydrogeology of Crystalline Basement Aquifers in Africa. Geological Society Special Publication No 66. Geological Society, London.

MOON, S.-K., WOO, N. C. AND LEE, K. S. 2004. Statistical analysis of hydrographs and water-table fluctuation to estimate groundwater recharge. Journal of Hydrology, 292**,** 198-209.

MUDZINGWA, B., 1998. Hard rock hydrogeology of the Nyatsime Catchment: Zimbabwe. MSc Thesis, ITC Enschede, The Netherlands.

MJANJA, R. 2000. A hydrochemical investigation of the groundwater resource around Chiweshe (upper Mazowe sub-catchment area). BSc Honours. Thesis, University of Zimbabwe, Harare, pp. 59.

NYAGWAMBO, N. L. 2006. Groundwater recharge estimation and water resources assessment in a tropical crystalline basement aquifer.

PHILLIPS, F. M. 1994. Environmental tracers for water movement in desert soils of the American Southwest. Soil Science Society of America Journal, 58**,** 15-24.

PIETERSEN, K. 2009. Aspects of groundwater management that is pertinent to basement aquifers in the Southern African Development Community (SADC). The Basement Aquifers of Southern Africa**,** 148.

PRATHAPAR, S. AND SIDES, R. 1993. A practical guide for estimating recharge from water table hydrographs, CSIRO, Institute of Natural Resources and Environment, Division of Water ….

REBOUÇAS, A. D. C. Groundwater development in Precambrian shield of South America and Westside Africa. IAH Congress on Hydrogeology of Hard Rocks, 1993.

SACS 1980. Stratigraphy of South Africa. Part 1. Geological Survey South Africa.

SCANLON, B. R., HEALY, R. W. AND COOK, P. G. 2002. Choosing appropriate techniques for quantifying groundwater recharge. Hydrogeology journal, 10**,** 18-39.

SCOT, P. AND WIJERS, B.E. 1992. Hydrogeology: groundwater resources, Annexure 3.5, Water resources planning of the Mogalakwena River Basin, situation assessment and development potential. Steffen, Robertson and Kirsten Consulting Engineers.

SELAOLO, E. T. 1998. Tracer studies and groundwater recharge assessment in the eastern fringe of the Botswana Kalahari: the Letlhakeng-Botlhapatlou Area, Vrije Universitet.

SIMMERS, I., HENDRICKX, J., KRUSEMAN, G. AND RUSHTON, K. 1997. Recharge of Phreatic Aquifers in (Semi-) Arid Areas: IAH International Contributions to Hydrogeology 19, AA Balkema. ed. I. Simmers, Rotterdam.

SMITH-CARRINGTON, A. AND CHILTON, P. 1983. Groundwater resources of Malawi. Department of Lands, Valuation and Water. Lilongwe, Republic of Malawi.

SOPHOCLEOUS, M. 1985. The role of specific yield in ground-water recharge estimations: A numerical study. Groundwater, 23**,** 52-58.

SOPHOCLEOUS, M. A. 1991. Combining the soilwater balance and water-level fluctuation methods to estimate natural groundwater recharge: practical aspects. Journal of hydrology, 124**,** 229-241.

STEYL, G. 2011. Estimation of representative transmissivities of heterogeneous aquifers. University of the Free State.

TAYLOR, R. AND HOWARD, K. 1998. Post-Palaeozoic evolution of weathered landsurfaces in Uganda by tectonically controlled deep weathering and stripping. Geomorphology, 25**,** 173-192.

TAYLOR, R. AND HOWARD, K. 2000. A tectono-geomorphic model of the hydrogeology of deeply weathered crystalline rock: evidence from Uganda. Hydrogeology Journal, 8**,** 279-294.

TITUS, R. 2002. Groundwater assessment and strategies for sustainable resource supply in arid zones: the Namaqualand case study, Water Research Commission.

TSANG, Y. W. AND TSANG, C. 1987. Channel model of flow through fractured media. Water Resources Research, 23**,** 467-479.

TSHIPALA, D. 2018. Conceptualisation of hydrogeological system in the crystalline aquifer of the Hout River Catchment, Limpopo Province. Master's dissertation. Wits University.

TWIDALE, C. R. AND ROMANÍ, J. R. V. 2005. Landforms and geology of granite terrains, CRC Press.

VAN TONDER, G., BOTHA, J., CHIANG, W.-H., KUNSTMANN, H. AND XU, Y. 2001. Estimation of the sustainable yields of boreholes in fractured rock formations. Journal of Hydrology, 241**,** 70-90.

VAN WYK, E., VAN TONDER, G. AND VERMEULEN, D. 2011. Characteristics of local groundwater recharge cycles in South African semi-arid hard rock terrains–rainwater input. Water SA, 37.

VARNI, M., COMAS, R., WEINZETTEL, P. AND DIETRICH, S. 2013. Application of the water table fluctuation method to characterize groundwater recharge in the Pampa plain, Argentina. Hydrological Sciences Journal, 58**,** 1445-1455.

WILLIAMS, L. J., ALBERTSON, P. N., TUCKER, D. D. AND PAINTER, J. A. 2004. Methods and hydrogeologic data from test drilling and geophysical logging surveys in the Lawrenceville, Georgia, area.

WOOD, W. W. AND SANFORD, W. E. 1995. Chemical and isotopic methods for quantifying ground-water recharge in a regional, semiarid environment. Ground Water, 33**,** 458-469.

WRIGHT, E. P. 1992. The hydrogeology of crystalline basement aquifers in Africa. Geological Society, London, Special Publications, 66**,** 1-27.

XU, Y. AND BEEKMAN, H. E. 2003. Groundwater recharge estimation in Southern Africa.

XU, Y. AND VAN TONDER, G. (2000). Recharge excel spreadsheet. Bloemfontein: The institution of groundwater studies.

XU, Y. AND VAN TONDER, G.J. (2001). Estimation of recharge using a revised CRD method. Water SA, 27(3):341-343

ABSTRACT

Communities residing near the Matlala Batholith are dependent on the groundwater resource for their water supply. The Matlala wellfield occurs near the south-eastern perimeter of the batholith outcrop and may in future supply local residents with water for drinking and domestic purposes. However, the groundwater level response to rainfall and the groundwater flow patterns within the study area are not well understood, and the risk of aquifer depletion exists if over-abstraction from the aquifer takes place. It is therefore important to understand the underlying aquifer system in terms of recharge and groundwater flow to allow determination of a sustainable abstraction rate. As a first step towards determining a sustainable yield for the wellfield, information on the recharge of the aquifer system is required.

In this study the groundwater recharge to the Matlala Batholith and surrounding gneissic host rock is estimated by evaluating historical groundwater level and chemistry data. However, the available historical data is sparse and contain large temporal and spatial gaps. This lack of complete, comprehensive, and recent data was a severe limitation to the recharge investigation. Despite the limitations associated with data scarcity, three methods were used to estimate the groundwater recharge in the study area from the available data, namely the chloride mass balance (CMB), water level fluctuation (WTF) and cumulative rainfall departure (CRD) methods.

For all three methods, the estimated recharge values varied significantly for the boreholes drilled around the Matlala Batholith. The large variations in the estimated recharge rates for the different boreholes indicate that different recharge conditions occur at these boreholes. The recharge rates are most likely affected by the depth of weathering and fracturing of the regolith in the vicinity of the different boreholes.

The average recharge rates estimated with the physical methods (WTF and CRD) were very similar (3.39% and 3.76% of the rainfall received) but differed from the estimate obtained with the CMB method (1.20% of the MAP). However, all three methods indicate low average recharge rates of well below 5%, in line with the results obtained during previous studies. These low recharge estimates should be used when calculating the sustainable abstraction rate from the aquifer system.

A way forward for future investigations at the Matlala wellfield includes: performing pumping tests on the high-yielding boreholes in the wellfield to investigate the flow regimes in the aquifers and to determine the aquifer hydraulic parameters, calculating sustainable abstraction rates using the results of the pumping tests, and developing a numerical model for the Matlala wellfield to investigate different pumping scenarios for future water supply purposes.

APPENDIX A

Geological Borehole Logs

BATHOLITH PROJECT: GEOLOGICAL LOG

Borehole number: G45524
Locality: Matlala Batholith (Matlala clinic)
Coordinates (degrees, minutes, seconds): Latitude: 23 44 29.8 Longitude: 29 03 31.0
Date drilled: 31/10/97
Blow yield: 1,0 l/s
Tested yield: Not tested
EC measurement: 63,4 mS/m
Water strikes: 12m, 14m, 26m, 34m
Water-level: 10,14m

Geological Log | Water-level and water strikes | Lithological description

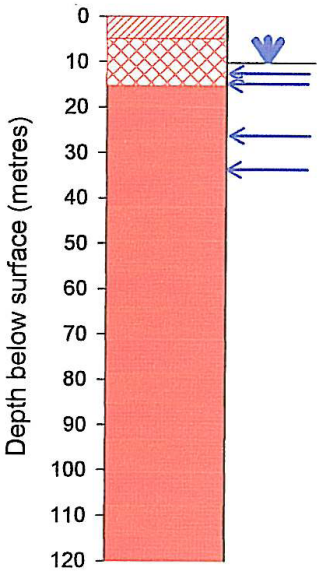

Weathered Matlala Granite (almost a diorite)

Fractured Matlala Granite (almost a diorite)

Solid Matlala Granite (almost a diorite)

BOREHOLE CONSTRUCTION

DRILLED HOLE:

165mm diameter: 12m - 120m
200mm diameter: 0m - 12m
250mm diameter: None
Total depth: 120m

CASING INSTALLED

Total length and diameter of innermost casing: 9m x 165mm
Length and diameter of other casing installed: None
Type of casing and wall thickness: Steel, 4mm
Length of plain innermost casing: 9m
Length of perforated casing: None
Location of perforations: None
Lenght and width of slots: None
Number of rows of slots: None

BATHOLITH PROJECT: GEOLOGICAL LOG

Borehole number: G45279
Locality: Matlala Batholith (Line 1)
Coordinates (degrees, minutes, seconds): Latitude: 23 45 49.5 Longitude: 28 57 16.4
Date drilled: 30/5/97
Blow yield: 1,0 l/s
Tested yield: Not tested
EC measurement: 511 mS/m
Water strikes: 18m to 21m
Water-level: 3,92m

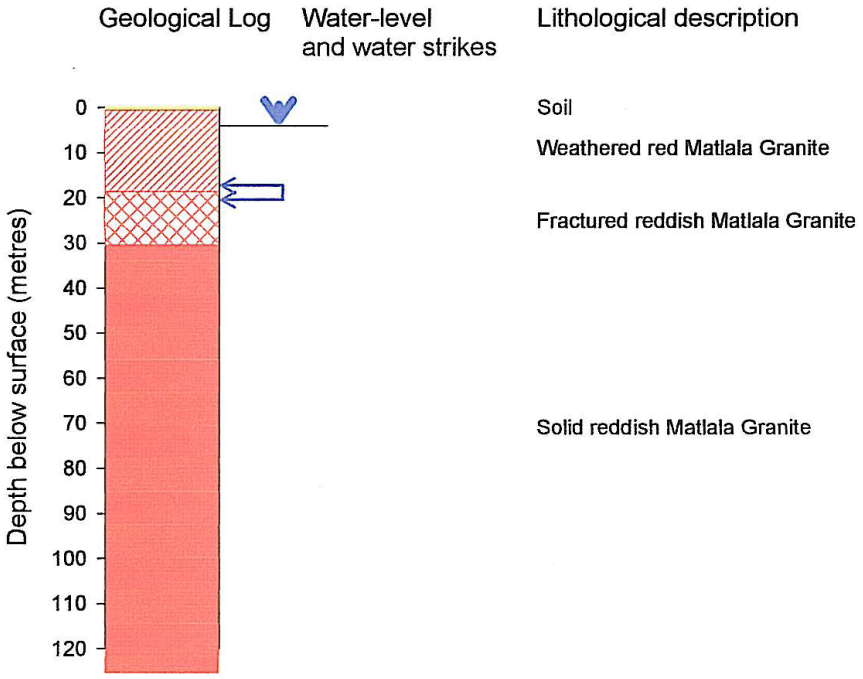

BOREHOLE CONSTRUCTION

DRILLED HOLE:

165mm diameter: 24m - 126m
200mm diameter: 0m - 24m
250mm diameter: None
Total depth: 126m

CASING INSTALLED

Total length and diameter of innermost casing: 18m x 165mm
Length and diameter of other casing installed: None
Type of casing and wall thickness: Steel, 4mm
Length of plain innermost casing: 18m
Length of perforated casing: None
Location of perforations: None
Lenght and width of slots: None
Number of rows of slots: None

BATHOLITH PROJECT: GEOLOGICAL LOG

Borehole number: G45185
Locality: Matlala Batholith (Line 6)
Coordinates (degrees, minutes, seconds): Latitude: 23 47 14.3 Longitude: 29 04 10.3
Date drilled: 5/8/97
Blow yield: < 0,1 l/s
Tested yield: Not tested
EC measurement: 59,9 mS/m
Water strikes: 39
Water-level: 5,54m

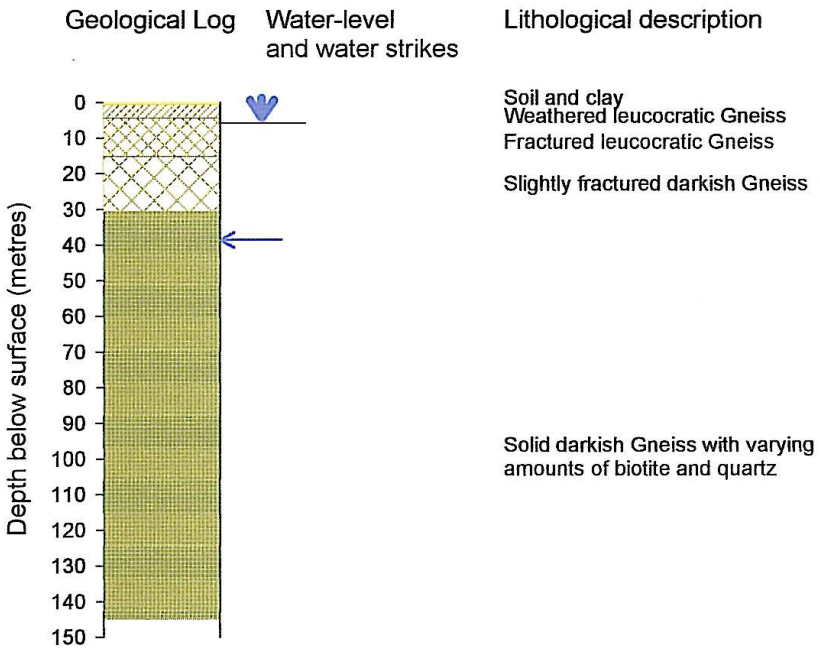

BOREHOLE CONSTRUCTION

DRILLED HOLE:

165mm diameter: 6m - 144m
200mm diameter: 0m - 6m
250mm diameter: None
Total depth: 144m

CASING INSTALLED

Total length and diameter of innermost casing: 6m x 165mm
Length and diameter of other casing installed: None
Type of casing and wall thickness: Steel, 4mm
Length of plain innermost casing: 6m
Length of perforated casing: None
Location of perforations: None
Lenght and width of slots: None
Number of rows of slots: None

APPENDIX B

Borehole Information

UTM35X (m)	UTM35Y (m)	Long (^{o}E)	Lat (^{o}S)	G No	Borehole No	Elevation (mamsl)	Weathered zone			Fractured zone			Aquifer
							Top elevation (mamsl)	Bottom elevation (mamsl)	Thickness (m)	Top elevation (mamsl)	Bottom elevation (mamsl)	Thickness (m)	Thickness (m)
710867	7367786	29.0695	-23.7873	G45185	H04 1047	1230	1230	1224	6	1224	1190	34	40
711189	7367515	29.0727	-23.7897	G45186	H04 1048	1225	1225	1210	15	1210	1135	75	90
710796	7367842	29.0688	-23.7868	G45187	H04 1046	1238	1238	1229	9	1229			
708926	7364679	29.0509	-23.8156	G45188	H04 0984	1268	1268	1259	9	1259	1218	41	50
708986	7364611	29.0515	-23.8162	G45189	H04 1049	1271	1271	1262	9	1262	1191	71	80
708428	7364797	29.046	-23.8146	G45281	H04 0991	1265	1265	1255	10	1255	1233	22	32
708773	7364670	29.0494	-23.8157	G45282	H04 0986	1262	1262	1227	35	1227	1192	35	70
708703	7364748	29.0487	-23.815	G45283	H04 0989	1259	1259	1240	19	1240	1186	54	73
709088	7364621	29.0525	-23.8161	G45284		1274	1274	1244	30	1244	1214	30	60
709574	7364403	29.0573	-23.818	G45285	H0 40987	1291	1291	1238	53	1238	1191	47	100
708642	7364771	29.0481	-23.8148	G45286	H04 0990	1291	1291	1273	18	1273	1236	37	55
708662	7364782	29.0483	-23.8147	G45287		1291	1291	1271	20	1271	1218	53	73
709006	7364611	29.0517	-23.8162	G45288	H04 0985	1291	1291	1264	27	1264	1226	38	65
710534	7368056	29.0662	-23.7849	G45294	H04 1044	1291	1291				1241		50
710313	7368237	29.064	-23.7833	G45295	H04 0982	1291	1291	1270	21	1270	1256	14	35
710222	7368316	29.0631	-23.7826	G45296	H04 0986	1291	1291	1279	12	1279	1256	23	35
710655	7367955	29.0674	-23.7858	G45297	H04 1045	1291	1291						
708866	7364757	29.0503	-23.8149	Matlala 1	H04-1457	1291	1291	1261	30	1261	1223	38	68
708966	7364623	29.0513	-23.8161	Matlala 2	H04-1049	1291	1291	1273	18	1273	1211	62	80
708864	7364657	29.0503	-23.8158	Matlala 3	H04-0986	1291	1291	1256	35	1256	1221	35	70
708863	7364602	29.0503	-23.8163	Matlala 4	H04-2281	1291	1291				1211		80
708951	7364324	29.0512	-23.8188	Matlala 5	H04-2264	1291	1291	1275	16	1275	1211	64	80
708718	7364427	29.0489	-23.8179	Matlala 6	H04-1459	1291	1291	1266	25	1266	1221	45	70
708627	7364461	29.048	-23.8176	Matlala 7	H04-1456	1291	1291	1266	25	1266			
708514	7364385	29.0469	-23.8183	Matlala 8	H04-2280	1291	1291						
708877	7364136	29.0505	-23.8205	Matlala 9	H04-2265	1291	1291	1275	16	1275	1242	33	49
708792	7363905	29.0497	-23.8226	Matlala 10	H04-2266	1291	1291	1276	15	1276	1266	10	25
708830	7363727	29.0501	-23.8242	Matlala 11	H04-2267	1291	1291	1282	9	1282	1239	43	52
708739	7363773	29.0492	-23.8238	Matlala 12	H04-2268	1291	1291	1264	27	1264	1239	25	52
708275	7364788	29.0445	-23.8147	Matlala 13	H04-2277	1291	1291	1274	17	1274			

UTM35X (m)	UTM35Y (m)	Long (^{o}E)	Lat (^{o}S)	G No	Borehole No	Elevation (mamsl)	Weathered zone			Fractured zone			Aquifer
							Top elevation (mamsl)	Bottom elevation (mamsl)	Thickness (m)	Top elevation (mamsl)	Bottom elevation (mamsl)	Thickness (m)	Thickness (m)
708469	7364796	29.0464	-23.8146	Matlala 14	H04-2274	1291	1291						
708487	7364674	29.0466	-23.8157	Matlala 15	H04-2278	1291	1291	1276	15	1276	1184	92	107
708334	7364665	29.0451	-23.8158	Matlala 16	H04-2275	1291	1291						
708376	7364753	29.0455	-23.815	Matlala 17	H04-2276	1291	1291	1262	29	1262	1181	81	110
708480	7364186	29.0466	-23.8201	Matlala 18	H04-2271	1291	1291	1255	36	1255	1214	41	77
708256	7364168	29.0444	-23.8203	Matlala 19	H04-2273	1291	1291	1259	32	1259	1211	48	80
708415	7363888	29.046	-23.8228	Matlala 20	H04-2269	1291	1291	1246	45	1246	1199	47	92
708273	7363946	29.0446	-23.8223	Matlala 21	H04-2270	1291	1291	1275	16	1275	1243	32	48
708671	7364704	29.0484	-23.8154	Matlala 22	H04-0988	1291	1291	1269	22	1269	1219	50	72
708679	7365214	29.0484	-23.8108	Matlala 23	H04-1460	1291	1291						
709071	7364876	29.0523	-23.8138	Matlala 24	H04-1461	1291	1291	1273	18	1273			
707922	7365745	29.0409	-23.8061	Matlala 25	H04-1458	1291	1291	1272	19	1272	1219	53	72